ROLL MOTION PARAMETER IDENTIFICATION USING RESPONSE IN RANDOM WAVES

XIA WU

Roll Motion Parameter Identification Using Response in Random Waves

BY

© XIA WU, B. Eng.

A Thesis Submitted To the School of Graduate Studies
in Partial Fulfillment of the Requirements for
the Degree of Master of Engineering

Faculty of Engineering and Applied Science
Memorial University of Newfoundland
December, 1992

St. John's *Newfoundland* *Canada*

ISBN 0-315-82621-5

Dedicated to

My Husband and Daughter

Abstract

The concept of the random decrement has been used successfully in the damping identification of linear systems. The formulation of the random decrement existing in the literature is based on the assumptions that the dynamic system is linear, time invariant and subjected to Gaussian, white noise excitation. Thus, the principle of superposition can be used in formulating the equation for the random decrement.

In this study, the concept of the random decrement is extended to nonlinear systems. Using the Fokker-Plank Equation approach, it can be shown that the random decrement formed by calculating the expected value of a stationary random rolling process satisfies the differential equation governing the free roll motion. It is also shown that, the autocorrelation function for the stationary nonlinear roll motion excited by a zero mean, Gaussian, white noise random process, satisfies a linearized free roll equation. Thus the random decrement and the autocorrelation function curves can be used for identifying the parameters in the nonlinear equation of free roll motion.

The validity, accuracy and reliability of the Random Decrement Technique in determining the parameters of the nonlinear equation for roll motion are investigated in this study. The technique is applied to roll motion obtained from: 1) computer simulation by using a fourth order Runge Kutta routine; 2) experiments of three ship models rolling in a towing tank; 3) full scale tests on a real fishing vessel. A method for evaluating the parameters in the nonlinear roll equation from free roll decay, the random decrement and the autocorrelation function is devel-

oped and presented in this study. This method is based on the theory of equivalent linearization. The application of the method provides accurate estimation for the parameters from both simulated and measured data.

It is shown that the random decrement and the autocorrelation function curves extracted from a history of nonlinear roll response to random excitation closely resemble the measured free roll decay curve. The predicted natural frequency obtained by either the random decrement or autocorrelation function method can be used to determine the value of the metacentric height for a ship rolling under the action of unknown random excitations. The damping coefficients estimated by either method are used to generate free roll decay curve which agrees well with the measured free roll decay curve.

This method does not rely on a model experiment and does not require the measurement of wave height. In addition, roll response of a ship can be easily measured with the ship underway. It is expected that the method would be particularly useful for assessing roll stability of a ship sailing in a realistic sea.

Acknowledgements

I would like to take this opportunity to express my sincere appreciation to my supervisor, Dr. M. R. Haddara for his support, guidance, patience and encouragement, which will be remembered forever.

I am deeply grateful to Dr. J. J. Sharp for his consideration of financial support and all generous help throughout my program. Mrs. Moya Crocker deserves many thanks for her patience and help in all aspects.

Special thanks to Dr. D. Muggeridge for providing me a computer and permitting me to use the towing tank. I owe a lot of thanks to Mr. Andrew Kuczora for his numerous help and assistance in my experiments.

I would also like to thank my fellow graduate students, Z. Tang, Z. Wang, B. Zou, K. Leung, S. Zhang and Y. Zhang for their helpful discussion and/or assistance in my experiments.

Dr. Momen Wishahy at C-CORE, who provided partial financial support and measuring instruments for the tank experiments and took charge of the real ship tests, is gratefully acknowledged.

Contents

List of Figures

List of Tables

List of Symbols

ϕ	roll angle
$\dot{\phi}$	roll velocity
$\ddot{\phi}$	roll acceleration
τ_{max}	time length of the random decrement
ϕ_s	selected angle of the random decrement
$\mu(\tau)$	random decrement function
$N(\phi, \dot{\phi})$	nonlinear damping moment per unit virtual inertia
$D(\phi)$	nonlinear restoring moment per unit virtual inertia
K(t)	wave exciting moment per unit virtual inertia
Ψ_0	variance of the excitation
δ	Dirac delta function
μ_1	expected value of roll angle
μ_2	expected value of roll velocity
$R_\phi(\tau)$	Autocorrelation function
b_e	equivalent linear damping coefficient
ω_e	equivalent natural frequency
ω_ϕ	roll natural frequency
ζ	non-dimensional linear damping coefficient
ϵ	non-dimensional nonlinear damping coefficient
α_1, α_2	nonlinear restoring coefficients
σ^2	variance of linear rolling motion
$S_\phi(f)$	spectral density function
PF	predominant frequency of spectral density

f_m	modal frequency of spectral density
H_s	significant wave height
F	Nyquist frequency
b_1	linear damping coefficient
b_2	quadratic damping coefficient
b_3	cubic damping coefficient
ω_d	damped natural frequency
R	roll angle amplitude
A	moment amplitude of sinusoidal wave component
ω_k	frequency of sinusoidal wave component
θ_k	phase angle of sinusoidal wave component
ω_b	low limit of wave band
ω_f	high limit of wave band
r	uniform random number
GM	transverse metacentric height
GZ	righting lever arm
KG	height of the center of gravity above keel
KM_T	height of transverse metacenter above keel

Chapter 1

Introduction and Literature Survey

1.1 Introduction

The roll motion of a ship under the excitation of waves may reach dangerously large amplitudes and may even result in ship capsizing. It is very important, therefore, to be able to predict the probability of roll amplitude reaching critical levels, for a ship sailing in a realistic sea. This is not a simple matter since the nonlinearities are present in both the damping and restoring moment terms. In addition, the stochastic nature of the wave excitation and the roll response make the analysis of roll motion more difficult. As a general theory for nonlinear system response to stochastic processes is not yet available, the progress in developing a satisfactory stochastic theory for ship rolling has been slowed.

So far, stability criterion for a ship at sea is still based on quasi-static considerations to ensure that the ship roll restoring characteristic satisfies specific criteria. The criterion dictates certain conditions on the minimum value of GM and the shape of the GZ curve. A sizeable number of small ships that satisfy this criterion are still being lost each year. The problem may be caused by ever changing

loading conditions, some of which may produce adverse effects on stability as in the case of fishing and warships [1]. Also, it may be caused by encountering severe environmental conditions brought about by the desire to increase the operating range of the ship. Dynamic instability is a third factor.

The initial value of GM and the shape of the GZ curve can be determined fairly easily using standard computer programs. But because of uncertainties regarding loading conditions, especially for a fishing vessel, the resulting errors in the calculation may render the results unsuitable for assessing the stability of the ship in certain sailing conditions. Also, these values are affected by the environmental conditions. It is thus best if we can determine these quantities from measurements obtained while the ship is at sea so that the safety criterion can be based on quasi-static as well as dynamic considerations.

Dynamic stability can be investigated using a second order differential equation in the rolling angle. The main parameters of this equation are: the moment of inertia (including the added moment of inertia), the damping moment, the restoring moment and the exciting moment. The equation can be normalized with respect to the moment of inertia. In this case we are left with only three quantities to determine. In principle, the restoring and the wave exciting moments can be determined using analytical methods provided that loading and wave conditions are well defined. As to the damping identification, a complete theoretical analysis of the problem is still beyond present capabilities.

As an alternative to theoretical prediction, based on fluid dynamic theory, one can attempt to estimate the ship roll parameters using empirical methods and parameter identification techniques. Kountzeris et al. [2] has shown that it is

possible to estimate all the parameters from experiments on a model rolling in irregular seas, if simultaneous records of the roll response and wave height are available. This approach is useful when studying the behaviour of scale models in a wave tank. However, for full scale ships at sea it is generally not possible to obtain time histories of the wave height in the vicinity of the ship. Thus, one has to rely on roll motion measurements only to predict roll parameters of a ship sailing in a random sea.

One of the main difficulties in the estimation of roll parameters from nonlinear rolling motion is the prediction of damping coefficients. The damping moment is a very important term in the roll equation because the roll amplitude of a ship is critically dependent on the magnitude of roll damping under resonant condition. Since the time of Froude, many efforts have been devoted to both theoretical and experimental studies concerning roll damping. Froude [3] demonstrated that both the damping and restoring moments varied in a distinctly nonlinear manner. He advanced the formulation of the linear plus quadratic velocity dependent damping moment. This formulation has been used almost exclusively for the last century. To overcome analytical difficulties arising from the use of the quadratic form, Haddara [4] introduced the linear plus cubic velocity dependent damping moment. Further, study of the form of the roll damping moment [5], shows that different models may be obtained using the same roll decay record.

An outline of the methods avaliable now in the literature for the prediction of nonlinear roll damping is given below.

1.2 Identification of Nonlinear Roll Damping

Various methods of analysing free roll tests, forced roll tests and roll tests in random waves have been developed for the prediction of the nonlinear roll damping coefficients.

1.2.1 Free Roll Tests

The free roll test is performed, in the absence of waves, by giving the model an initial roll amplitude and then releasing it. A free roll test is probably the simplest way to measure roll damping of a ship or a model. There are several methods for the analysis of free roll tests from which nonlinear damping coefficients can be determined.

Froude Energy Method equates the energy loss due to damping in each half-cycle to the work done by the restoring lever in reducing the roll amplitude. The method, suitable for the use with linear restoring, was devised for linear + quadratic damping by Froude [3] and extended to linear + cubic damping by Dalzell [6]. Over one century since it was first proposed, the Froude Method has been used as the standard for free roll decay analysis, apparently without any criticism. However, the errors in calculating the slope of the roll decay curve make this method the most sensitive to the distortion at the start of the decay curve.

Quasi-linear Method is simply a linear analysis technique used to determine the nonlinear damping coefficients from the equivalent linear damping coefficient for ships with linear restoring. The method assumes that the energy loss due to damping during a half cycle of roll is the same when linear and nonlinear damping are used. The quasi-linear method is the least complex of all methods, but gives

the least confidence in the results [7].

Averaging Technique of Krylov and Bogoliubov [5, 6] assumes that the motion during the free-decay is sinusoidal with slowly-varying amplitude and phase, and that for any cycle the rates of change of amplitudes and phase are constant and equal to their average values during the cycle. Dalzell [6] investigated the quadratic and cubic models using the averaging technique to find an equation for the rate of decay of the peaks of the roll decay curve as a function of damping parameters. Haddara [5] used a stochastic version of the same procedure to investigate different damping models including angle dependent components. This method usually yields fairly accurate results for velocity dependent components of the damping moment but it is only suitable for linear restoring moment which is unrealistic for large amplitude motion.

Perturbation Method makes the preliminary assumption that the nonlinear terms in the equation of motion are small compared to the linear terms. The nonlinear equation is then replaced by a series of linear equations. Mathisen and Price [8] used perturbation approach to analyse free roll response of a ship. The method usually gives good fit to the measured decay but is valid only for small nonlinearity and capable of dealing with simple forms of damping and linear restoring moments.

Roberts Energy Method [9] formulates an energy loss function which is related to the amplitude of roll motion, and the parameters of the roll damping moment. It is therefore similar in principle to the Froude energy method although, in producing an expression for the damping coefficients rather than the slope of the decay curve. The method is able to include nonlinear restoring moment, but it

is critically dependent on high-quality experimental data and requires numerical fairing of the decay curve.

All of the above mentioned methods are only suitable for linear restoring moment except the Roberts Method which is capable of dealing with nonlinear restoring moments. Besides, these methods are limited to either small nonlinearities or simple forms of damping. To avoid the drawbacks of these methods, Bass and Haddara [10] introduced the 'DEFIT Method' and the 'Energy Approach'.

DEFIT Method is a parameter identification technique based on fitting the experimental data to the solution of an assumed differential equation. In this method, the linear damping is estimated primarily and the remaining parameters can be simply 'guessed'. The sum of the squared errors between the observed value and the predicted value is then minimized using an algorithm due to Levenberg and Marquardt [11]. This method avoids the possible errors raised from the theoretical assumptions used in the other methods.

Energy Approach uses the concept that the decremental rate of the total energy in free roll motion is equivalent to the rate of energy dissipated by the roll damping. The roll angle decay curve is used to calculate the roll velocity at equally spaced instants of time. The total energy is evaluated from the roll angle and the roll velocity at the same time instants. A parametric form for the damping moment is assumed and the damping coefficients are obtained by the least squares method.

Since DEFIT Method and Energy Approach make use of the values of the whole curve, not the peak values only, they are especially useful in situations where only a couple of cycles in a decay curve are available. Besides, the methods are suitable for

the the analysis of large rolling motion and large nonlinearities presented in both damping and restoring moments. Third, they are capable of dealing with a rather general form of the roll damping moment. Thus angle dependent components can be included.

1.2.2 Forced Roll Tests

The forced roll test involves applying a pure sinusoidal wave and measuring the roll response of the model to wave excitation. To obtain the values of nonlinear damping coefficients directly through a steady-state forced roll experiment, we would probably need numerical techniques to fit the data. Such an attempt does not seem to have been done. Instead, it is usual to assume some additional relations concerning energy consumption, linearity of damping and its independence of roll angle. Since a single sine-wave roll test is not sufficient for nonlinear damping coefficients to be determined, a number of sinusoidal tests conducted with differing input frequencies or amplitudes are needed. For determining nonlinear damping in regular waves, three methods are commonly used.

Quasi-linear Methods [7] analyze each steady forced roll using a linear technique. The resulting damping is treated as an equivalent linear value and expressed as a function of linear restoring coefficient or measured phase angle. From the variation of equivalent linear damping with roll amplitudes of a set of forced roll tests, the nonlinear damping coefficients can be determined by using a linear least-squares fit.

Energy Method [7] equates the energy dissipated by the damping in a cycle to the work done by the wave exciting moment. This gives an expression for the part of the forcing moment that is in phase with the roll velocity. The non-

linear damping coefficients are determined from the equivalent linear damping. This method produces the same expression as the quasi-linear method using phase angles.

Perturbation Method usually makes use of higher harmonics in roll response, and is therefore inappropriate where the response is nearly sinusoidal. Mathisen and Price [8, 12] used this technique to investigate linear + cubic damping and also used higher harmonics in the forcing moment to produce sinusoidal roll motion. The method has been proved virtually useless in practice [7].

It is expected that forced roll tests give a more accurate estimate of roll damping, simply because forced roll can reach steady state, while free roll is transient. However, since a sequence of tests at a range of excitation frequencies or amplitudes are needed in order to deduce values of the nonlinear damping parameters, the forced roll test is less employed than free roll test.

1.2.3 Roll Tests in Random Waves

The random roll test is carried out with the model rolling under the excitation of random waves. From both theoretical and practical point of view, the prediction of roll parameters in random waves is extremely difficult, especially in the situation where only roll measurements are available.

Roberts et al. [13] developed a method using roll measurements only to estimate roll parameters of nonlinear roll motion in random waves. It is based on the method of stochastic linearization and utilizes various theoretical results relating to the energy envelope of the roll response, including its probability distribution and its correlation function. The method seems to yield good results when tested using digitally generated data. Results using real data were not presented.

In the attempt to use Roberts Method for the analysis of random roll response, it is found that the method was not applicable to real data. It is also found that the method is valid for simulated data only in particular situations such as: systems with nearly zero damping or linear restoring moment. When a nonlinear restoring term was added to the parameters given in the paper as cases 2 and case 3, incorrect and even unreasonable results were obtained by this method. For the simulated data of a ship model with realistic damping and nonlinear restoring moments, the method gave serious biased estimates. For an accurate prediction of large amplitude roll, it is necessary to include nonlinear restoring moment terms in the equation of motion, and also the damping moment of a realistic ship model could not be that small. Thus this method can not be used as a practical tool even for some digitally generated data.

1.3 Random Decrement Technique

The Random Decrement Technique was developed in the late 1960's by Cole [14]. It was originally developed as a technique for determining damping characteristics of models being tested in wind tunnels. Subsequently, the method was used to measure damping of soils, bridges, platforms, etc [15, 16]. The method has achieved rather widespread use, especially in the aerospace industry, for measuring damping of aircraft models in a wind tunnel and aircrafts in flight [17]. It also made the detection of flaws in structures possible by monitoring their dynamic characteristics [18]. In fact, the technique is a general method of analysis that is applicable to a wide class of problems in which a system is subjected to an unknown random input and the only measured quantity is the system response.

The concept of the Random Decrement is based on the assumption that the random response of a linear time invariant damped system subjected to a zero-mean, white noise, Gaussian process is composed of two parts: a deterministic part and a random part. By averaging enough samples of the same random response, the random part will average out, leaving only the deterministic part [19]. It can be shown that the deterministic part that remains is the free decay response from which the natural frequency and damping can be predicted. Hence the Random Decrement technique uses the free decay response of a system under random excitation to identify its vibration parameters, namely natural frequency and damping.

1.4 The Scope of this Study

As stated above, there is a recognized need to develop a method for the identification of the parameters in the equation describing the rolling motion of a ship sailing in a realistic seaway using roll motion measurements only. An ongoing research in this work is to investigate the feasibility and accuracy of the Random Decrement Method used for nonlinear ship roll motion.

The theoretical basis of extending the random decrement technique for use with the nonlinear roll motion has been developed by Haddara [1]. Using the Fokker-Planck Equation and a first-order approximation, it can be proved that the expected value of the nonlinear roll response to stationary, time invariant, Gaussian, white noise excitation satisfies the differential equation describing the free roll motion. It has also been shown that the autocorrelation function of the nonlinear roll response satisfies an equivalent linear equation of free roll motion.

Therefore, the random decrement or autocorrelation function curve can be used as an approximate of free roll decay for identifying the parameters in nonlinear roll equation.

Using the random decrement technique to identify the parameters in the nonlinear roll equation is particularly useful because the measurement of roll motion can be taken when a ship is in a seaway. The following are some of the anticipated advantages of this method:

1. In this method, roll measurements are taken with the ship in real loading condition. Thus the dynamic stability of the ship can be more realistically and accurately investigated than quasi-static consideration.

2. Since the method uses roll measurements only, it could be applied for a ship rolling under the action of unknown random excitations of a realistic sea.

3. The method does not rely on a model experiment which not only costs money but also causes scale errors.

4. Ship's transverse stability at sea can be assessed during the actual motion without interrupting the service of the ship or requiring a special measurement for the input.

The main objective of this study is to present the application of the random decrement technique for parametric identification from the nonlinear roll motion of a ship subject to random waves. In order to investigate the validity and the accuracy of the random decrement method used for nonlinear roll motion, a reliable and accurate estimation method is demanded for evaluating the roll parameters from free roll decay, random decrement and autocorrelation curves. A new estimation

method using equivalent linearization is developed and presented in this study. The method is capable of including nonlinear damping and nonlinear restoring moments and suitable for the analysis of both simulated data and measured data. The method provides accurate estimation of roll parameters from free roll decay as well as from the resulting curves, referred to as the random decrement and the autocorrelation curves.

Chapter 2 presents the theoretical basis of the analytical methods used in this study. The random decrement and the autocorrelation function methods are introduced for estimating the free decaying nonlinear roll response of a ship from its stationary response in random waves. The proposed method for evaluating the parameters from free roll decay is also described.

In Chapter 3, the analytical methods introduced in Chapter 2 are tested by applying them to simulated data generated using a fourth order Runge Kutta routine. The estimated parameters from the free roll decay and the random decrement are compared with the known values used in the simulation.

In Chapter 4, the validity and accuracy of the same methods used for the simulation are examined using the experimental data of three fishing vessel models rolling in a towing tank. The effects of different nonlinear damping moments and different wave excitations on the random decrement are investigated.

Chapter 5 displays the analysis and the results of the real ship tests conducted for a ship sailing in a realistic sea. The same methods are verified by using real roll data taken in a seaway.

Chapter 2

Analytical Methods

In this chapter, the analytical methods for parametric identification of nonlinear roll motion in random waves are described. Three methods – Random Decrement, Autocorrelation Function and Spectral Density Function could be used in determining the natural frequency and roll damping of a ship subject to a randomly varying excitation. These methods share one characteristic: no knowledge of the excitation is required as long as it is a zero mean, Gaussian, white noise random process. To determine all relevant parameters from the random decrement, autocorrelation function and free roll decay curves, a new estimation method is developed and presented in this Chapter.

2.1 Random Decrement Method

2.1.1 Random Decrement for Linear Systems

The random decrement is an averaging technique which is usually used for the damping identification of linear systems. In this technique one is able to obtain the free decay curve of the system from its steady state random response. Thus, the natural frequency and damping of the system are identified from the in-situ

response without interrupting the service or requiring a special measurement for the input.

Illustrated in Figure 2.1, the Random Decrement Technique consists of dividing a record of random response into N segments of equal lengths τ_{max} which can possibly overlap. Each segment begins at a selected amplitude, that is, ϕ_s = constant. Also, the initial slopes of the segments alternate between positive and negative values so that one half will have initial positive values and the other half will have initial negative values. These segments are then ensemble averaged and represented mathematically as

$$\mu(\tau) = \frac{1}{N}\sum_{i=1}^{N}\phi_i(t_i+\tau) \qquad 0 \le \tau \le \tau_{max} \tag{2.1}$$

where

$$\begin{aligned} & \phi_i(t_i) = \phi_s && && i = 1,2,3,\cdots,N \\ if \quad & \dot{\phi}_i(t_i) \ge 0 && then \quad && i = 1,3,5,\cdots,N-1 \\ if \quad & \dot{\phi}_i(t_i) \le 0 && then \quad && i = 2,4,6,\cdots,N \end{aligned}$$

The function $\mu(\tau)$ gives the conditional expected value of the random process which is called the random decrement (signature).

Since for linear systems the superposition law applies, the response can be decomposed into three parts: response due to initial displacement, response due to initial velocity and response due to excitation. When enough segments are averaged together, the part caused by the initial velocity cancels out because the positive and negative initial slopes are taken alternately and their distribution is random. The part caused by the excitation vanishes because, by definition, the excitation is a zero-mean, Gaussian, white noise process. Thus, only the

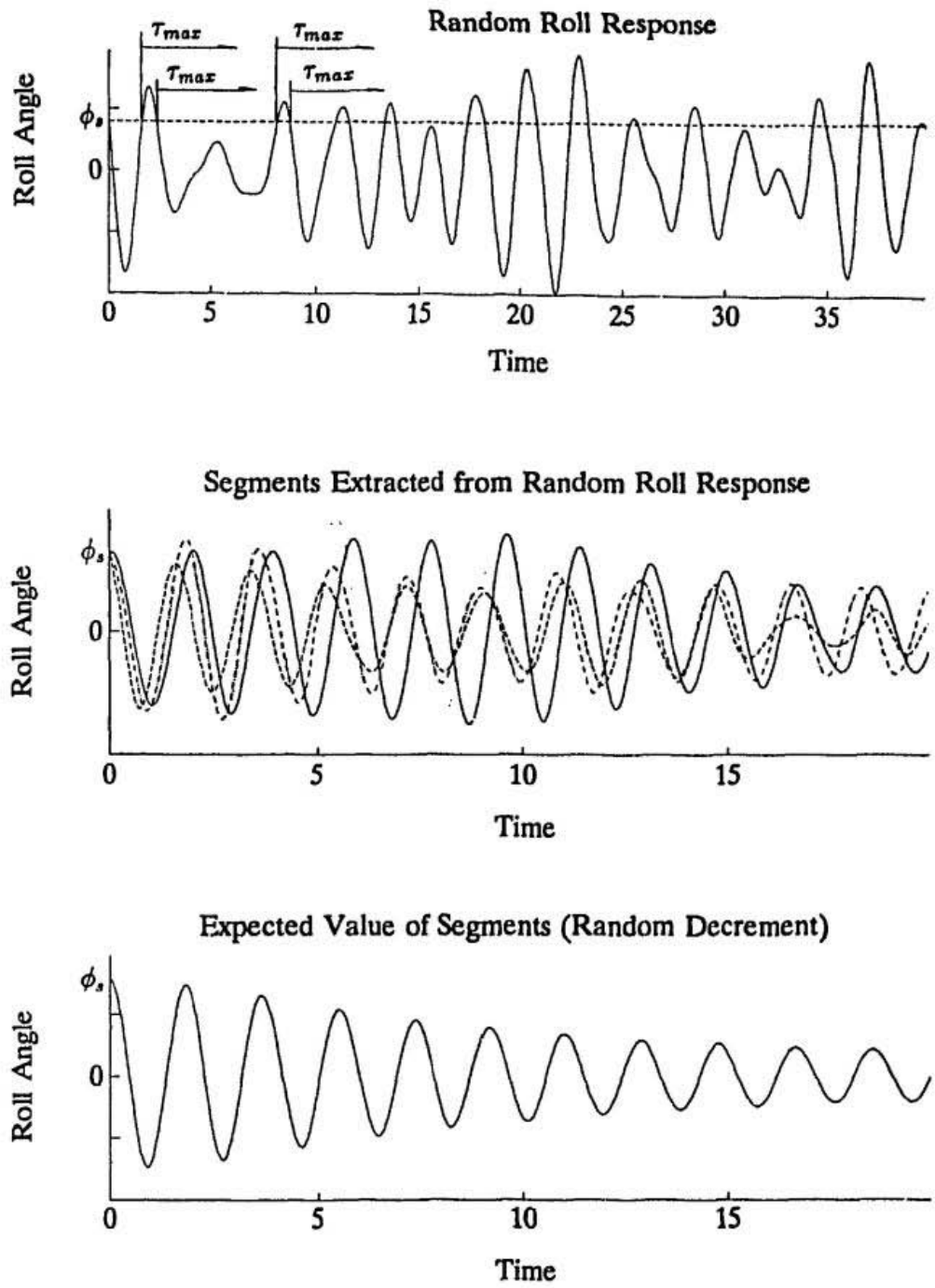

Figure 2.1: Extraction of Random Decrement

part caused by the initial displacement is left, which is the random decrement representing the free decay curve for a linear system.

A more extensive mathematical derivation of the random decrement was developed by Reed [20] for linear systems.

2.1.2 Random Decrement for Nonlinear Systems

In general, for nonlinear systems the separation of responses can not be made since the principle of superposition does not apply. However, we can use the Fokker-Planck Equation to show that the random decrement is an approximation to the free decay curve. The procedure given by Haddara [1] is outlined below.

The nonlinear roll motion of a ship in random beam seas can be mathematically modelled by a second-order ordinary, nonlinear differential equation.

$$\ddot{\phi} + N(\phi, \dot{\phi}) + D(\phi) = K(t) \tag{2.2}$$

where ϕ is the roll angle. $\dot{\phi}$ and $\ddot{\phi}$ are the first and second derivatives with respect to time, respectively. $N(\phi, \dot{\phi})$ and $D(\phi)$ are the nonlinear damping and restoring moments per unit virtual inertia, respectively. K(t) is the wave exciting moment per unit virtual inertia.

It is assumed that the wave excitation K(t) is a stationary random Gaussian process which satisfies the following equations.

$$< K(t) > = 0$$

$$< K(t_1)K(t_2) > = \Psi_0 \, \delta(t_1 - t_2)$$

where δ is the Dirac delta function, Ψ_0 is the variance of the excitation and the symbol <> means the ensemble average of the process.

Using the following change of variables

$$\begin{array}{l} y_1 = \phi \\ y_2 = \dot{\phi} \end{array} \qquad and\ let \qquad Y(t) = \begin{bmatrix} y_1 \\ y_2 \end{bmatrix}$$

Then, Equation (2.2) can be expressed as

$$\begin{aligned} \dot{y_1} &= y_2 \\ \dot{y_2} &= -N(y_1, y_2) - D(y_1) + K(t) \end{aligned}$$

The stochastic process Y(t) is assumed to be a Markov process. A Markov process satisfies the following conditional probability equation:

$$P_n(x_n t_n \mid x_1 t_1, x_2 t_2, \cdots, x_{n-1} t_{n-1}) = P_2(x_n t_n \mid x_{n-1} t_{n-1})$$

Thus the process $Y(t)$ may be described by the conditional probability density function, $P_2(y_1, y_2, t \mid y_{10}, y_{20})$ where y_{10} and y_{20} are the initial values of the angle and velocity of roll motion. One can show that P_2 satisfies the following partial differential equation [1]:

$$\frac{\partial P}{\partial t} = -\frac{\partial}{\partial y_1}(y_2 P) + \frac{\partial}{\partial y_2}(N + F)P + \frac{\Psi_0}{2}\frac{\partial^2 P}{\partial y_2^2} \tag{2.3}$$

where P represents $P_2(y_1, y_2, t \mid y_{10}, y_{20})$. The solution of equation (2.2) subject to the initial condition

$$P(y_1, y_2, t \mid y_{10}, y_{20}) = \delta(y_1 - y_{10})\ \delta(y_2 - y_{20})$$

as $t \to 0$, yields the conditional probability density function which describes the process Y(t) completely.

In order to obtain an equation describing the expected value propagation, we rewrite Equation (2.3) as

$$\frac{d}{dt} P(y_1, y_2, t \mid y_{10}, y_{20})$$
$$= \frac{P(y_1, y_2, t + dt \mid y_{10}, y_{20}) - P(y_1, y_2, t \mid y_{10}, y_{20})}{dt}$$
$$= -\frac{\partial}{\partial y_1}(y_2 P) + \frac{\partial}{\partial y_2}(N + F)P + \frac{\Psi_0}{2}\frac{\partial^2 P}{\partial y_2^2} \tag{2.4}$$

Multiplying equation (2.4) by y_1 and integrating the equation with respect to y_1 and y_2 from $-\infty$ to ∞ gives

$$\frac{1}{dt}\int_{-\infty}^{\infty}\int_{-\infty}^{\infty} y_1 \left[P(y_1, y_2, t + dt \mid y_{10}, y_{20}) - P(y_1, y_2, t \mid y_{10}, y_{20})\right] dy_1 dy_2$$
$$= \frac{\mu_1(t + dt) - \mu_1(t)}{dt} = \dot{\mu}_1 \tag{2.5}$$

$$\int_{-\infty}^{\infty}\int_{-\infty}^{\infty} y_1 \left[-\frac{\partial}{\partial y_1}(y_2 P) + \frac{\partial}{\partial y_2}(N + F)P + \frac{\Psi_0}{2}\frac{\partial^2 P}{\partial y_2^2}\right] dy_1 dy_2$$
$$= \mu_2 - \int_{-\infty}^{\infty} \left(y_1 y_2 P \Big|_{y_1=-\infty}^{y_1=\infty}\right) dy_2 +$$
$$\int_{-\infty}^{\infty} y_1 \left[(N + F)P \Big|_{y_2=-\infty}^{y_2=\infty}\right] dy_1 + \frac{\Psi_0}{2}\int_{-\infty}^{\infty} y_1 \left(\frac{\partial P}{\partial y_2}\Big|_{y_2=-\infty}^{y_2=\infty}\right) dy_1 \tag{2.6}$$

where μ_1 and μ_2 are the expected values of y_1 and y_2 respectively. Assuming the following boundary conditions:

$$y_1 y_2 P \Big|_{y_1=-\infty}^{y_1=\infty} = (N + F)P \Big|_{y_2=-\infty}^{y_2=\infty} = \frac{\partial P}{\partial y_2}\Big|_{y_2=-\infty}^{y_2=\infty} = 0$$

and equating equation (2.5) and (2.6), we obtain

$$\dot{\mu}_1 = \mu_2 \tag{2.7}$$

We then repeat the same process using y_2 and get

$$\dot{\mu}_2 = - < N(y_1, y_2) + D(y_1) >$$

This equation can be expanded in its Taylor series about μ_1 and μ_2. Retaining the first-order terms only gives

$$\begin{aligned}\dot{\mu_2} &= -< N(\mu_1,\mu_2) + D(\mu_1) \\ &\quad + \left[(y_1-\mu_1)\frac{\partial}{\partial y_1} + (y_2-\mu_2)\frac{\partial}{\partial y_2}\right][N(\mu_1,\mu_2) + D(\mu_1)] > \\ &= -N(\mu_1,\mu_2) - D(\mu_1) \end{aligned} \tag{2.8}$$

Substituting equation (2.7) into equation (2.8), we get

$$\ddot{\mu_1} + N(\mu_1,\dot{\mu_1}) + D(\mu_1) = 0 \tag{2.9}$$

From this equation, we can see that the expected value of the random roll motion satisfies a first order approximation to the differential equation of its free roll motion.

Based on this principle, we apply the random decrement technique to the non-linear roll motion of a ship in irregular seas. The random decrement curve is extracted from a time history of roll angle measurements taken when a ship is in a seaway.

2.2 Autocorrelation Function

The autocorrelation function $R_\phi(\tau)$ for random data $\phi(t)$ describes the general dependence of the values of the data at one time, on the values at a later time. An estimate for the autocorrelation between the values of $\phi(t)$ at time t and time $(t+\tau)$ may be obtained by taking the product of the two values and averaging them over the observation time T. Mathematically, the autocorrelation function is represented by

$$R_\phi(\tau) = E[\phi(t)\phi(t+\tau)] = \lim_{T\to\infty}\frac{1}{T}\int_0^T \phi(t)\phi(t+\tau)dt \tag{2.10}$$

For discrete data, the autocorrelation function can be calculated using the formula

$$R_\phi(k) = \frac{1}{n}\sum_{t=1}^{n-k} \phi(t)\phi(t+k) \tag{2.11}$$

where $k = 0, 1, \cdots, K$ and $1 \leq K < n$.

It has been shown by Vandiver [21] that the autocorrelation function of the response of a linear time invariant system excited by a zero mean, stationary, Gaussian random process is linearly related to its random decrement.

For nonlinear systems, the autocorrelation function of the random roll response satisfies an equivalent linear differential equation governing the free roll motion, see Haddara [22].

The elements of the autocorrelation matrix of the process Y(t) are defined by

$$C_{ik}(\tau) = \int\int y_{i0}\, y_k P(Y, \tau \mid Y_0) P_s(Y_0) dY dY_0$$

where $P_s(Y)$ is the steady state probability function and it is independent of t and Y_0.

If we multiply both sides of equation (2.4) by $y_{i0}\, y_k P_s(Y_0)$ and integrate the two sides of the equation from $-\infty$ to ∞, we get the following differential equations describing the elements of the correlation matrix:

$$\begin{aligned}
\dot{C_{11}}(\tau) &= C_{12}(\tau) \\
\dot{C_{21}}(\tau) &= C_{22}(\tau) \\
\dot{C_{12}}(\tau) &= - < y_{10}\,(N + D) > \\
\dot{C_{22}}(\tau) &= - < y_{20}\,(N + D) >
\end{aligned}$$

Using a Gaussian closure technique, the four equations can be combined in one approximate differential equation for the autocorrelation function C_{11} of the roll

angle

$$\ddot{C_{11}} + b_e\dot{C_{11}} + \omega_e^2 C_{11} = 0 \tag{2.12}$$

where b_e and ω_e are the equivalent linear damping and equivalent natural frequency, respectively.

If the damping and restoring moment take the form

$$N(y_1, y_2) = 2\zeta\omega_\phi(y_2 + \epsilon y_2^3)$$

$$D(y_1) = \omega_\phi^2(y_1 + \alpha_1 y_1^3 + \alpha_2 y_1^5)$$

then the equivalent linear damping and natural frequency are given by

$$b_e = 2\zeta\omega_\phi(1 + 3\epsilon\omega_\phi^2\sigma^2)$$

$$\omega_e^2 = \omega_\phi^2(1 + 3\alpha_1\sigma^2 + 15\alpha_2\sigma^4)$$

where σ^2 is the variance of linear rolling motion.

Equation (2.12) shows that the autocorrelation function of a nonlinear, time invariant, system excited by a zero mean, stationary, Gaussian, white noise random process satisfies the differential equation describing the free motion of an equivalent linear system.

2.3 Power Spectral Density

The spectral analysis of time series data is very important since it provides important information such as resonant frequency and damping ratio. The resonant frequency, also called predominant frequency (PF) or modal frequency f_m, can be found as the peak frequency of the spectral density. The damping ratio of a linear system undergoing random excitation can be obtained from the spectral density

using the half power bandwidth. This method introduced into ship motion studies by St. Denis and Pierson [23] are used successfully for the study of other motions such as pitch and heave. However, it is inappropriate for roll motion because of the nonlinear nature of ship rolling.

A power spectral density (PSD) describes the distribution of energy as a function of frequency. The power in an infinitesimal frequency interval divided by the width of that interval yields the density.

Spectral density functions can be computed in three ways: the Fast Fourier Transform Method, the Correlation Function (Blackman-Tukey) Method and the Bandpass Filter Method. Different methods are based on three different computational definitions of PSD and all of them are asymptotically equivalent. In this study, we will use the Fast Fourier Transform Method for spectral analysis.

The spectral density function $S_\phi(f)$ defined in the frequency domain can be evaluated from a random process $\phi(t)$ defined in the time domain by applying the Fourier transform as follow:

$$S_\phi(f) = \frac{1}{N}\sum_{n=1}^{N}\frac{2}{T}\left|\int_0^T \phi(t)e^{-i2\pi ft}dt\right|^2$$

The computer program for this method uses MATLAB subroutines to get the spectral density of discrete roll data. A frequency vector is created with the Nyquist frequency defined as

$$F = \frac{1}{2\Delta t}$$

where Δt is the time interval of two measurements being taken.

The area under the spectral density function is equal to the average energy of

a random process with respect to time. That is

$$\overline{P}_{\phi} = \int_0^{\infty} S_{\phi}(f)df$$

In a situation when the power spectral density is uniform over infinite range of frequency, the signal is called white noise.

2.4 The Proposed Method for Parameter Estimation

As shown in the previous sections, the random decrement and autocorrelation function can be used to describe approximately the equation of free roll motion given by

$$\ddot{\phi} + N(\phi, \dot{\phi}) + D(\phi) = 0 \tag{2.13}$$

The nonlinear roll damping moment $N(\phi, \dot{\phi})$ is commonly expressed in one of the following two forms:

1) Linear + quadratic form: $N(\phi, \dot{\phi}) = b_1\dot{\phi} + b_2\dot{\phi}|\dot{\phi}|$

2) Linear + cubic form: $N(\phi, \dot{\phi}) = b_1\dot{\phi} + b_3\dot{\phi}^3$

The restoring moment $D(\phi)$ in Equation (2.13), following Bass and Haddara [10], can be expressed as

$$D(\phi) = \omega_{\phi}^2(\phi + \alpha_1\phi^3 + \alpha_2\phi^5) \tag{2.14}$$

where ω_{ϕ} is the natural frequency and α_1 and α_2 are the nonlinear restoring coefficients.

The righting lever arm GZ describes the statical stability of a ship. It varies with the heel angle of the ship and its center of gravity. For a specified center of

$$\dot{\psi} = \omega_e(R) = \omega_\phi + \dot{\theta}$$

The linearized parameters b_e and ω_e are defined by the following functions

$$b_e = \frac{\epsilon}{\pi R\omega_\phi}\int_0^{2\pi} f(R\cos\psi, -R\omega_\phi \sin\psi)\sin\psi d\psi \tag{2.18}$$

$$\omega_e^2 = \omega_\phi^2 - \frac{\epsilon}{\pi R}\int_0^{2\pi} f(R\cos\psi, -R\omega_\phi \sin\psi)\cos\psi d\psi \tag{2.19}$$

For systems with linear plus quadratic form of damping, the term $\epsilon f(\phi, \dot{\phi})$ in equation (2.16) becomes

$$\epsilon f(\phi, \dot{\phi}) = -(b_1\dot{\phi} + b_2\dot{\phi}|\dot{\phi}| + \alpha_1\omega_\phi^2\phi^3 + \alpha_2\omega_\phi^2\phi^5) \tag{2.20}$$

Substituting this equation into equation (2.18) and (2.19) respectively and using

$$\phi = R\cos\psi, \quad \dot{\phi} = -R\omega_\phi \sin\psi$$

we obtain

$$b_e = b_1 + \frac{8R\omega_\phi}{3\pi}b_2 \tag{2.21}$$

$$\omega_e^2 = \omega_\phi^2\left(1 + \frac{3}{4}\alpha_1 R^2 + \frac{5}{8}\alpha_2 R^4\right)$$

For systems with linear plus cubic form of damping, the expression for $\epsilon f(\phi, \dot{\phi})$ becomes

$$\epsilon f(\phi, \dot{\phi}) = -(b_1\dot{\phi} + b_3\dot{\phi}^3 + \alpha_1\omega_\phi^2\phi^3 + \alpha_2\omega_\phi^2\phi^5)$$

Repeating the same process as above, we get

$$b_e = b_1 + \frac{3}{4}R^2\omega_\phi^2 b_3 \tag{2.22}$$

$$\omega_e^2 = \omega_\phi^2\left(1 + \frac{3}{4}\alpha_1 R^2 + \frac{5}{8}\alpha_2 R^4\right) \tag{2.23}$$

It can be seen that systems with the same form of restoring moment but different forms of damping moment have the same expression for the natural frequency.

gravity, the GZ curve can be approximated by

$$GZ(\phi) = GM(\phi + \alpha_1\phi^3 + \alpha_2\phi^5) \tag{2.15}$$

where GM is the transverse metacentric height. It denotes the distance from the center of gravity to the metacenter, positive upward. The value of GM is determined from an inclining test.

To determine the values of α_1 and α_2, Equation (2.15) is fitted by a least-squares technique.

To evaluate the natural frequency and the damping parameters, the method of equivalent linearization given by Krylov and Bogoliubov [24] is applied here. This technique assumes that a given nonlinear differential equation can be replaced by an equivalent linear differential equation with the property that the solution of the two equations can be made to differ from each other by an error of the order ϵ^2.

The nonlinear differential equation (2.13) can be rewritten as the form

$$\ddot{\phi} + \omega_\phi^2\phi = \epsilon f(\phi, \dot{\phi}) \tag{2.16}$$

Its equivalent linear equation is given by

$$\ddot{\phi} + b_e\dot{\phi} + \omega_e^2\phi = 0 \tag{2.17}$$

If one follows the theory of the first approximation, one starts with a solution of the form

$$\phi = R\cos\psi = R\cos(\omega_\phi t + \theta)$$

where R and ψ are given by the differential equation of the first approximation:

$$\dot{R} = \frac{\epsilon}{2\pi\omega_\phi}\int_0^{2\pi} f(R\cos\psi, -R\omega_\phi\sin\psi)\sin\psi d\psi$$

Still, equation (2.23) cannot be used directly to predict the natural frequency from the measured frequency which is available from a decay curve. We know that the measured frequency is equal to the damped natural frequency ω_d, while the relationship between the damped natural frequency and the equivalent natural frequency can be found from the equivalent linear equation (2.17). That is

$$\omega_d = \sqrt{\omega_e^2 - b_e^2/4} \tag{2.24}$$

By combining equation (2.23) and (2.24), a new formula for predicting the natural frequency of a nonlinear system from its decay curve is developed. It is expressed as

$$\omega_\phi = \sqrt{\frac{\omega_d^2 + b_e^2/4}{1 + \frac{3}{4}\alpha_1 R^2 + \frac{5}{8}\alpha_2 R^4}} \tag{2.25}$$

The equivalent damping coefficient b_e can be calculated from a decay curve using the formula

$$b_e = \frac{4}{T} \ln\left(\frac{\phi_k}{\phi_{k+1}}\right)$$

where T is the period of a cycle. ϕ_k and ϕ_{k+1} are two sequent peak amplitudes.

b_e and R vary from cycle to cycle in a decay curve. Using the mean values of b_e and R in equation (2.25), we have

$$\omega_\phi = \sqrt{\frac{\omega_d^2 + \overline{b}_e^2/4}{1 + \frac{3}{4}\alpha_1 \overline{R}^2 + \frac{5}{8}\alpha_2 \overline{R}^4}} \tag{2.26}$$

This formula provides a practical tool for predicting tne natural frequency of a nonlinear system using the information available from a decay curve.

The nonlinear damping coefficients are determined using a least squares method to fit Equation (2.21) or (2.22) in which roll angle amplitude R takes the average

of two sequent peak amplitudes. That is

$$R = \frac{\phi_k + \phi_{k+1}}{2}$$

The method described above is suitable for roll motion with nonlinear damping and nonlinear restoring moments. The results show that this method provides considerably accurate estimation for both the natural frequency and the damping coefficients.

Chapter 3

Numerical Simulation

The use of numerical simulation gives a controlled test for the validity of the Random Decrement Method used for nonlinear roll motion and the accuracy of the proposed method for parameter estimation from free roll decay curve. It allows a direct comparison between the estimated parameters and their true values which were used in the simulation. Another advantage is that the sample length can be increased progressively to test for optimum sample length.

3.1 Estimation from Free Roll Decay

For validation purposes, the proposed method for parameter estimation from free roll decay is first applied to some simulated free roll decay data, where the values of the parameters are known. The following nonlinear roll equation was used to generate the free roll decay data

$$\ddot{\phi} + b_1\dot{\phi} + b_3\dot{\phi}^3 + \omega_\phi^2(\phi + \alpha_1\phi^3 + \alpha_2\phi^5) = 0 \tag{3.1}$$

To obtain the numerical solution of the nonlinear differential Equation (3.1), we express the equation as a set of first order differential equations. A numerical solution of these equations is then obtained using a fourth order Runge Kutta

Table 3.1: True and Estimated Parameters in Free Decay Equation

Case	Comparison		b_1	b_3	ω_ϕ	α_1	α_2
1	Known Values		0.0800	0.2563	3.4468	0.1480	-1.5676
	Estimated Values	dt=0.05 sec	0.0803	0.2576	3.4503	0.1480	-1.5676
		dt=0.01 sec	0.0801	0.2560	3.4469	0.1480	-1.5676
2	Known Values		0.0750	0.3187	3.3684	0.1723	-1.6896
	Estimated Values	dt=0.05 sec	0.0748	0.3209	3.3672	0.1723	-1.6896
		dt=0.01 sec	0.0749	0.3193	3.3672	0.1723	-1.6896
3	Known Values		0.0797	0.3443	3.1762	0.2024	-1.8402
	Estimated Values	dt=0.05 sec	0.0793	0.3474	3.1760	0.2024	-1.8402
		dt=0.01 sec	0.0796	0.3445	3.1760	0.2024	-1.8402
4	Known Values		0.0826	0.3540	3.0068	0.2580	-2.1184
	Estimated Values	dt=0.05 sec	0.0825	0.3564	3.0091	0.2580	-2.1184
		dt=0.01 sec	0.0825	0.3544	3.0062	0.2580	-2.1184
5	Known Values		0.0767	0.4062	2.7679	0.3258	-2.4581
	Estimated Values	dt=0.05 sec	0.0766	0.4087	2.7697	0.3258	-2.4581
		dt=0.01 sec	0.0767	0.4061	2.7670	0.3258	-2.4581
sample duration 20 seconds							

routine. Its algorithm uses a fixed step size for convenience in processing the discrete data. The generated free roll decay records were then used to evaluate the rolling parameters. To predict the natural frequency and the damping coefficients, a computer program was written based on equations (2.26) and (2.22).

Five cases were considered and different time intervals were used for the integration of the free roll equation. The true values and the predicted values of the parameters are given in Table 3.1. It is seen that very accurate parameter estimates are obtained for all of the cases. It is also noted that the time interval of 0.01 second gives more accurate results than that of 0.05 second. However, results obtained using an interval of 0.05 seconds are still very good. We can expect that an even more accurate estimation could be obtained if one uses a shorter

time interval. Thus, it may be concluded that the proposed method achieves high accuracy in estimating the parameters when applied to simulated free roll decay data.

3.2 Simulation of Roll in Random Waves

To generate random roll data, we used the following differential equation describing the nonlinear roll motion in random waves.

$$\ddot{\phi} + 2\zeta\omega_\phi(\dot{\phi} + \epsilon\dot{\phi}^3) + \omega_\phi^2(\phi + \alpha_1\phi^3 + \alpha_2\phi^5) = \sum_{k=0}^{n} A\sin(\omega_k t + \theta_k) \qquad (3.2)$$

ζ and ϵ are the nondimensional linear and nonlinear damping coefficients, respectively. The random wave excitation is simulated by superposing a large number of sinusoidal functions with the same amplitude A, varying frequencies ω_k and random phase angles θ_k. The expressions for ω_k and θ_k are

$$\begin{aligned} \omega_k &= \omega_b + \frac{k}{n}(\omega_f - \omega_b) \qquad & k = 0, 1, \cdots, n \\ \theta_k &= 2\pi r & 0 \le r \le 1 \end{aligned}$$

ω_k varies between frequency limits ω_b and ω_f which define a band-limited white noise. r is an uniform random number chosen such that the phase angle varies between 0 and 2π. The wave exciting moment used in Equation (3.2) is composed based on the method given by Borogman [25] to ensure that the excitation is a broad band random process.

The rolling motion of a 1.5 meter model was simulated using the parameters shown in Table 3.2 for the five cases considered. The excitation moment used in the simulation was composed of 70 sinusoidal components with the same amplitude of 0.07 per sec^2 and varied frequencies. The limits of the frequency band, ω_b and

Table 3.2: Parameters Used in the Simulation

Case	GM (cm)	ω_ϕ	ζ	ϵ	α_1	α_2
1	5.29	3.4468	0.0116	3.204	0.1480	-1.5676
2	4.91	3.3684	0.0111	4.249	0.1723	-1.6896
3	4.51	3.1762	0.0126	4.320	0.2024	-1.8402
4	3.92	3.0068	0.0137	4.286	0.2580	-2.1184
5	3.38	2.7679	0.0139	5.296	0.3258	-2.4581

ω_f took the values of 2.0 and 5.0 rad/sec, respectively. The time interval for the integration was chosen to be 0.05 second and the sample length was 1200 seconds for each record.

Five random roll records were generated using a fourth order Runge-Kutta routine to get the numerical solution of equation (3.2).

3.3 Estimation from Random Roll Response

3.3.1 Random Decrement and Autocorrelation Curves

To extract the random decrement from random roll data, a computer program is written based on the method described in chapter 2. This program involves three steps: 1) using interpolation to find the start time t_i of each segment corresponding to a selected angle ϕ_s; 2) picking up the segments from each start time to a time length τ_{max} and using cubic spline interpolation to get uniform time interval; 3)

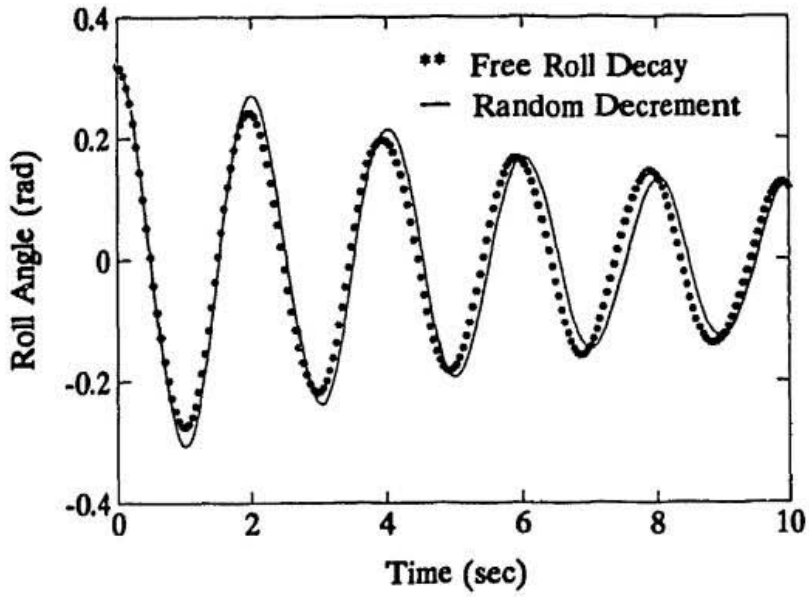

Figure 3.1: Comparison of Random Decrement and Free Decay

taking the ensemble average of these segments.

The initial roll angle of the random decrement has been chosen to be equal to the significant amplitude of roll response so that a reasonable number of segments is taken. For the five random decrement curves, the initial angles ranged from 0.32 to 0.35 radian and the numbers of segments ranged from 80 to 192.

The autocorrelation function was calculated from the whole record of roll angle using a program based on equation (2.11). For comparison, the free decay curves were generated by the numerical integration of equation (3.2) with the excitation term set to zero.

The three decay curves: random decrement, autocorrelation and free roll decay are compared in Figure 3.1 and Figure 3.2. It is seen that the random decrement and the autocorrelation function resemble to a large extent the free roll decay

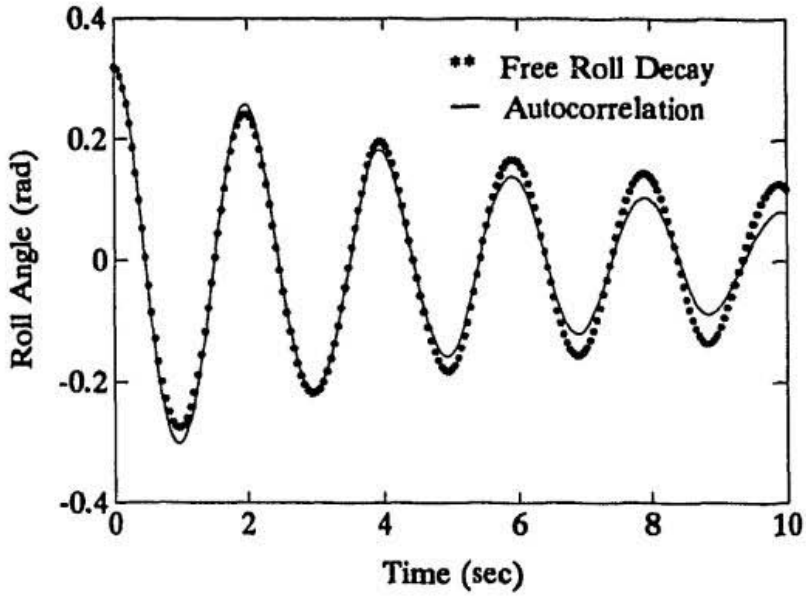

Figure 3.2: Comparison of Autocorrelation and Free Decay

curve. The results have been shown for one case only because the results for the other cases are very much similar.

3.3.2 Prediction of Natural Frequency

As was explained previously, the natural frequency can be predicted by one of three methods: the random decrement, the autocorrelation function and the power spectral density. All of them were calculated from the stationary random response of the roll equation. The values for the natural frequency predicted by each of the above mentioned methods are given in Table 3.3, together with the exact value used for the generation of the random roll response. The results were obtained from the random decrement and the autocorrelation function curves of 20 seconds long.

It is clear that the values of the natural frequency obtained using the autocor-

Table 3.3: Natural Frequencies Predicted by Three Methods

Case	GM (cm)	Given Values ω_ϕ (r/s)	Random Decrement ω_ϕ (r/s)	Auto-Correlation ω_ϕ (r/s)	Spectral Density ω_ϕ (r/s)
1	5.29	3.4468	3.4252	3.4639	3.4975
2	4.91	3.3684	3.3816	3.3231	3.3748
3	4.51	3.1762	3.1785	3.1500	3.1907
4	3.92	3.0068	2.9692	3.0125	3.0680
5	3.38	2.7679	2.7335	2.7726	2.8225

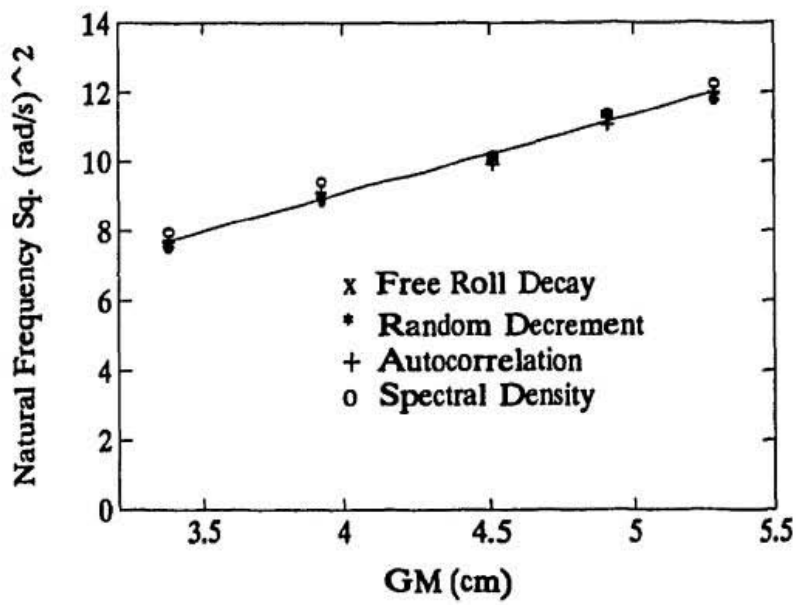

Figure 3.3: Predicted Values for the Natural frequency

Table 3.4: Goodness Fit of ω_ϕ^2 Versus GM

Parameter	Free Decay	Random Decrement	Auto-Correlation	Spectral Density
m	2.2334	2.3264	2.1867	2.1707
R^2	0.9919	0.9855	0.9899	0.9871

relation function or the random decrement are both very good estimates for the actual natural frequency used in simulation. The square of the natural frequency versus the metacentric height is shown in figure 3.3.

It can be seen from the plot that their relationship is best represented by a linear equation in the form

$$\omega_\phi^2 = m\overline{GM}$$

where m is a constant. To compare the goodness of the fit of the least squares line to the fitted data, we use the square of correlation coefficient R^2 as a measure, R^2 is defined as

$$R^2 = \frac{[\ Cov\ (GM, \omega_\phi^2)\ ]^2}{Var(GM)\ Var(\omega_\phi^2)} \tag{3.3}$$

where Var and Cov represent variance and covariance, respectively. The nearer the value of R^2 to one the better the fit. The values of m and R^2 obtained using the four methods are given in table 3.4.

The results of linear regression show that the square of the natural frequency obtained using the random decrement, autocorrelation function or spectral density

Table 3.5: Known and Estimated Parameters Using Random Decrement

Case	Comparison	ω_ϕ	ζ	ϵ	α_1	α_2
1	Known Values	3.4468	0.0116	3.2040	0.1480	-1.5676
	Estimated Values	3.4252	0.0148	3.3295	0.1480	-1.5676
2	Known Values	3.3684	0.0111	4.2490	0.1723	-1.6896
	Estimated Values	3.3816	0.0125	5.7447	0.1723	-1.6896

function is linearly related to the metacentric height of the model. Thus, the estimated natural frequency by one of these techniques can be used to predict the instantaneous value of the metacentric height of a ship at sea where a free roll test cannot be obtained.

3.3.3 Damping Identification

Since the random decrement or the autocorrelation function is a first order approximation of free roll decay for nonlinear systems, we use the same estimation method as previously used for free roll decay to identify damping parameters from the resulting curves. The damping coefficients estimated from the random decrement curves are shown in table 3.5 for the first two cases given in Table 3.3.

It has been difficult to determine unique values for the damping parameters in the other three cases. The reason being that there is usually a trade off between the two unknown damping parameters. This is a problem that has been observed

in all methods which uses the least squares technique for estimating the linear and nonlinear damping coefficients, see Haddara and Wu [26].

Figures 3.4 and 3.5 show the comparison between the true free decay curves and the estimated decay curves which were generated using the parameters predicted by the random decrement and the autocorrelation function techniques. The first four cases in Table 3.2 are shown here.

It is seen that the damping parameters estimated from the random decrement and the autocorrelation function produce free decay curves which compare well with the actual free decay curve.

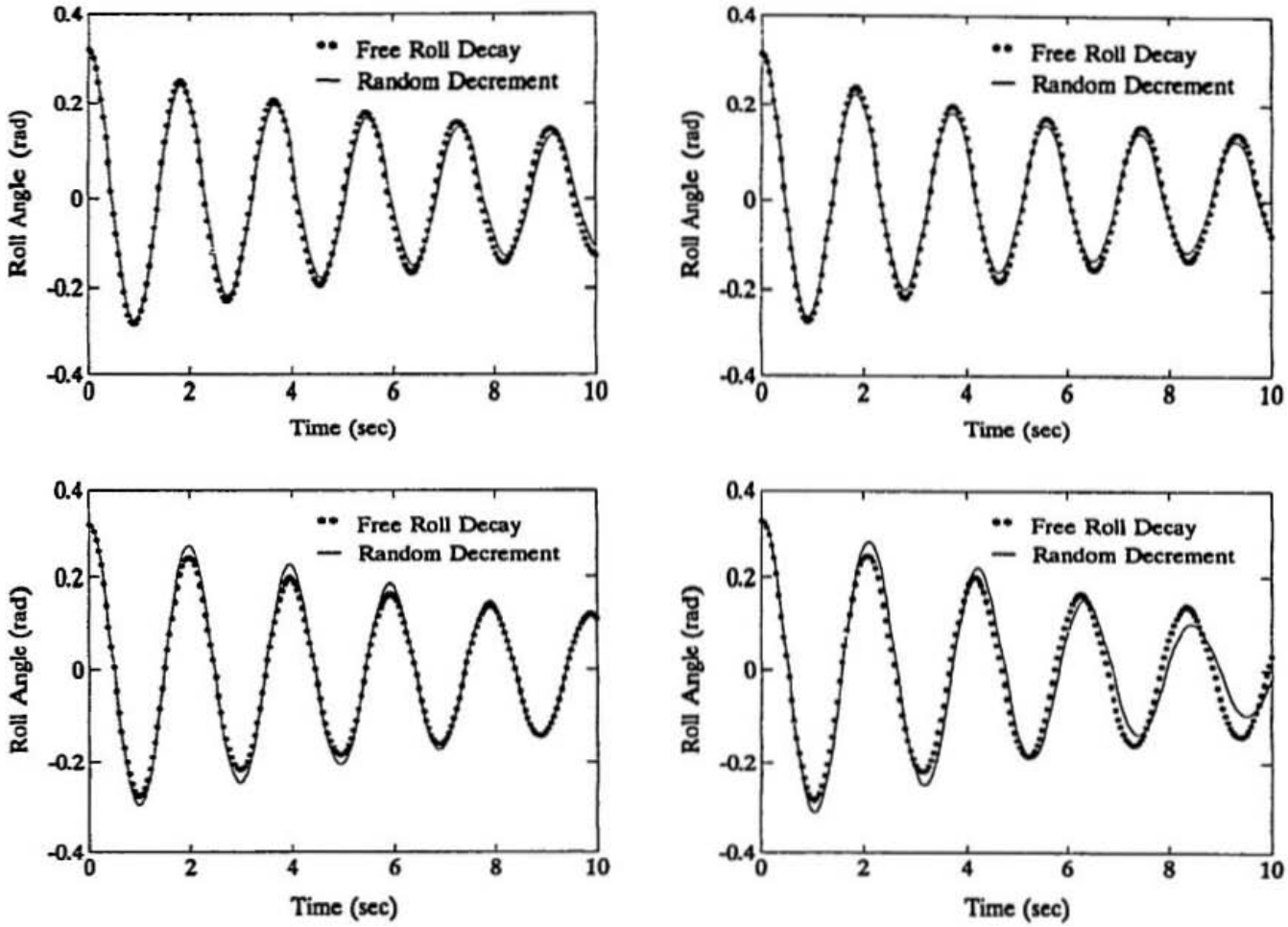

Figure 3.4: Free Decay and the Estimate of Random Decrement

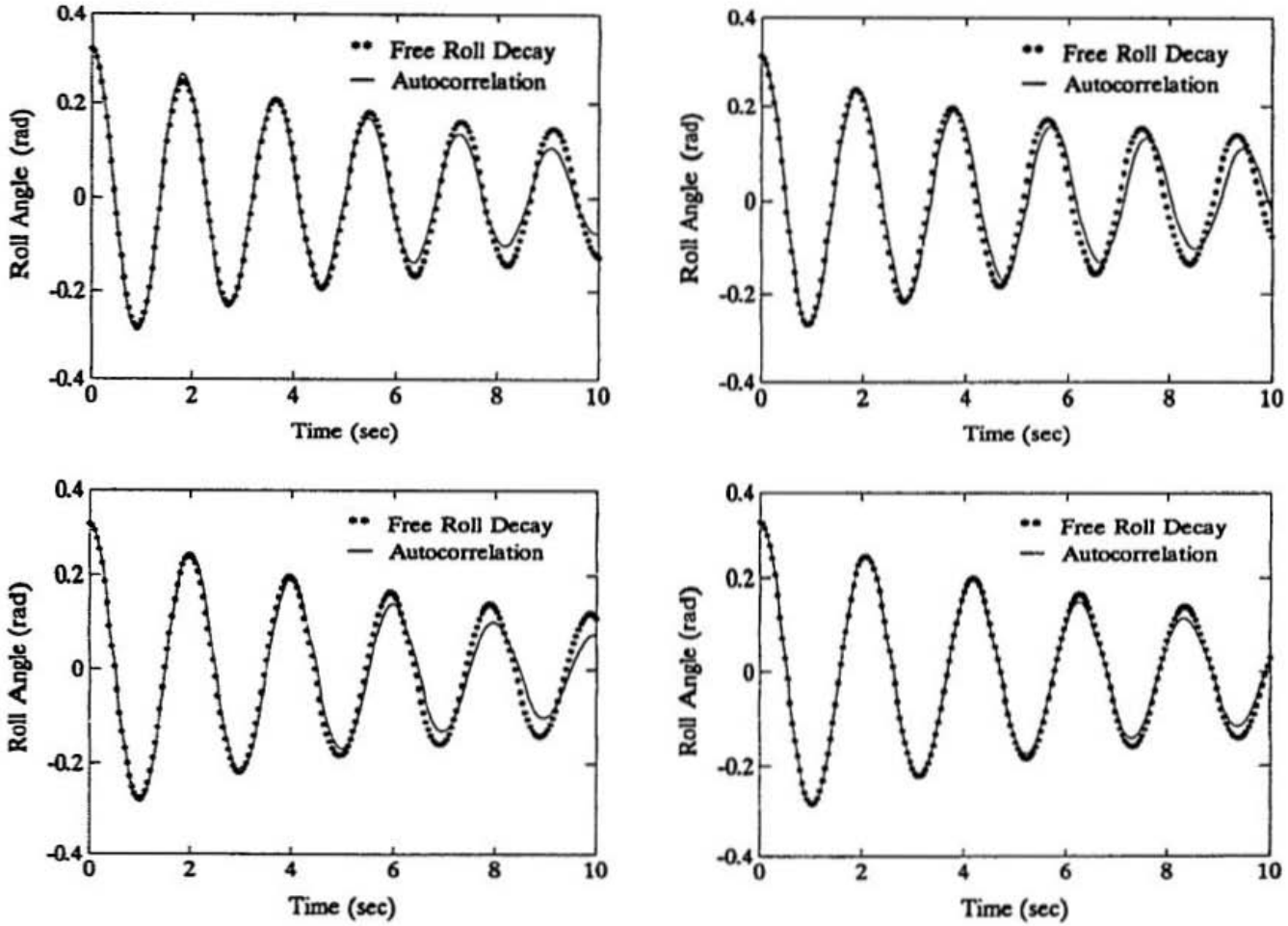

Figure 3.5: Free Decay and the Estimate of Autocorrelation

Chapter 4

Experimental Study

Although in the last chapter, we already verified the validity and accuracy of the random decrement method and the proposed estimation method for simulated data, the use of real roll data is of ultimate importance in demonstrating the value of the methods because real data reflect the physical response of a system to true environment. Unlike simulated data which are obtained from an assumed equation, real data are always corrupted to some extent by random "noise" which arises from methods of measurement. Model experiments in a wave tank can simulate to a certain extent real ships at sea, and also allow the methods to be tested in a realistic but controlled environment. Furthermore, model experiments enable us to assess the reliability of the method for different models under various loading conditions and various wave excitations.

4.1 Experiments

The rolling experiments were performed on three fishing vessel models in the towing tank of Memorial University of Newfoundland. The inside dimensions of the tank are 58.27 m in length, 4.57 m in width, and 3.04 m in depth, as shown in figure

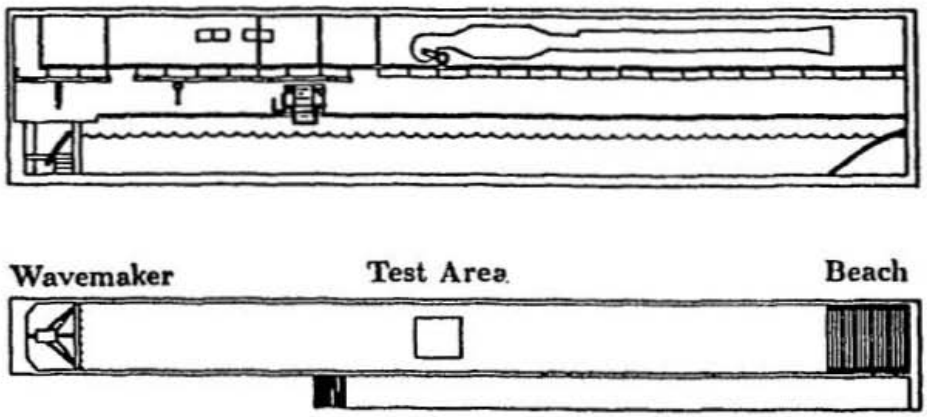

Figure 4.1: Towing Tank Layout

4.1. The hydraulically operated, piston-type wave generator is installed behind the waveboard at one end of the tank and a wave absorbing beach is located at the other end of the tank to reduce the reflected and standing waves. Both regular and irregular waves, in a frequency range between 0.3 and 1.3 Hz, can be generated through the translatory motion of the waveboard driven by a hydraulic actuator. The actuator is controlled by a MTS closed-loop, servo-controlled system.

Since no forward speed is involved in the experiment, the model was positioned across the tank at the test area shown in Figure 4.1. The waves generated by the wavemaker at one end of the tank approached the model from its side with an encounter angle of 90 degree, namely a beam sea.

4.1.1 The Models

Three fishing vessel models: M363, M365, M366 were used in the model experiment. They belong to the 'less-than 25 metre' class and have similar dimensions but varying hull forms. M363 has long hard chine, deep skeg, significant vertical

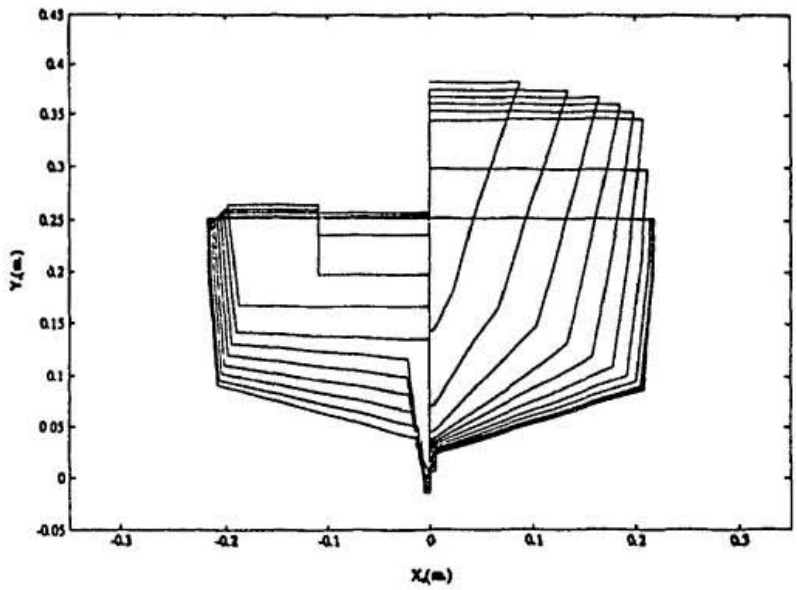

Figure 4.2: Body Plan of M363

prismatic coefficient and low rise of floor. M365 has a much higher center of gravity, also a higher transverse metacenter. M366 has a rounded hull form and the smallest Midship Section Coefficient C_m . The body plans of the three models are shown in Figures 4.2 - 4.4 and their particulars are given in table 4.1

Before the experiments, the models were prepared to meet the requirements specified in the hydrostatic particulars list provided by the model builder, Institute for Marine Dynamics, National Research Council of Canada. This work involves balasting the model until the required waterline is reached and then arranging the weights in the model to adjust the center of gravity and the radius of gyration. After being ballasted and trimmed in the above way, each model has the proper draft, center of gravity and roll natural frequency.

In the procedure of adjusting the mass distribution in the model, the center

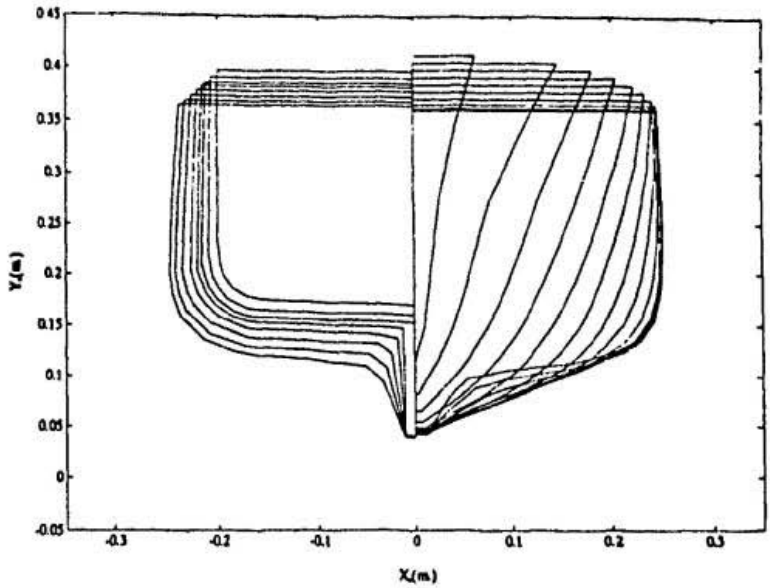

Figure 4.3: Body Plan of M365

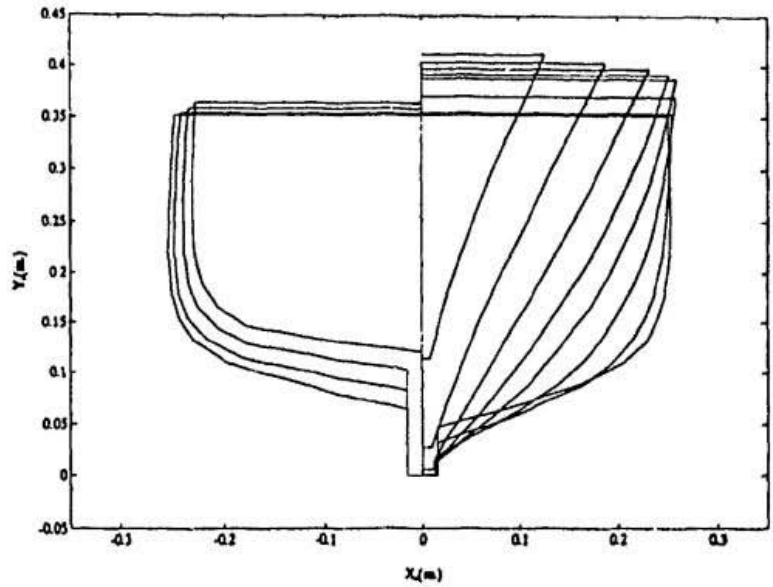

Figure 4.4: Body Plan of M366

Table 4.1: Particulars of Three Models

Model	M363	M365	M366
Scale	1:12	1:9.1	1:6.8
LWL (m)	1.551	1.336	1.568
Beam (m)	0.507	0.542	0.506
Draft (m)	0.221	0.215	0.205
LCB (m)	-0.109	-0.052	-0.1375
Mass (kg)	80	55	69.5
GM (m) at OG=0	0.031	0.0326	0.0451
ω (r/s) at OG=0	2.7362	3.2693	3.1762
α_1 at OG=0	1.2832	-0.3851	0.2024
α_2 at OG=0	-1.3293	-2.5141	-1.8402

of gravity and the roll natural frequency need to be checked repeatedly. The roll natural frequency of the model can be roughly estimated by conducting a free roll test and recording the time required by the model to perform a specific number of roll cycles. The vertical position of the center of gravity is usually estimated from an inclining test.

4.1.2 Test Setup

Two different techniques are usually used for measuring roll motion. The first uses a dynamometer and the second uses a gyroscope. Both of them were used in the experiments. The experiment on Model M363 was conducted a couple of months earlier than the experiments on the other two models.

For model M363, a dynamometer was attached to the model to measure the roll angle. The dynamometer is composed of a linear bearing, a pivot and an angular induction transducer. As shown in figure 4.5, the model was attached to the pivot through a platform with adjustable height. The pivot was connected to a rod which goes through the linear bearing. This set up prevents the model from motions other than rolling and heaving. By adjusting the height of the platform, the rolling centre and the gravity centre of the model were both changed to achieve the variation of transverse metacentric height GM.

A wave probe was set up at a location 2.25 meters away from the model in the direction towards the wavemaker to monitor the time history of the wave height. The signals from the dynamometer and the wave probe were sent through a filter and stored on a microcomputer. The microcomputer was connected to a data acquisition unit: a two channel digital signal analyzer. The roll response and the wave height could be observed during a test.

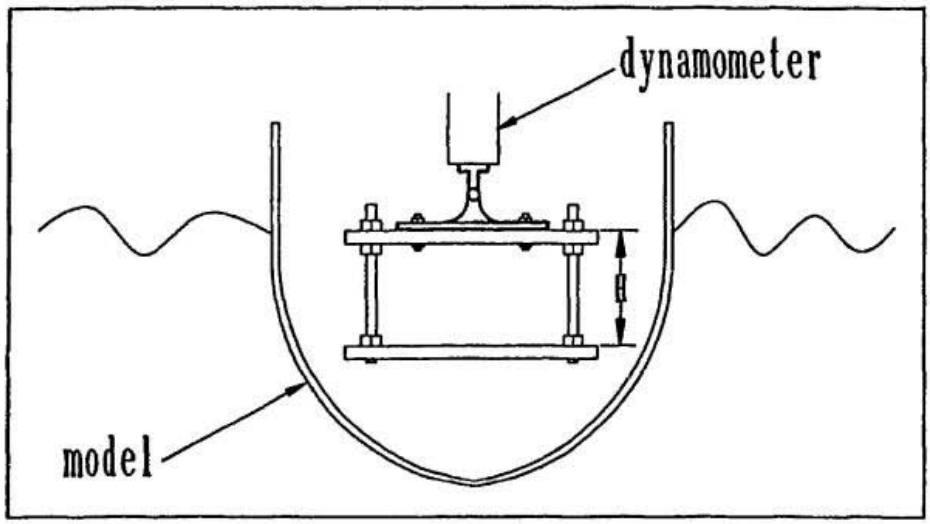

Figure 4.5: Test Setup for M363

For models M365 and M366, a gyroscope was installed on the model to measure the roll angle. Figures 4.6 and 4.7 are the photographs of the test arrangement. A portable computer was used to download data acquisition programs to the data logger. The signal of roll motion from the gyroscope was input to the data logger through a cable. The signal from the wave probe was also sent to the data logger. The sample rate was set by a frequency counter. All instruments used here are portable so that they can be used later in the real ship tests.

The model was tethered from its bow and stern by two strings running through a pair of pulleys. The line joining the two tethering points in the bow and stern passes through the center of gravity of the model. The pulleys were fixed at the end of two angle steel bars attached firmly to the opposite sides of the carriage. Two small weights were fastened at the end of the two strings, which provided the model with small adjustments for flexibility. The sway and roll modes are

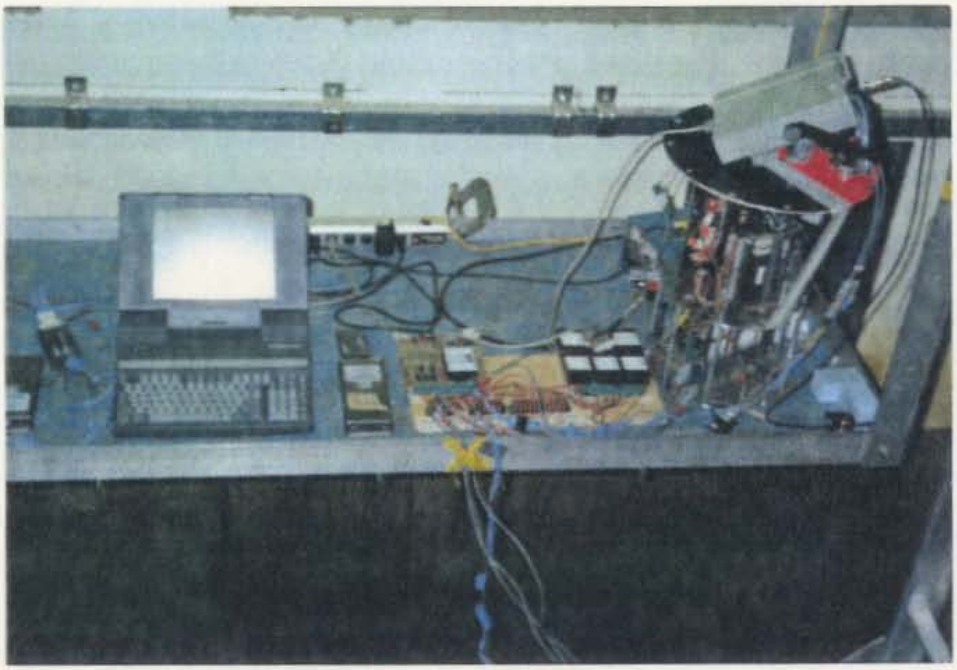

Figure 4.6: Instruments for M365 and M366

Figure 4.7: Test Setup for M365 and M366

normally coupled but this coupling was found to be weak and negligible. The center of gravity of the model was changed by moving a set of weights vertically in the model. Thus the different GM values were obtained.

Random wave generation consists of five steps: 1) definition of the target wave spectrum. 2) synthesis of a random target wave train with an energy distribution defined by the target spectrum 3) calculation of the control signal for the wave machine. 4) generation and measurement of the waves in the towing tank. 5) spectral analysis of the measured wave train and comparison with the desired target spectrum.

The unidirectional JONSWAP sea-spectrum was used for random rolling experiments as it is a reasonable representation of a North Atlantic wave energy distribution. This spectrum, expressed as a function of frequency, is given by

$$S(f) = \frac{A}{f^5}\exp(-B/f^4)\gamma^a$$

where

$$A = \frac{5}{16}\frac{H_s^2 f_m^4}{\gamma^{\frac{1}{3}}}, \qquad B = \frac{5}{4}f_m^4, \qquad a = \exp\left[-\frac{(f-f_m)^2}{2\sigma^2 f_m^2}\right]$$

The JONSWAP spectrum depends on four parameters. They are significant wave height H_s, wave modal frequency f_m, peak enhancement factor γ and shape parameter σ. The following values proposed by Ewing [27] were used in the experiments:

$$\gamma = 3.3$$
$$\sigma = 0.07 \quad \text{for} \quad f \leq f_m$$
$$\sigma = 0.09 \quad \text{for} \quad f > f_m$$

Wave modal frequency f_m or wave predominant frequency (PF) is the peak

frequency of a wave spectrum. The significant wave height is the average of the one-third highest waves, which is defined as $H_s = 4\sqrt{m_o}$ where m_o is the area under the wave spectrum.

4.1.3 Roll Tests in Random Beam Waves

The rolling tests were performed for each model at a series of GM values. During the experiment, the mass of each model remained constant but the centre of gravity changed vertically to give a series of different GM values. For each model at each GM value, the experiment included three parts: inclining test, free roll tests and roll tests in random beam waves.

The purpose of the inclining test is to check the value of the transverse metacentric height GM for each loading condition. To avoid error from measurements, the small weight was moved transversely through five positions on the model and 9 measurements were taken for each case. Tables A.1 to A.3 in Appendix A give the inclining test data for the three models in each case. The ratio of the highest GM value to the lowest GM value for M363, M365 and M366 was 1.52, 1.8 and 1.57, respectively.

In order to compare the results from the random decrement and the autocorrelation function curves with those from the free roll decay curve, a set of free roll tests were carried out at each GM value for each model. In each set of free roll tests, the model was heeled respectively to port and starboard at 5 different initial angles ranging from 5 to 15 degrees. For M363, the measurements were taken at a rate of 20 points per second and the test duration was 25 seconds. For M365 and M366, the sampling rate was 21.3 points per second and the duration of the sample was also 25 seconds.

Following the inclining tests and the free roll tests, the roll tests in random beam waves were performed with the model at the same loading condition. The wave modal frequency was chosen to be close to the roll natural frequency of the model. To see the effect of different wave height on the random decrement, the model in each loading condition was subjected to two wave spectra with the same modal frequency but different significant wave heights. The effect of varying the wave modal frequency on the random decrement was also studied. In one loading condition, Model M365 and M366 each was subjected to the wave excitations generated respectively from three wave spectra which had the same significant wave height but different wave modal frequencies. The three wave modal frequencies were so chosen such that one of them is near the model natural frequency, the other is higher and the third is lower than the model natural frequency. Every random roll test was recorded twice in the same loading condition and the same wave excitation for investigating the reliability of the results provided by the random decrement method.

The sample rate of the random roll tests was kept the same as free roll tests, while the sample duration of each record lasts for 400 seconds in order to meet stationarity requirements and provide enough data.

4.2 Results and Discussion

This section will focus on: 1) the validation of the proposed estimation method using experimental roll data; 2) the feasibility of the random decrement method for different nonlinear systems; 3) the reliability of the results obtained from the roll response to different wave excitations.

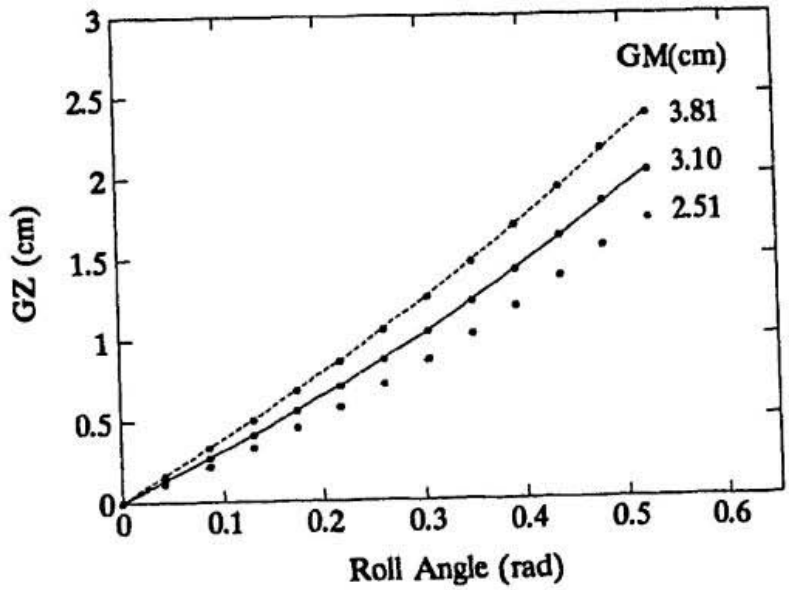

Figure 4.8: GZ Curves of M363

4.2.1 Analysis of Free Roll Data

To determine the roll parameters from free roll response, the estimation method used in the previous chapter is applied here. As explained in chapter 2, the non-linear restoring coefficients for a specified center of gravity can be obtained from GZ curve fit by a least-squares technique. Figures 4.8 to 4.10 show the GZ curves of each model for different GM values.

It is seen that equation 2.14 provides very good estimate for the restoring moment for the three models. From the regressions of GZ curves, the nonlinear restoring coefficients α_1 and α_2 were evaluated as shown in Table 4.2.

The values of the natural frequency and damping parameters given in Table 4.2 were estimated using the same computer program used previously in the analysis of simulated data. It is seen in Table 4.2 that M363 has the highest linear and

Table 4.2: Parameters Estimated from Free Roll Decay

Model	GM(cm)	b_1	b_3	ω_ϕ	α_1	α_2
M363	3.81	0.0648	0.4433	2.8051	1.0130	-1.0800
	3.10	0.1572	2.0321	2.7362	1.2832	-1.3293
	2.51	0.2239	7.2033	2.2068	1.6240	-1.6437
M365	4.31	0.1113	0.7052	3.6126	-0.3319	-1.8996
	3.61	0.0941	0.8368	3.4100	-0.3640	-2.2695
	3.26	0.0951	0.8352	3.2693	-0.3851	-2.5141
	2.75	0.1070	0.8357	3.0178	-0.4257	-2.9818
	2.39	0.1067	0.9946	2.7675	-0.4647	-3.4322
M366	5.29	0.0819	0.2957	3.4466	0.1480	-1.5676
	4.91	0.0780	0.3048	3.3595	0.1723	-1.6896
	4.51	0.0797	0.3443	3.1762	0.2024	-1.8402
	3.92	0.0826	0.3540	3.0068	0.2580	-2.1184
	3.38	0.0811	0.3988	2.7673	0.3258	-2.4581

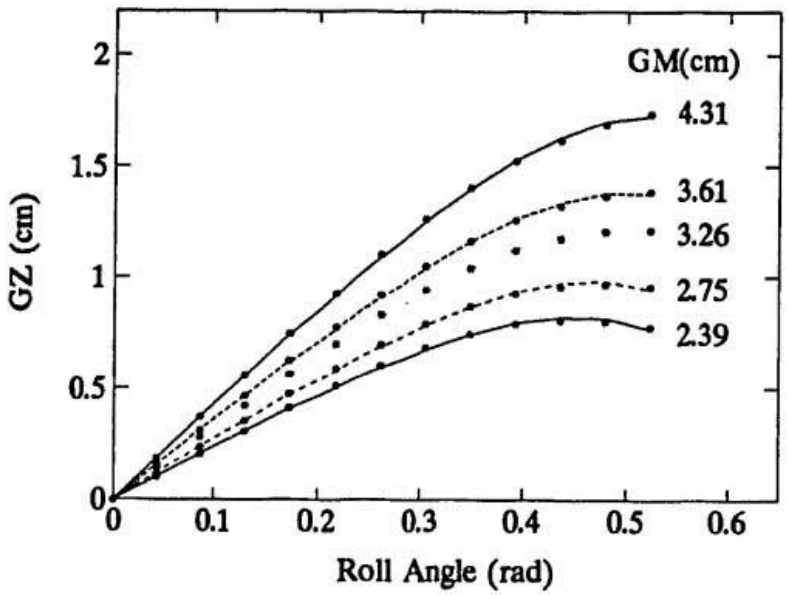

Figure 4.9: GZ Curves of M365

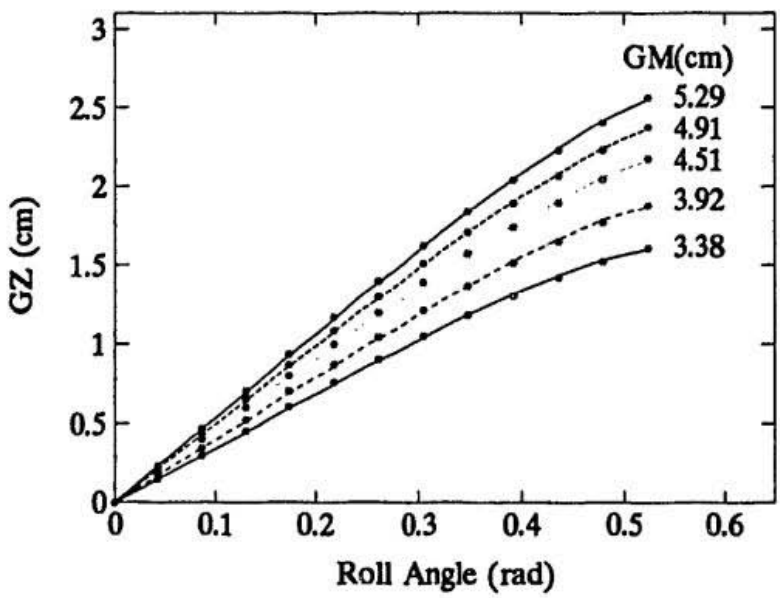

Figure 4.10: GZ Curves of M366

nonlinear damping among the three models because of the effects of its long hard chine, deep skeg and low rise of floor. M366 has lower linear and nonlinear damping than M365 because M366 has higher rise of floor.

To test the accuracy of the estimation by the proposed method, the predicted parameters were used to regenerate free roll decay curves which were then compared with the originally measured free roll decay curves. Fig. B.1 through Fig. B.13 in the Appendices show this comparison for all GM values of the three models.

It is seen that the predicted free decay curves are almost identical to the measured free decay curves in all cases. The excellent agreement indicates that Equation (3.1) is a very good mathematical model for free roll motion. And also the method used here is very accurate and reliable for parametric identification from measured free roll data.

4.2.2 Analysis of Random Roll Data

By using the same programs outlined in the last chapter, the random decrement and autocorrelation function have been calculated from the stationary random roll records. Each record contains 8001 sample points for M363 and 8518 points for M365 and M366. Although the sample size used in the experiments is much smaller than that used in the simulation, it still reaches stationarity and provides good results for most tests.

As stated in Chapter 2, the random decrement and the autocorrelation function of a nonlinear system satisfy approximately the differential equation describing free roll motion. Thus we can in principle estimate the parameters in the free roll equation from the random decrement and the autocorrelation function both of which can be calculated from random roll records. The estimated free decay curves

were generated using the free roll equation and the parameters predicted from the random decrement and the autocorrelation function. Fig. C.1 through Fig. C.13 in Appendix C display the comparison of the random decrement curve with its estimated free decay curve for all cases of the three models. The comparison of the autocorrelation function curve with its estimated free decay curve is illustrated in Fig. D.1 through Fig. D.13 for all cases.

We can see from the plots that the estimated curves generated using free roll equation agree well with the random decrement and the autocorrelation function curves. That means the random decrement and the autocorrelation function satisfy the same equation describing free roll motion. Therefore, the estimation method presented in this work can be used to obtain quite accurate estimations for the parameters in the roll equation using the random decrement or the autocorrelation function.

For comparison purposes, the random decrement and the autocorrelation function curves are plotted with the corresponding free decay curve with the same initial angle and the same GM value. Figures 4.11 to 4.13 show the comparison of the random decrement and the free roll decay for the different models. Figures 4.14 through 4.16 compare the shapes of the autocorrelation function curve and the free roll decay curve for the same cases.

It is seen that both the random decrement and the autocorrelation function curves closely resemble the actual free roll decay curves for M365 and M366. Such resemblance for M363 is reasonable but not as good as in the cases of M365 and M366 due to the large nonlinear damping of M363. These results are expected because of the first-order approximation used in the derivation of the random

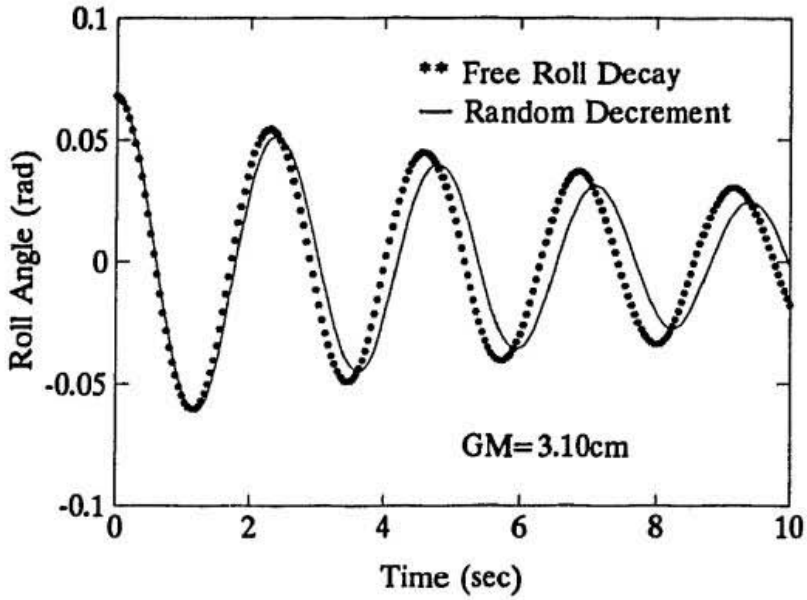

Figure 4.11: Comparison of Random Decrement and Free Decay (M363)

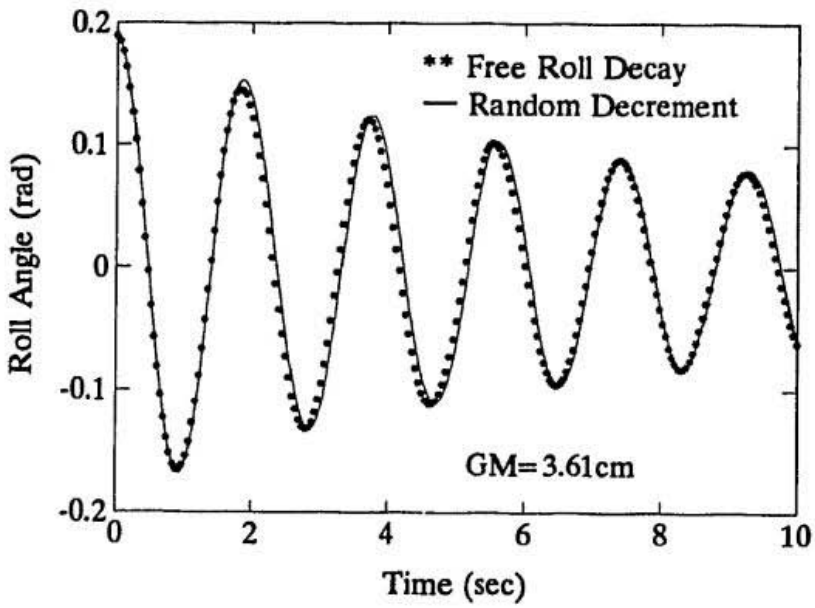

Figure 4.12: Comparison of Random Decrement and Free Decay (M365)

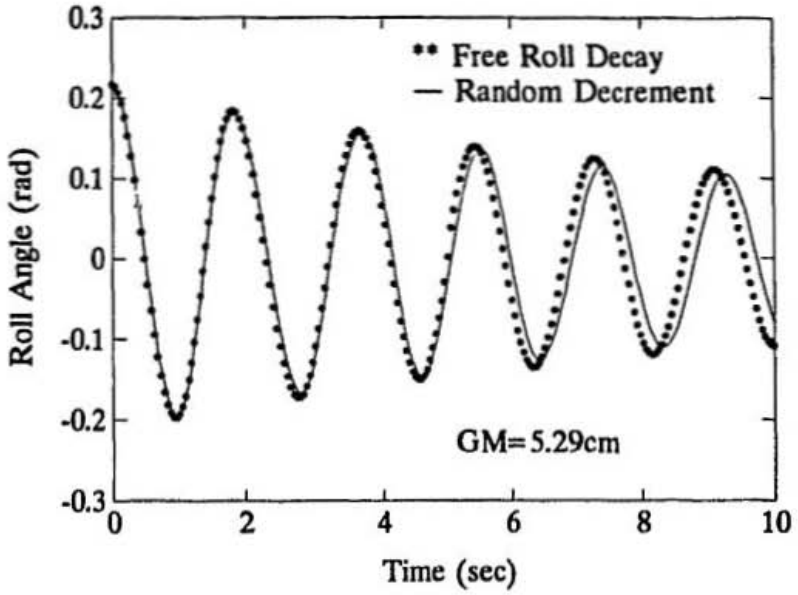

Figure 4.13: Comparison of Random Decrement and Free Decay (M366)

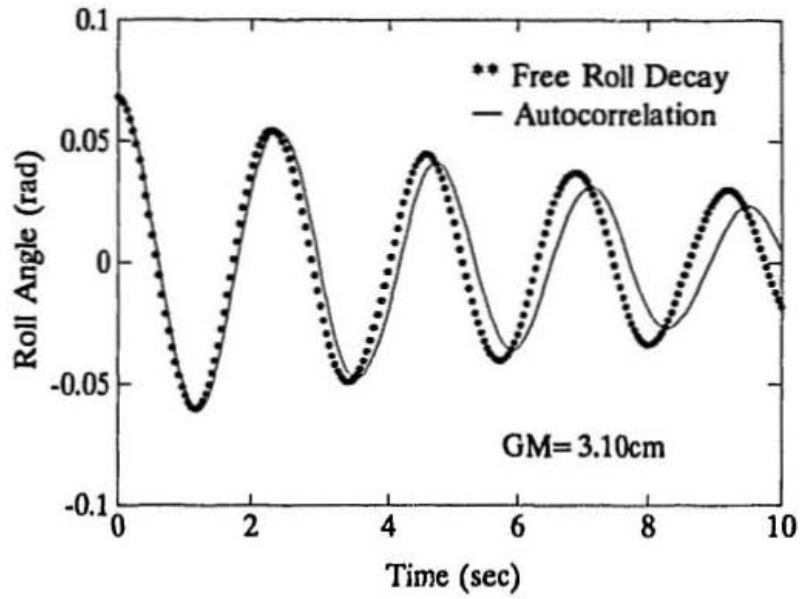

Figure 4.14: Comparison of Autocorrelation and Free Decay (M363)

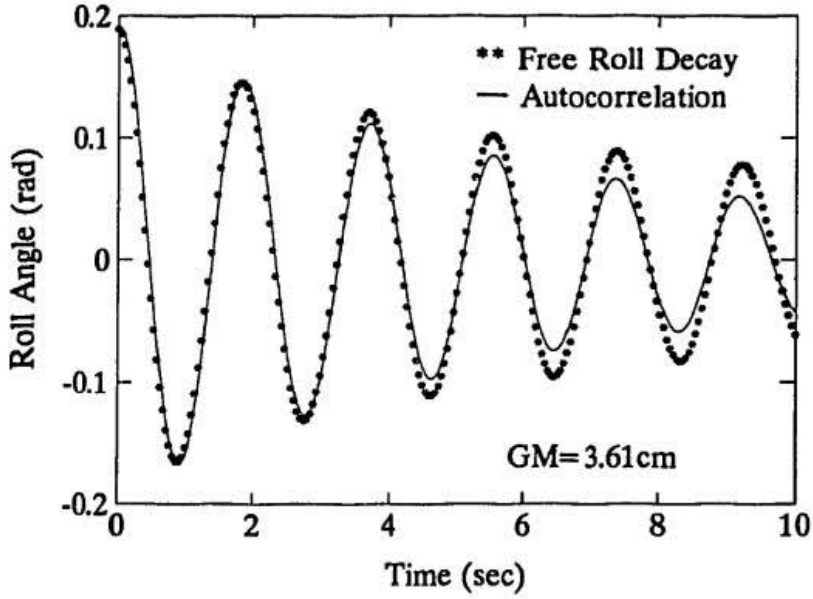

Figure 4.15: Comparison of Autocorrelation and Free Decay (M365)

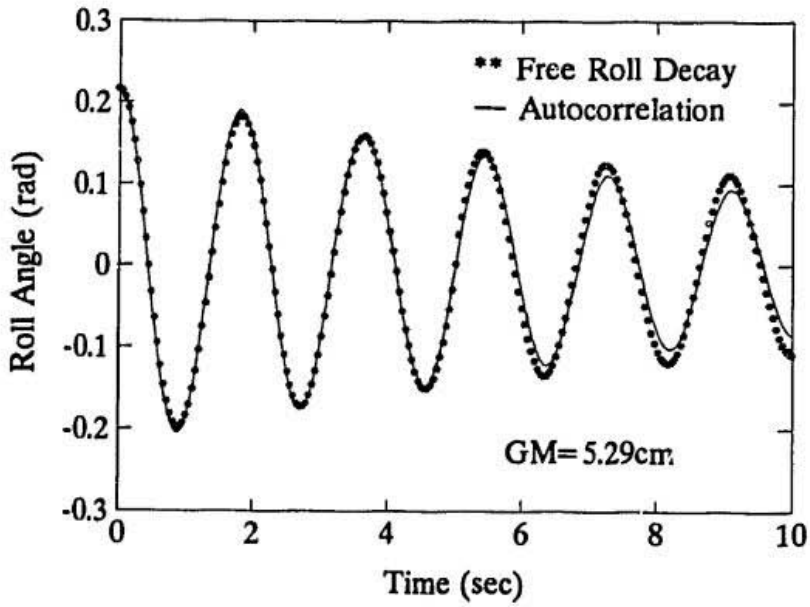

Figure 4.16: Comparison of Autocorrelation and Free Decay (M366)

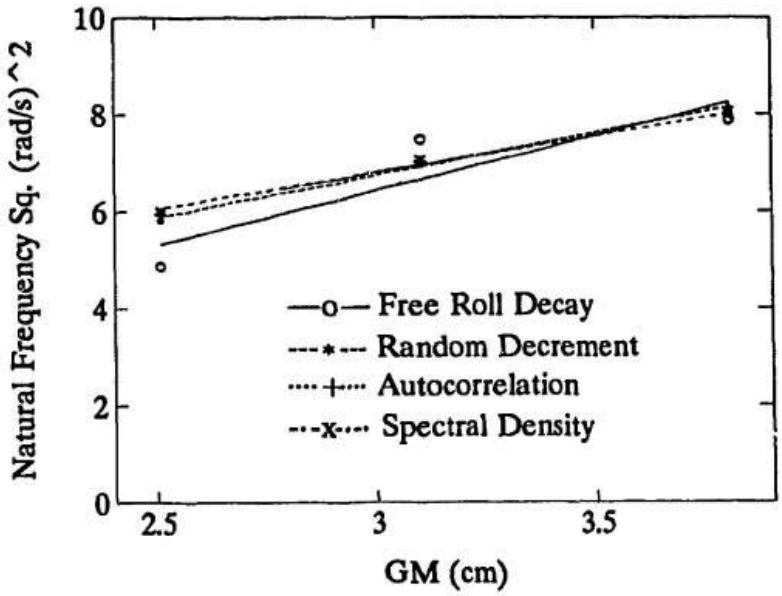

Figure 4.17: ω_ϕ Predicted from Four Methods (M363)

decrement. In the autocorrelation function, the nonlinearities in the damping and restoration are replaced with equivalent linear quantities. As a consequence, the system with larger nonlinearity would produce larger errors in calculation of the random decrement and the autocorrelation function. Also, M363 experiments were conducted with the model constrained against sways while models M365 and M366 were allowed to sway. Restraining sway seems to influence the accuracy of the parameter identification.

The natural frequencies predicted using three methods: the random decrement, the autocorrelation function and the power spectral density are compared with those estimated from the free roll decay curves. The plots of the square of the natural frequency versus GM value are shown in figures 4.17 to 4.19 for the three models. It seems that M366 gives the best results and M363 gives larger errors. It is seen that both the random decrement method and the autocorrelation

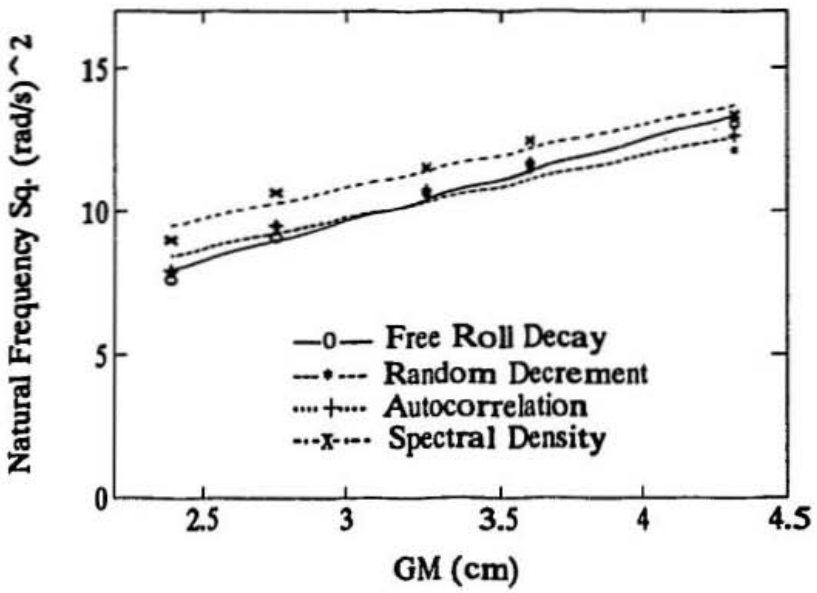

Figure 4.18: ω_ϕ Predicted from Four Methods (M365)

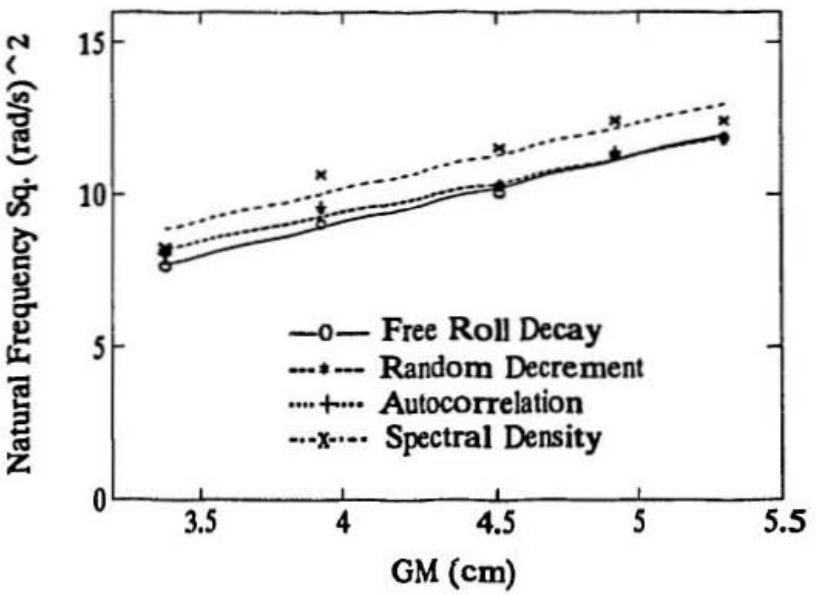

Figure 4.19: ω_ϕ Predicted from Four Methods (M366)

function method provide very good estimates for the natural frequency obtained from free roll decay. The method of power spectral density seems to give more biased estimates for all of the models and it tends to over estimate the values of the natural frequency. The results obtained form the random decrement and the autocorrelation methods are very close to each other. From a linear regression, one can find that the natural frequency predicted using the autocorrelation function curve is slightly more accurate than those obtained from the random decrement.

The relationship between the square of natural frequency and the GM value is demonstrated by the straight lines obtained using a least-squares fit. To predict instantaneous value of the GM for varied loading conditions, one can use this relationship and the natural frequency predicted from either the random decrement or the autocorrelation function curve.

Table 4.3 compares the damping values predicted from the random decrement curves with those from the free roll decay curves. It is seen that the random decrement can be used to approximately estimate the nonlinear damping coefficients. The results from the three models show that the system with smaller nonlinear damping would allow more accurate estimation for damping. Damping estimates obtained from the random decrement and autocorrelation function were used to generate free roll decay curves which agreed well with the original free roll decay curve. However, it must be mentioned that not all of the random roll tests have been successfully used as a substitute for actual free roll decay in the prediction of nonlinear damping coefficients. This problem is partially caused by the transfer of energy between the different components of damping. It is also caused by the first-order approximation used in the derivation of the random decrement and the

Table 4.3: Parameters from Random Dec. and Free Decay

Model	Comparison	b_1	b_3	ω_ϕ	α_1	α_2
M363	Free Decay	0.1509	2.0270	2.7453	1.2832	-1.3293
	Random Dec.	0.2041	1.7636	2.6737	1.2832	-1.3293
M365	Free Decay	0.0894	0.7987	3.4052	-0.3640	-2.2695
	Random Dec.	0.1079	0.5702	3.4053	-0.3640	-2.2695
M366	Free Decay	0.0933	0.2412	3.4643	0.1480	-1.5676
	Random Dec.	0.0971	0.2897	3.3942	0.1480	-1.5676

autocorrelation function. Other reasons have been pointed out in Chapter 3. The effect of wave excitation on the random decrement may be another reason.

This discrepancy may be improved by using the middle parts of the random decrement and free decay curves since we find that the middle part of the two decay curves are more similar. This is because the start of free decay is often distorted and the tails of the random decrement and free decay curves are even worse.

Overall, the accuracy of nonlinear damping estimation by random decrement method seems to critically depend on the nonlinear damping value, the accuracy of roll measurements and some other factors to be determined.

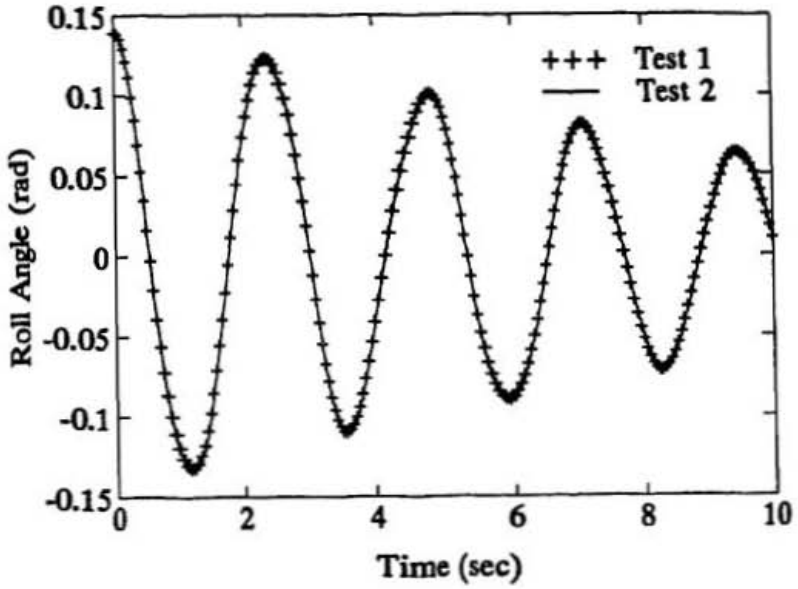

Figure 4.20: Random Decrement from Repeated Tests (M363)

4.2.3 Reliability of the Random Decrement Method

If the wave excitation is a stationary, zero mean, Gaussian, white noise random process, the random decrement curve should be dependent only on the system characteristics and independent of the wave excitation. Neither the type nor the intensity of the input should affect the scale and the form of the random decrement curve. This point is investigated here in three ways: 1) to test whether the random decrement curve is repeatable under the random excitation defined by the same wave spectrum. 2) to see if the change of significant wave height affects the random decrement curve. 3) to see the effect of different wave modal frequencies on the random decrement curve.

Figures 4.20 through 4.22 each shows two random decrement curves extracted from the repeated tests conducted in random waves with the same wave spectrum.

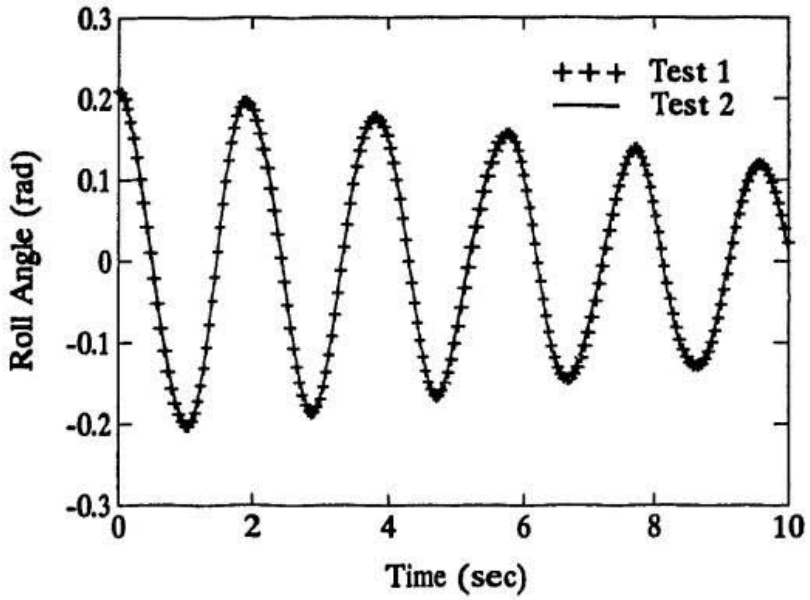

Figure 4.21: Random Decrement from Repeated Tests (M365)

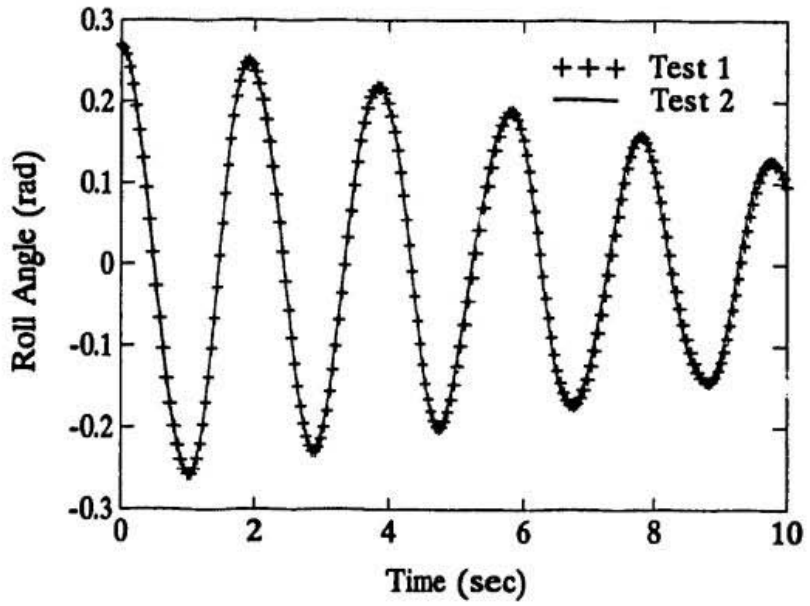

Figure 4.22: Random Decrement from Repeated Tests (M366)

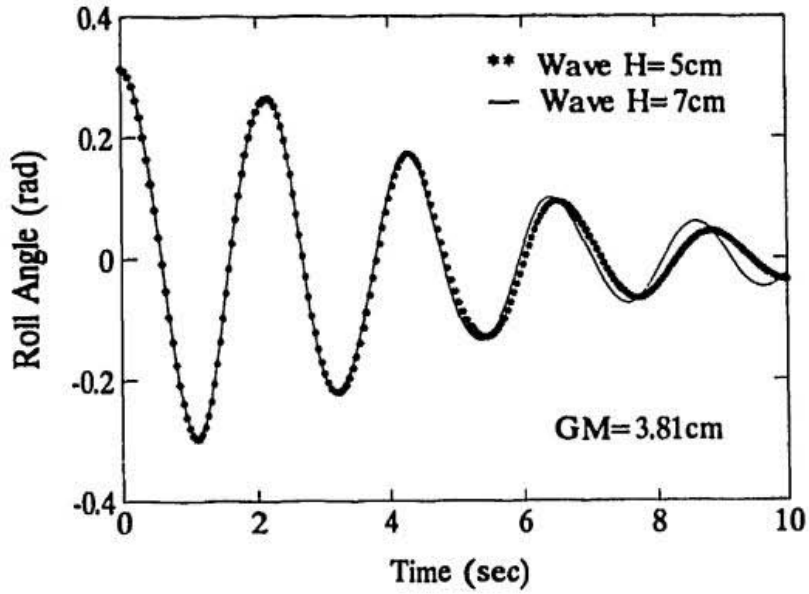

Figure 4.23: Effect of Wave Height on Random Decrement (M363)

Although the time histories of wave excitation in the two tests are different and the time series of roll response are also different, the random decrement curves from two records of random roll response are almost identical. The marvelous resemblance obtained for three models show that the random decrement method can produce repeatable decrement curves from the nonlinear roll response subject to the wave excitations with the same spectrum. This is important for ensuring a reliable and unique solution of the roll parameters to be obtained.

In figures 4.23 through 4.25, the two random decrement curves are obtained from the two roll tests which were conducted in random waves generated from two wave spectra. The two wave spectra have different significant wave heights and the same modal frequency. Although the significant amplitude of the two random roll records are much different, their random decrement curves closely resemble each other. The good results for three models leads to the conclusion that the effect

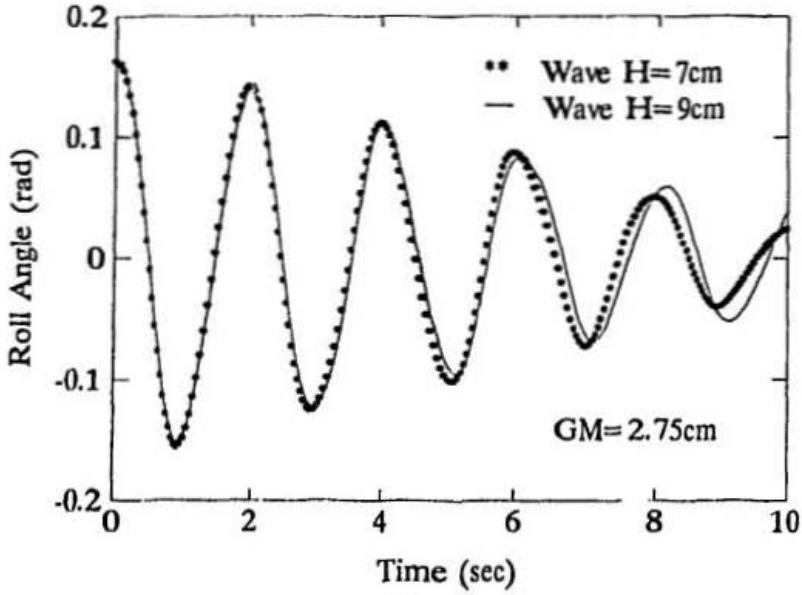

Figure 4.24: Effect of Wave Height on Random Decrement (M365)

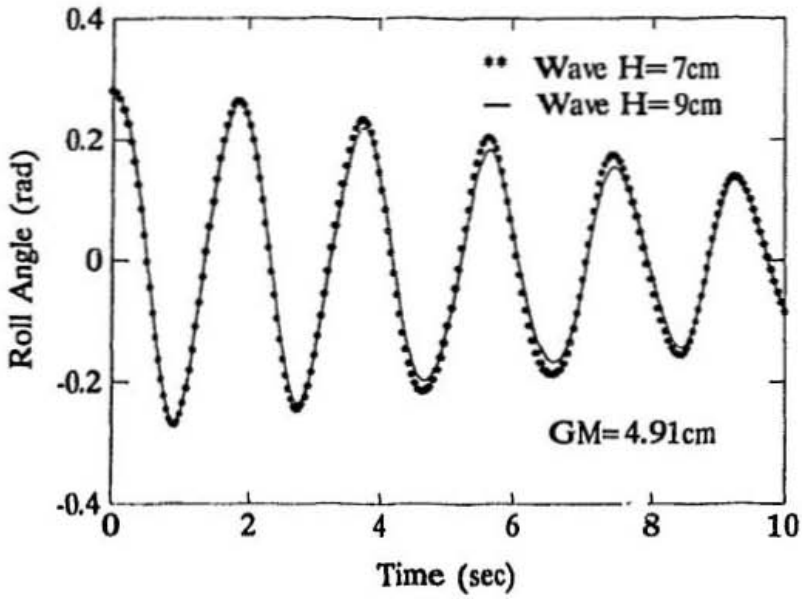

Figure 4.25: Effect of Wave Height on Random Decrement (M366)

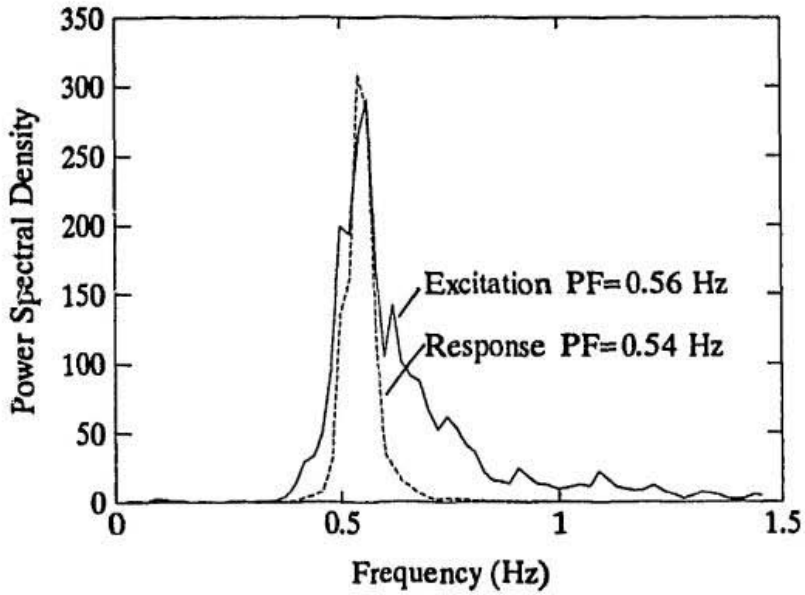

Figure 4.26: Wave Modal Frequency Close to Model ω_ϕ

of varying significant wave height on the random decrement is weak and can be neglected.

Figures 4.26 through 4.28 show the spectra of both wave excitation and roll response for Model M365. Three wave spectra with different modal frequencies and the same significant wave height were used in the experiments on Model M365 and M366 to investigate the effect of wave modal frequency on the random decrement curve. The results for M365 are shown here and the results for M366 are very much similar. In Figure 4.26, the wave modal frequency is close to the natural frequency of the model. While in Figure 4.27 and Figure 4.28, the modal frequencies of the wave spectra are different from the natural frequency of the model: one of them is higher and the another is lower than the natural frequency of the model.

It can been seen that in the resonant condition, the model reached largest amplitude of roll motion while in the other two situations, the average energy of

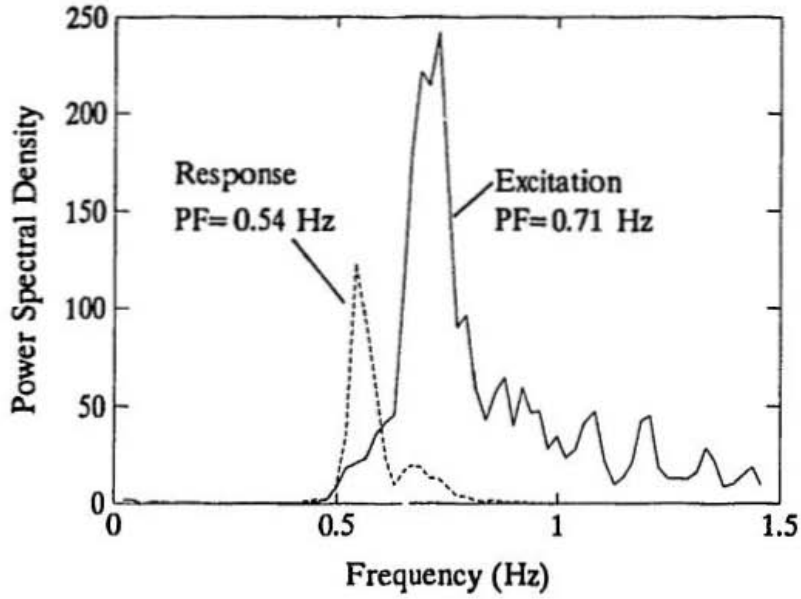

Figure 4.27: Wave Modal Frequency Higher Than Model ω_ϕ

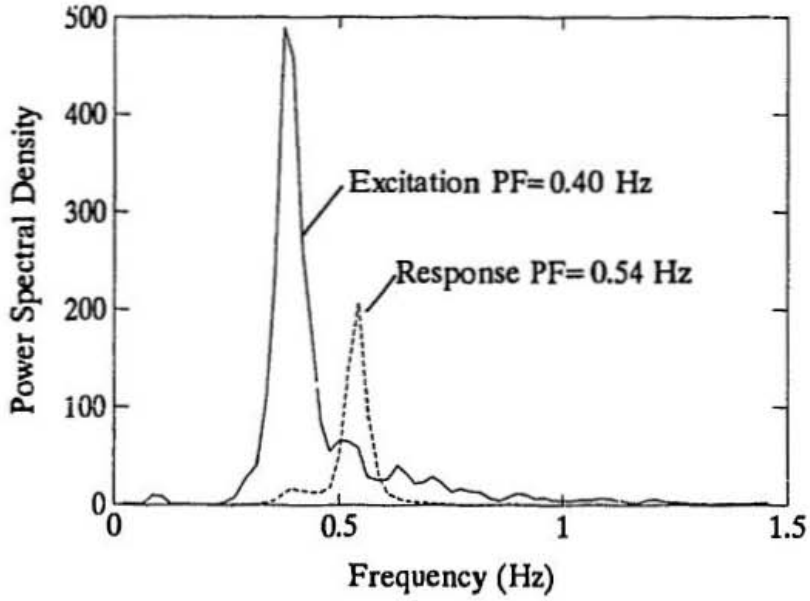

Figure 4.28: Wave Modal Frequency Lower Than Model ω_ϕ

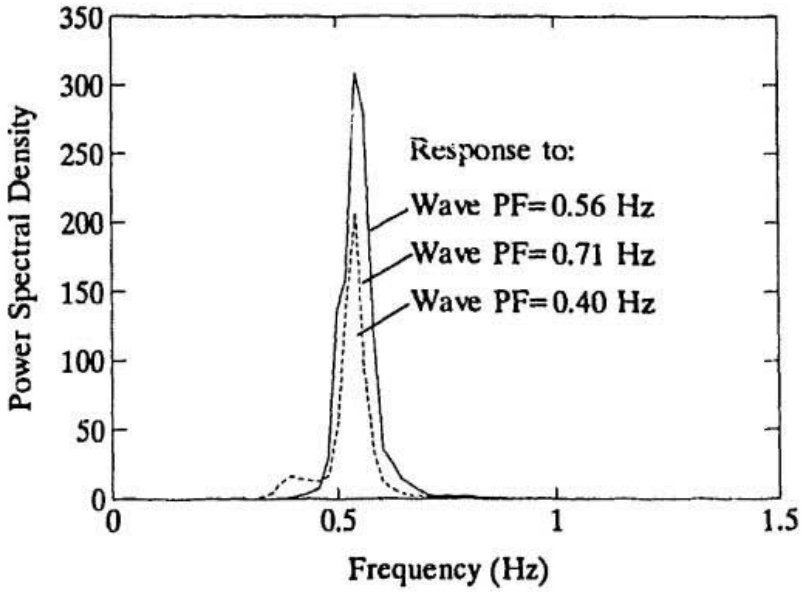

Figure 4.29: Roll Response to Different Wave Modal Frequencies

the roll response were much smaller. The three spectra of roll response are plotted together in Figure 4.29. Although the modal frequencies of the input are different in the three tests, the modal frequencies of roll response are almost the same.

Figure 4.30 compares two random decrement curves obtained from the roll response shown in Figures 4.27 and 4.28. It is observed that there exists large difference between the two random decrement curves. One explanation to this problem is that JONSWAP spectrum which was used for generating random waves is different from the white noise spectrum that was assumed in the derivation of the random decrement. When the modal frequency of excitation is away from the natural frequency of the system, the wave spectrum is not sufficiently broader than the response band-width. The problem may also be caused in the calculation of the expected values. The numbers of segments for forming the random decrement curves are largely different when the same initial angle is used for both large

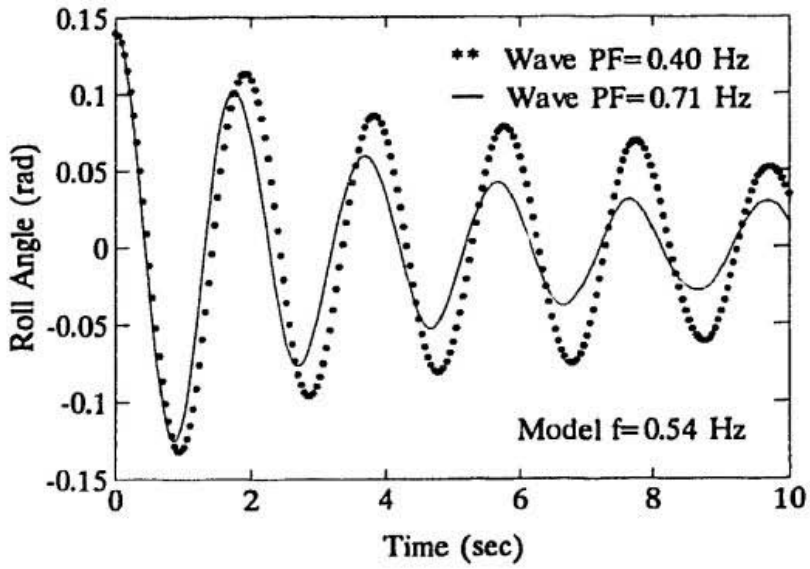

Figure 4.30: Effect of Wave Modal Frequency on Random Decrement

and small amplitude roll records. When the number of segments is limited by the length of a record, the ensemble average of the segments may not represent the ture random decrement. The nonlinear damping is probably another reason to cause the random decrement curve to change with the random excitation. For linear systems, the scale and form of the random decrement curve remain unchanged even when the ambient random excitation changes. For nonlinear systems, the independence of the random decrement on the modal frequency of input needs to be further studied.

Chapter 5

Full Scale Ship Tests

In this chapter, the random decrement method will be used in the analysis of the real ship response in an irregular sea. The wave pattern of an actual sea is rather complex and the wave surface varies from time to time and place to place, depending on wind speed and direction. Since the free roll test and the measurement of wave excitation are not avaliable for a ship at sea, one has to rely on roll measurements only to predict roll parameters for assessing the stability of the ship against capsizing.

5.1 Ship Roll Tests at Sea

The real ship tests were carried out on the fishing vessel "Newfoundland Alert" during its fishing trip at sea in September 1992. The particulars of the ship are given in Table 5.1 and the ship layout is shown in Figure 5.1. The instruments used for measuring roll motion of the ship are the same as those used in the experiments for M365 and M366. Since the period of roll motion for the ship is much longer than that of the models, the measurements of roll angle were taken every 0.25 second for 20 to 40 minutes for each record.

Table 5.1: General Particulars of the Ship

Vessel's Name	Newfoundland Alert
Type of Vessel	Fishing Vessel
Length Between Perpendicular	32.80 meters
Breadth Moulded	10.00 meters
Depth Moulded	6.80 meters
Summer Load Draft	4.011 meters
Displacement at S.L.W.L.	673 tons
Lightship Weight	406 tons
Date Keel Laid	February 25, 1988
Builder	Marystown Shipyard Limited

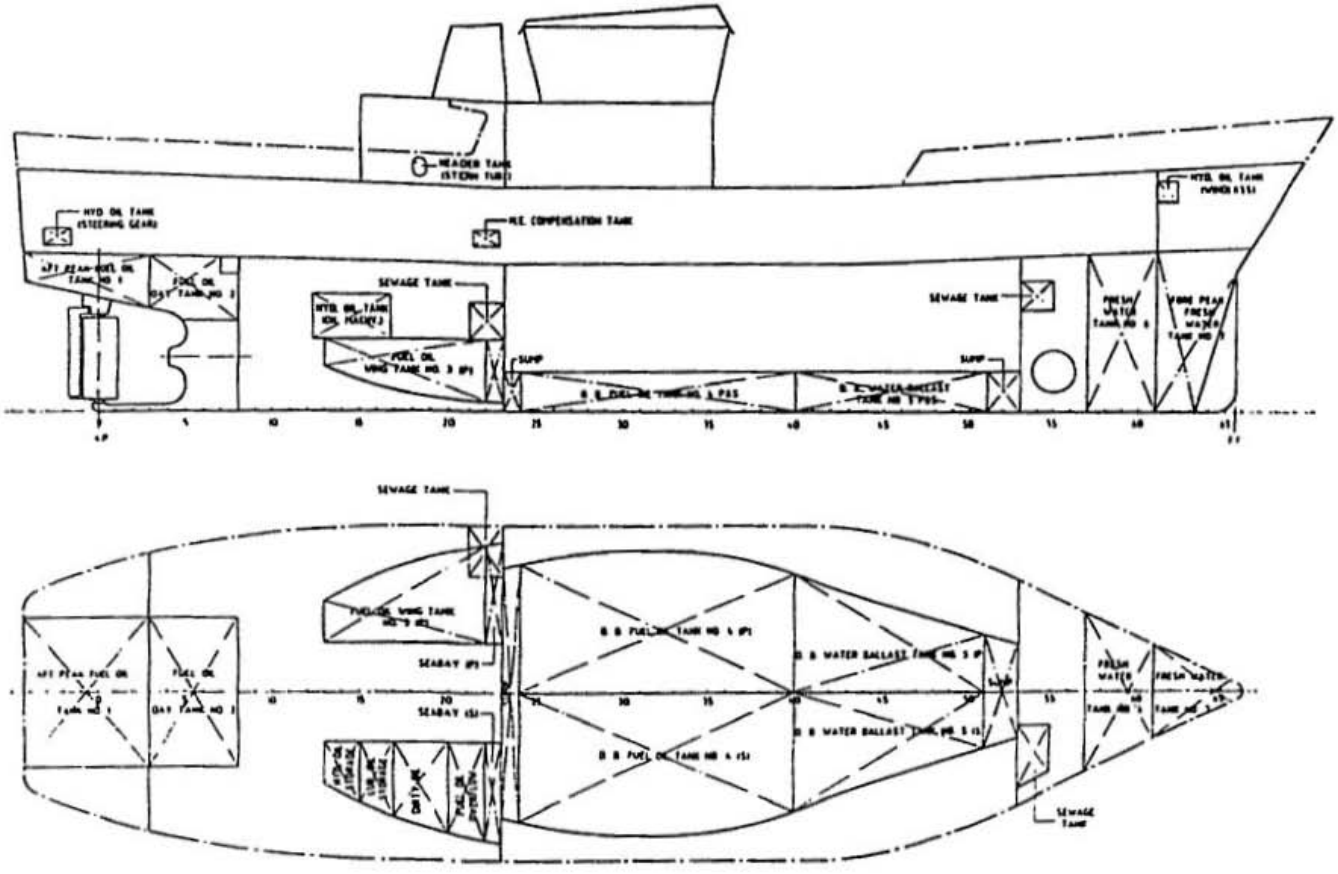

Figure 5.1: Full Scale Ship Layout

5.2 Calculations of Loading Conditions

The loading condition of the ship changed from time to time during the trip because of the change in weight of the catch, the consumption of fuel and fresh water and some other changes in either weight or location. To find the instantaneous GZ curve and GM value of the vessel, we need to calculate the weight and the center of gravity of each item causing the changes of mass and mass distribution of the vessel. In addition, there are several tanks located in the ship (see Figure 5.1). When the tanks are partially filled with liquid, the stability of the ship is adversely affected by what is known as "Free Surface Effect", which causes a loss in GM. The Free Surface Correction can be calculated using the formula

$$F/S\ Correction = \frac{Total\ Free\ Surface\ Moment}{Displacement\ of\ Vessel} \qquad \frac{(t.m)}{t} \tag{5.1}$$

The center of gravity of the vessel KG can be corrected by

$$KG_{fluid} = KG_{solid} + F/S\ Correction \tag{5.2}$$

and the metacentric height GM is obtained from

$$GM_{fluid} = KM_T - KG_{fluid} \tag{5.3}$$

where KM_T is the height of transverse metacenter above keel.

Three loading conditions are reported in Table E.1 through E.3 in the Appendices. The consumed fuel, fresh water and provisions were calculated on the basis of assumed consumption rate during the trip. The weight of ice and boxes used for the catch were considered to be proportional to the weight of fish. To calculate the center of gravity of each item changing in weight and the free surface moment

Table 5.2: Hydrostatic Data of Three Conditions

Item	Condition 1	Condition 2	Condition 3
Displacement (t)	605.07	607.69	614.33
Draft (m)	3.7433	3.7539	3.7806
$KM_T(m)$	4.8554	4.8573	4.8623
KG_{solid} (m)	3.9475	3.9464	3.9397
F/S Correction (m)	0.2090	0.2018	0.1939
KG_{fluid} (m)	4.1565	4.1483	4.1336
GM_{fluid} (m)	0.6989	0.7091	0.7287

of each tank, a computer program was written to interpolate some relevant data given in the Stability Booklet of the ship for a series of loading conditions. The hydrostatic data were calculated using equation (5.1) through (5.3) and the results are shown in Table 5.2 for the three loading conditions.

The statical stability (GZ) curve for a certain loading condition is obtained using the following equation

$$GZ = KN - KG_{fluid} \sin\theta$$

The KN values can be derived from the Stability Booklet of the ship by interpolating the given KN values for a series of displacement values. Figure 5.2 shows the GZ curve for one loading condition.

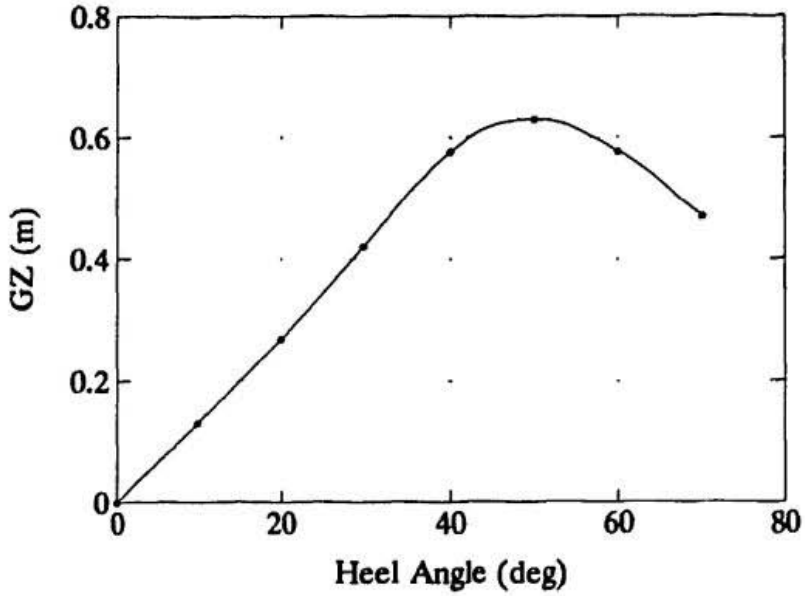

Figure 5.2: GZ Curve of the Ship

5.3 Results and Discussion

Figures 5.3 and 5.4 show the random decrement curves extracted from the roll response of the ship in an irregular sea. For a real ship sailing in a sea, six degrees of freedom of motion and forward speed are involved. In addition, the ship is subject to varied sea states. Therefore, the situation of a ship at sea is more complicated than in numerical simulation or in experiments.

However, good results were obtained from the ship roll records with a shorter sample length and a larger sample interval than those used in the simulation and the experiments. One explanation is that the frequency band of the sea waves may be broader than the assumed mathematical model for the simulation and also than the wave spectra used in the experiments. Another reason is that the wave excitation of the actual sea is a true random process. Thus, the real ship tests can

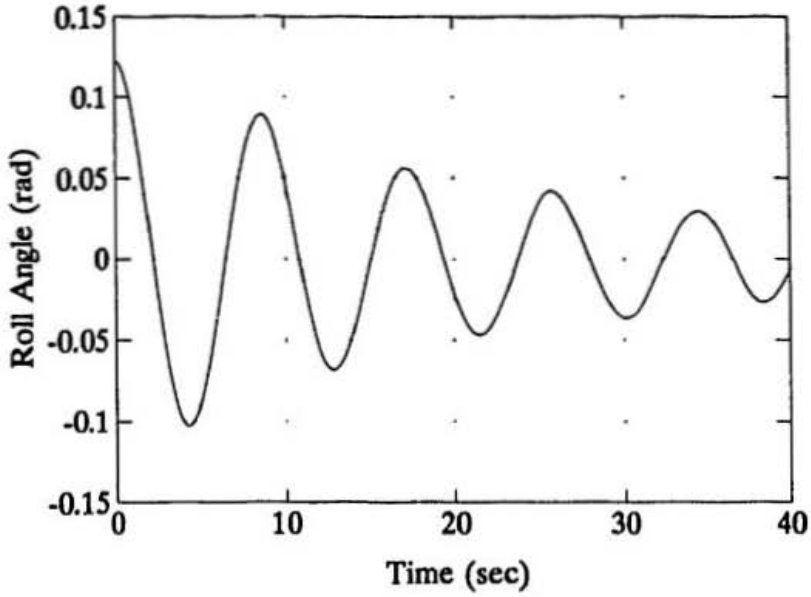

Figure 5.3: Random Decrement (Ship: GM=0.6989m)

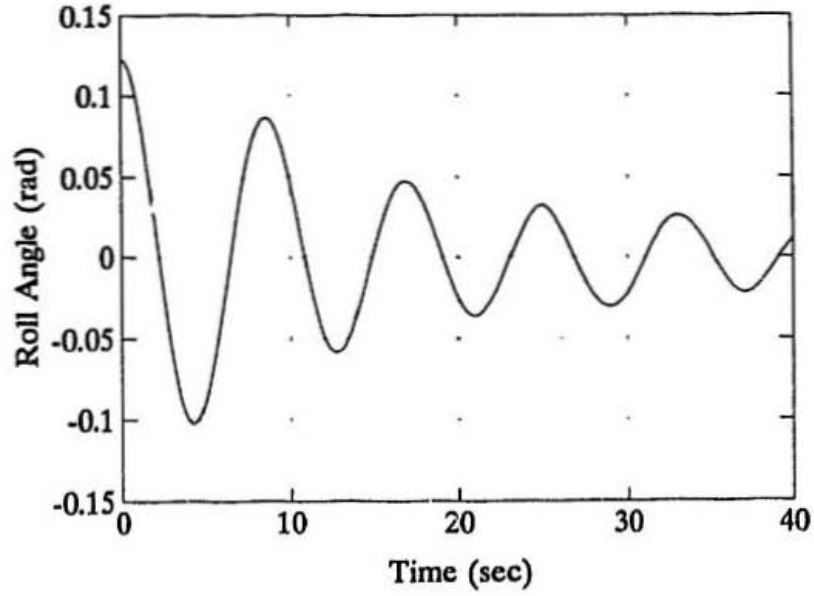

Figure 5.4: Random Decrement (Ship: GM=0.7287m)

Table 5.3: Parameters Estimated from Random Decrement

Case	GM (m)	b_1	b_3	ω_ϕ	α_1	α_2
1	0.6989	0.0733	3.2782	0.7350	0.4025	-0.4818
2	0.7091	0.0775	4.5473	0.7401	0.3910	-0.4747
3	0.7287	0.0868	3.5923	0.7653	0.3671	-0.4611

use less segments to form an equally accurate random decrement curve.

Table 5.3 shows the parameters predicted from the random decrement curves for the three loading conditions. Good estimate of damping parameters have been obtained from the nonlinear roll motion of a ship in a realistic sea.

Figure 5.5 displays the comparison of the random decrement and the autocorrelation function curves. It is seen that the two curves agree reasonably well with each other. Thus we may use random decrement for parametric identification and use the autocorrelation function method to check the estimation.

Figure 5.6 shows the plot of the square of natural frequency against GM value obtained from the three methods. Due to the small variation in the value of GM for three loading conditions, the spectral density method fails to tell the change of natural frequency with the GM value. However, both the random decrement method and autocorrelation method not only succeeded to distinguish the small changes in the natural frequency with different loading conditions but also gave the results satisfying the linear relationship between the square of the natural

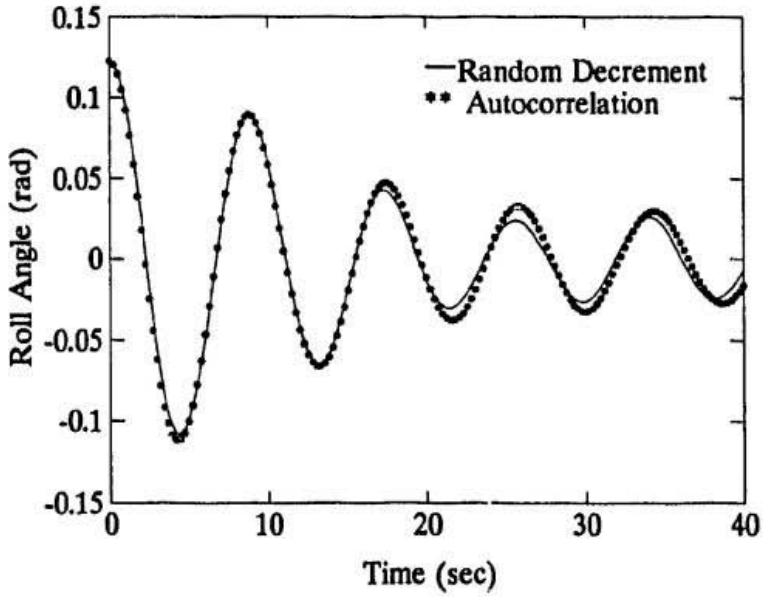

Figure 5.5: Random Decrement and Autocorrelation (GM=0.7091m)

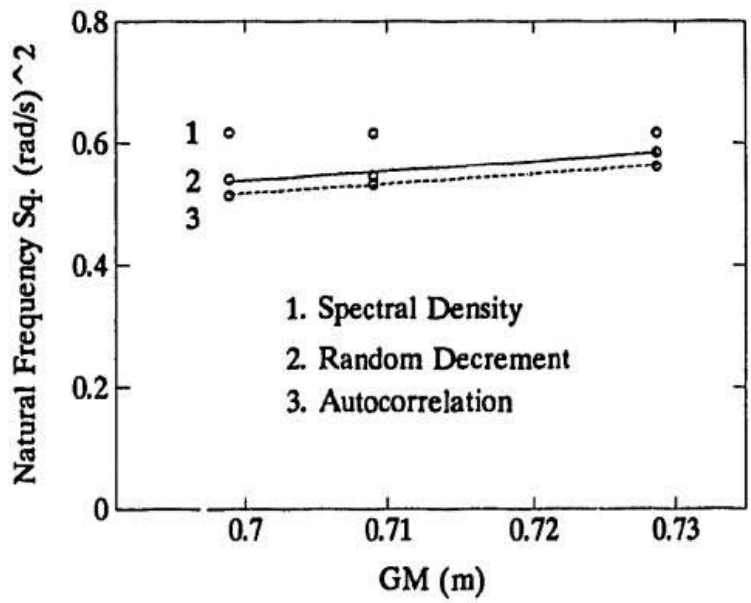

Figure 5.6: Natural Frequency Predicted by Three Methods

frequency and the GM value. The results from the random decrement and the autocorrelation function methods are very close to each other. As in numerical simulation and model experiments, the power spectral density method produced the highest values for the natural frequency.

As the wave excitation was beyond control in the real ship tests, some measurements were taken when the roll motion was small. Consequently small initial angles were used in forming the random decrement curves. It is found that using an initial angle smaller than 5 degree tends to produce bad random decrement curves. This is because the data become quite noisy for small roll motion. It is also found that if the random decrement method fails to provide good estimation from noisy data in the case of small roll motion, the autocorrelation method or spectral density method correspondingly provide bad results too.

Chapter 6

Conclusions and Recommendations

6.1 Conclusions

In this study, the difficulties with the parameter identification from nonlinear roll motion of a ship in random waves were overcome by the use of the Random Decrement Method. The applicability of this technique as applied to nonlinear systems was investigated using computer generated data, model experimental data and real ship test data. The validation of the method covered various loading conditions, different hull shapes, different nonlinear damping moments and different wave spectra. It has been shown that the free roll response for the nonlinear rolling motion can be either obtained from a calculation of the propagation of the expected value of the roll motion in a random sea, usually referred to as the random decrement, or from the calculated autocorrelation function of the stationary random rolling response. In both cases the measurement of the random excitation is not required.

The values of the natural frequency predicted from the random decrement or the autocorrelation function showed good agreement with those obtained from

the actual free roll decay. The power spectral estimation provided more biased results than either the random decrement or the autocorrelation function method, especially in the situation when GM value varied slightly. It has also been shown that the square of the natural frequency is linearly related to the magnitude of GM. Thus the natural frequency obtained by the random decrement method or the autocorrelation method can be used to find an estimate for the instantaneous metacentric height for a ship at sea.

It is very interesting that for some noisy data obtained in case of small roll motion, the three methods: random decrement, autocorrelation function and spectral density produced equally bad results.

The comparison between the estimated decay curve obtained from the random decrement with the actual free decay curve showed reasonably close agreement, which indicate that it is possible to use the random decrement as a substitute of the free roll decay for nonlinear damping identification. However, the variance of the damping coefficients obtained from the random decrement seems still considerably large for some cases. Several factors may cause this problem. First, the nonlinearity of the damping would affect the accuracy of the damping estimation from the random decrement. Second, a first order approximation was used to derive the expected value propagation. Third, the exciting moment used in the simulation and the experiments departed from the Gaussian white noise which was assumed in the theoretical formulation.

The results of the three models have proved that the system with smaller damping nonlinearity gives more accurate estimation for both the natural frequency and the damping parameters. This point was verified by comparing the accuracy of the

parameter estimation and the resemblance between the free roll decay, the random decrement and the autocorrelation function curves for three models.

Comparing the results from the numerical simulation, the model experiments and the real ship tests, one sees that the real ship tests used smaller sample size or less segments to form an equally accurate random decrement curve. The numerical simulation needs the longest record to get a random decrement curve with the same accuracy. The damping coefficients obtained from the real ship tests show smaller variance than either the numerical simulation or the model experiment. It seems more errors occur in the damping identification from the experimental tests. The reasons might be: the spectra used in the experiments for generating random waves were narrower than the wave spectra affected by realistic sea. The simulation used a limited-band excitation composed of a number of sinusoidal components which may not be truly random as a realistic sea.

The technique described here opens up the possibility to assess the roll stability of a ship in real loading condition using its roll measurements taken in a seaway. The whole procedure developed in this work will serve as an useful tool for the prediction of roll parameters in the nonlinear equation of roll motion. This will provide a means for immediate estimation of the margin against capsizing for a ship sailing in a realistic sea.

6.2 Recommendations

Based on the results of this study, the following major recommendations have been drawn and should be pursued in further research.

1. In the theoretical approach, a more rigorous method for obtaining the expected value propagation may improve the accuracy of damping estimation from the random decrement.

2. A method which can deal with a non-white excitation should be developed.

3. The effect of wave modal frequency on the random decrement from nonlinear roll motion needs to be further investigated.

4. For real ship tests, large change in loading condition is recommended in order to cover large range of GM values in the study.

References

[1] Haddara, M. R. "On the Random Decrement for Nonlinear Rolling Motion", Proceedings of the Eleventh International Conference on Offshore Mechanics and Arctic Engineering, Vol. II, Safety and Reliability, pp. 321-324, 1992.

[2] Kountzeris, A., Roberts, J. B. and Gawthrop, P. J., "Estimation of Ship Roll Parameters from Motion in Irregular Seas", Transactions of the Royal Institution of Naval Architects, Vol. 132, pp. 253-266, 1991.

[3] The Papers of William Froude, The Institution of Naval Architects, London, 1955.

[4] Haddara, M. R., "On the Stability of Ship Motion in Regular Oblique Waves", International Shipbuilding Progress, Vol. 18, No. 207, pp. 416-434, 1971.

[5] Haddara, M.R., " A Note on the Effect of Damping Moment Form on Rolling", International Shipbuilding Progress, Vol. 31, No. 363, pp. 285-290, 1984.

[6] Dalzell, J. F., "A Note on the Form of Ship Roll Damping," Journal of Ship Research, Vol. 22, No. 3, pp. 178-185, 1978.

[7] Spouge, J. R., "Non-linear Analysis of Large Amplitude Roll Experiments", International Shipbuilding Progress, Vol. 35, No. 403, pp. 271-324, 1988.

[8] Mathisen, J. B. and Price, W. G., "Estimation of Ship Roll Damping Coefficients," Trans. of the Royal Institute of Naval Architects, Vol. 127, pp. 295-307, 1985.

[9] Roberts, J. B., "Estimation of Non-linear Ship Roll Damping from Free-decay Data," Journal of Ship Research, Vol. 29, No. 2, pp. 127-138, 1985.

[10] Bass, D. W. and Haddara, M. R., "Nonlinear Models of Ship Roll Damping," International Shipbuilding Progress, Vol.35, No. 401, pp. 5-24, 1988.

[11] Levenberg, K., "A Method for the Solution of Certain Problems in Least Squares", Quart. Journ. of Appl. Math., Vol. 2, pp. 164-168, 1944.

[12] Mathisen, J. B. and Price, W. G., "Determination of Linear Plus Cubic Ship Roll Damping Coefficients", NMI Report R187, April 1984.

[13] Roberts, J. B., Dunne, J. F. and Debonos, A., " Estimation of Ship Roll Parameters in Random Waves", Proceedings of the Tenth International Conference on Offshore Mechanics and Arctic Engineering, Vol. II, Safety and Reliability, pp. 97-106, 1991.

[14] Cole, H. A., "On-The line Analysis of Random Vibrations", Paper No. 68-288, Proceedings of the AIAA/ASME 9th Structures, Structural Dynamics and Materials Conference, Palm Springs California, 1968.

[15] Aggour, M. S., Yang, J. C. S. and Al-Sanad, H. "Application of the Random Decrement Technique in the Determination of Damping of Soils ", in Pro-

ceedings of the 7th European Conference on Earthquake Engineering, Vol. 2, pp. 337-344, Greece, 1982.

[16] Yang, J. C. S., Aggour, M. S., Dagalakis, N., and Miller, F., "Damping of an Offshore Platform Model by Random Dec Method", in Proceedings of the Second ASCE/EMD Specialty Conference on Dynamic Response of Structures, American Society of Civil Engineers, New York, pp. 819-832, 1981.

[17] Brignac, W. J., Ness, H. B. and Smith, L. M., "The Random Decrement Technique Applied to the YF-16 Flight Flutter Tests", in Proceedings of the 16th AIAA/ASME/SAE Structures Conference, Vol. 2, pp. 1-8, American Institute of Aeronautics and Astronautics, New York, 1975

[18] Ibrahim, S. R., "Random Decrement Technique for Model Identification of Structures", The AIAA Journal of Spacecraft and Rockets, Vol. 14, No. 11, 1977.

[19] Al-Sanad, H., Aggour, M. S. and Yang, J. C. S., "Dynamic Shear Modulus and Damping Ratio from Random Loading Tests", Geotechnical Testing Journal, GTJODJ, Vol. 6, No. 3, pp. 120-127, 1983.

[20] Reed, R. E., " Analytical Aspects of Randomdec Analysis", in Proceedings of the 20th AIAA/ASME/ASCE/AHS Structures, Structural Dynamics and Materials Conference, Vol. 1, pp. 404-409, American Institute of Aeronautics and Astronautics, New York, 1979.

[21] Vandiver, J. K., " A Mathematical Basis for the Random Decrement Vibration Signature Analysis Technique", Journal of Mechanical Design, Vol. 104, pp. 307-313, 1982.

[22] Haddara, M. R. "A Note on the Power Spectrum of Nonlinear Rolling Motion", International Shipbuilding Progress, Vol. 30, No. 342, pp. 41-43, 1983.

[23] St. Denis, M. and Pierson, W. J., "On the Motions of Ships in Confused Seas," Trans. SNAME, Vol. 61, pp. 280-357, 1953.

[24] Hagedorn, P., "Non-linear Oscillations", Oxford Science Publications, pp. 348-351, 1988.

[25] Borgman, L. E. "Ocean Wave Simulation for Engineering Design", Journal of Waterways and Harbors Division, Proceedings of the ASCE, pp. 557-583, 1969.

[26] Haddara, M. R. and Wu, X., "Parameter Identification of Nonlinear Rolling Motion in Random Seas", to be published in International Shipbuilding Progress.

[27] Ewing, J. A., "Some Results from the Joint North Sea Wave Project of Interest to Engineers", . Symposium of the Dynamics of Marine Vehicles and Structures in Waves, London, England, pp. 41-46, 1974.

[28] Haddara, M.R. "A Modified Approach for the Application of Fokker-Planck Equation to the Nonlinear Ship Motions in Random Waves", International Shipbuilding Progress, Vol. 21, no.242, pp. 283-288, 1974.

[29] Haddara, M. R. and Bennett, P. "A Study of the Angle Dependence of Roll Damping Moment", Ocean Engineering, Vol. 16, No. 4, pp. 411-427, 1989.

[30] Al-Sanad, H., "Effect of Random Loading on Modulus and Damping of Sands", Ph.D. Thesis, University of Maryland, College Park, MD, 1982.

[31] Caughey, T. K. and Stumpt, H.J. "Transient Response of a Dynamic System Under Random Excitation", Journal of Applied Mechanics, pp. 563-566, Dec. 1961.

[32] Caughey, T. K. "Derivation and Application of the Fokker-Planck Equation to Discrete Nonlinear Dynamic Systems Subjected to White Random Excitation", the Journal of the Acoustical Society of America, Vol. 35, No. 11, pp. 1683-1692, 1963.

[33] Himeno, Y. "Prediction of Ship Roll Damping, State of the Art", College of Engineering, The University of Michigan. Report No. 239, 1981.

Appendix A

Model Inclining Test Data

Table A.1: Inclining Test Data of M363

	Case 1		Case 2		Case 3	
d (cm)	ϕ (deg)	θ (deg)	ϕ (deg)	θ (deg)	ϕ (deg)	θ (deg)
0	-0.03		0.02		0.04	
10.5 S	0.37	0.40	0.51	0.49	0.64	0.60
21.0 S	0.75	0.38	1.00	0.49	1.24	0.60
10.5 S	0.36	0.39	0.52	0.48	0.65	0.59
0	-0.04	0.40	0.03	0.49	0.04	0.61
10.5 P	-0.45	0.41	-0.44	0.47	-0.57	0.61
21.0 P	-0.84	0.39	-0.94	0.50	-1.16	0.59
10.5 P	-0.44	0.40	-0.46	0.48	-0.54	0.62
0	-0.05	0.39	0.02	0.48	0.04	0.58
GM	3.81 cm		3.10 cm		2.51 cm	
KG	25.92 cm		26.63 cm		27.22 cm	

Table A.2: Inclining Test Data of M365

	Case 1		Case 2		Case 3		Case 4		Case 5	
d (cm)	ϕ (deg)	θ (deg)	ϕ (deg)	θ (deg)	ϕ (deg)	θ (deg)	ϕ (deg)	θ (deg)	ϕ (deg)	θ (deg)
0	0.01		0.02		0.04		0		0	
8.5 S	0.42	0.41	0.51	0.49	0.58	0.54	0.62	0.62	0.73	0.73
17 S	0.85	0.43	1.02	0.51	1.12	0.54	1.27	0.65	1.49	0.76
8.5 S	0.42	0.43	0.51	0.51	0.57	0.55	0.62	0.65	0.73	0.76
0	0.02	0.40	0.03	0.48	0.04	0.53	0	0.62	0	0.73
8.5 P	-0.39	0.41	-0.45	0.48	-0.48	0.52	-0.65	0.65	-0.72	0.72
17 P	-0.79	0.40	-0.94	0.49	-1.05	0.57	-1.32	0.67	-1.48	0.76
8.5 P	-0.39	0.40	-0.46	0.48	-0.48	0.57	-0.65	0.67	-0.73	0.75
0	0.02	0.41	0.02	0.48	0.04	0.52	-0.02	0.63	0	0.73
GM	4.31 cm		3.61 cm		3.26 cm		2.75 cm		2.39 cm	
KG	28.75 cm		29.45 cm		29.80 cm		30.31 cm		30.67 cm	

Table A.3: Inclining Test Data of M366

d (cm)	Case 1		Case 2		Case 3		Case 4		Case 5	
	ϕ (deg)	θ (deg)	ϕ (deg)	θ (deg)	ϕ (deg)	θ (deg)	ϕ (deg)	θ (deg)	ϕ (deg)	θ (deg)
0	0.10		-0.01		0.05		0.03		0.03	
10.5 S	0.44	0.34	0.34	0.35	0.43	0.38	0.48	0.45	0.54	0.51
21.0 S	0.76	0.32	0.69	0.35	1.81	0.38	0.91	0.43	1.05	0.51
10.5 S	0.44	0.32	0.34	0.35	0.43	0.38	0.46	0.45	0.53	0.52
0	0.10	0.34	-0.01	0.35	0.05	0.38	0.01	0.45	0.03	0.50
10.5 P	-0.23	0.33	-0.37	0.36	-0.34	0.39	-0.45	0.46	-0.49	0.52
21.0 P	-0.55	0.32	-0.72	0.35	-0.73	0.39	-0.86	0.41	-1.00	0.51
10.5 P	-0.23	0.32	-0.37	0.35	-0.35	0.38	-0.43	0.43	-0.50	0.50
0	0.10	0.33	-0.01	0.36	0.04	0.39	0.02	0.45	0.03	0.53
GM	5.29 cm		4.91 cm		4.51 cm		3.92 cm		3.38 cm	
KG	24.70 cm		25.08 cm		25.48 cm		26.07 cm		26.61 cm	

Appendix B

Free Roll Decay and its Estimated Curve

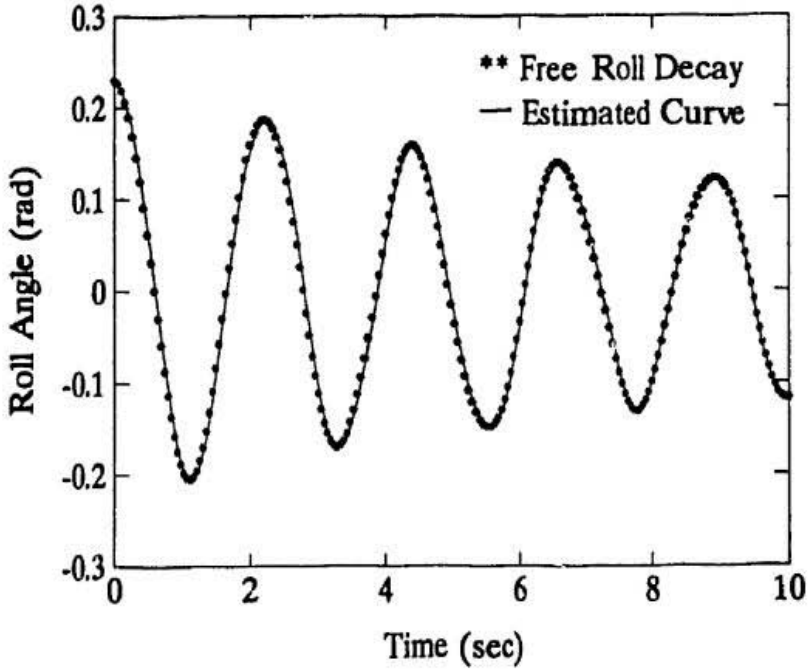

Fig. B.1: Free Decay and its Estimated Curve (M363: GM=3.81cm)

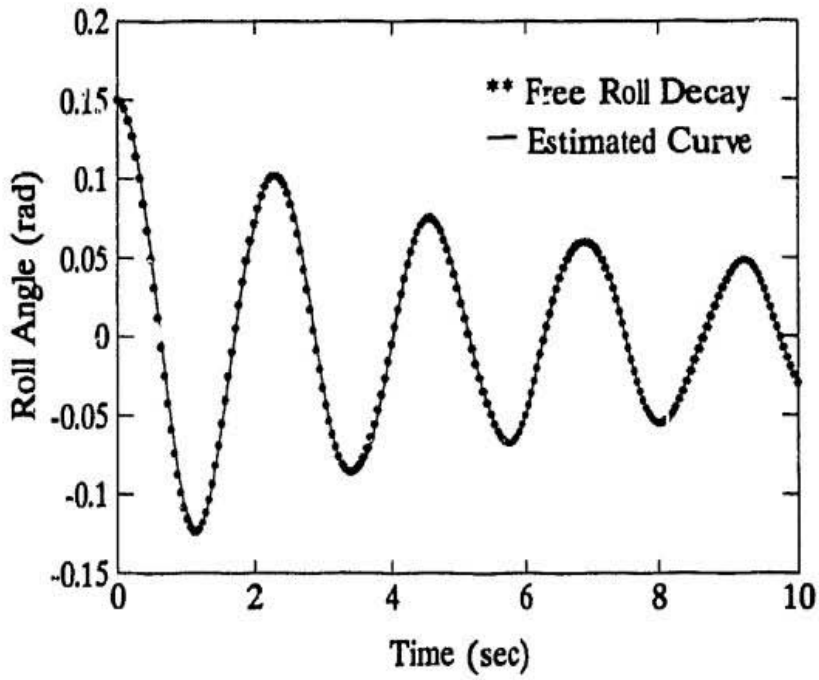

Fig. B.2: Free Decay and its Estimated Curve (M363: GM=3.10cm)

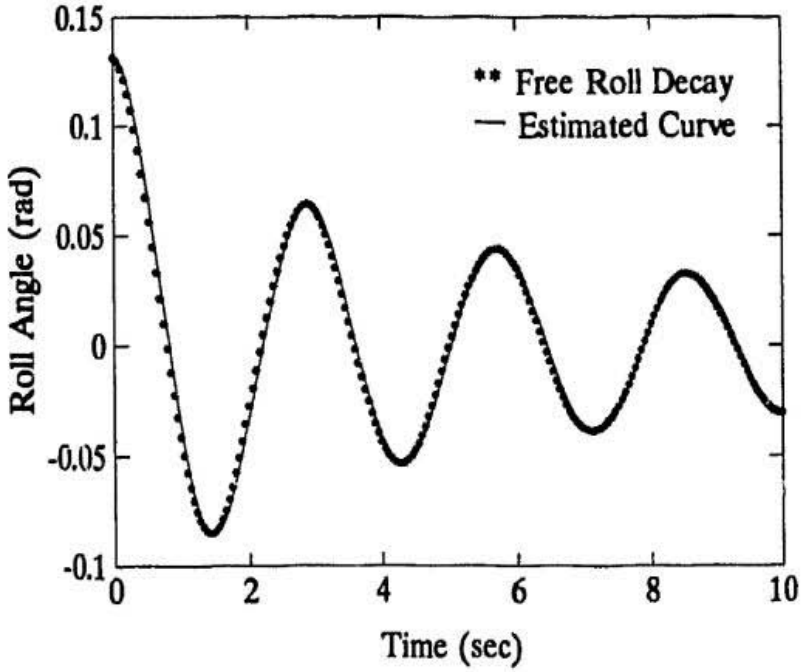

Fig. B.3: Free Decay and its Estimated Curve (M363: GM=2.51cm)

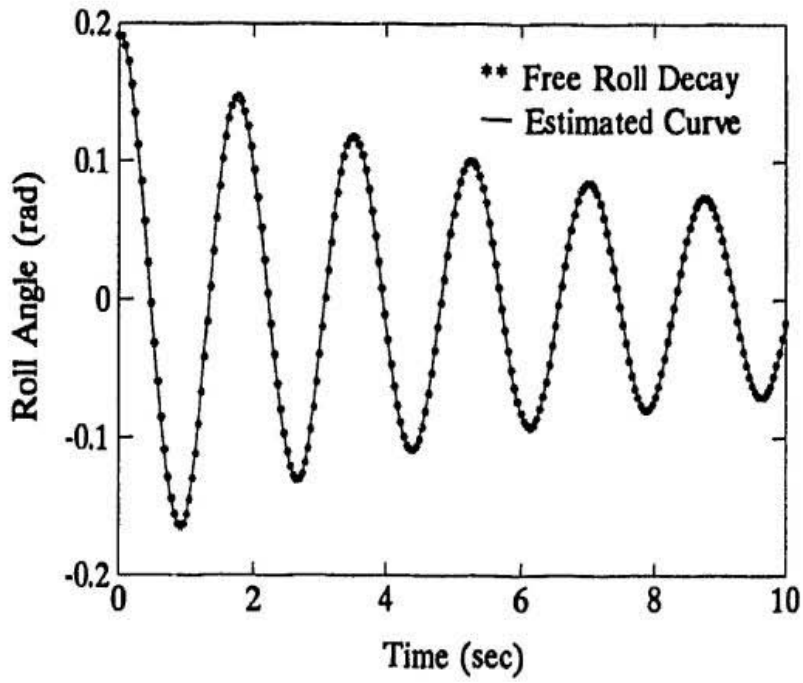

Fig. B.4: Free Decay and its Estimated Curve (M365: GM=4.31cm)

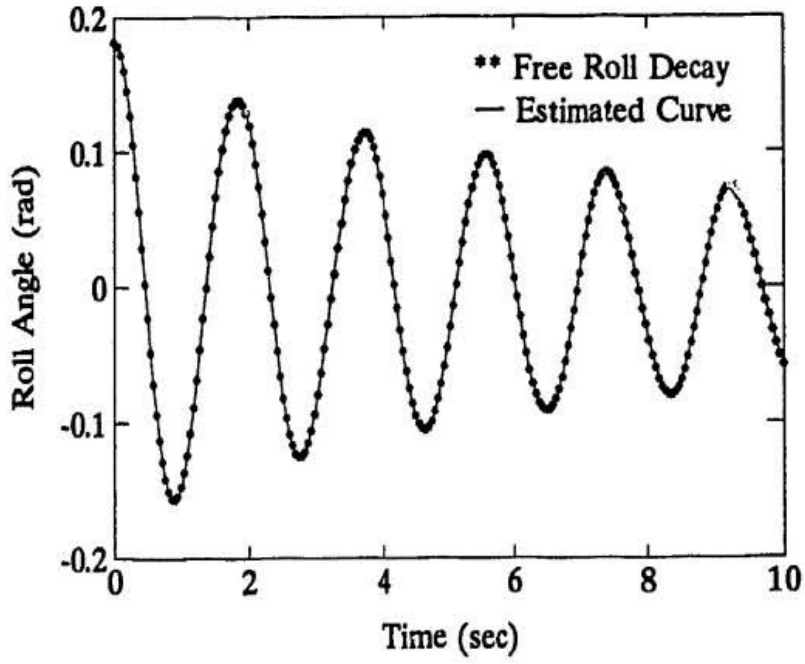

Fig. B.5: Free Decay and its Estimated Curve (M365: GM=3.61cm)

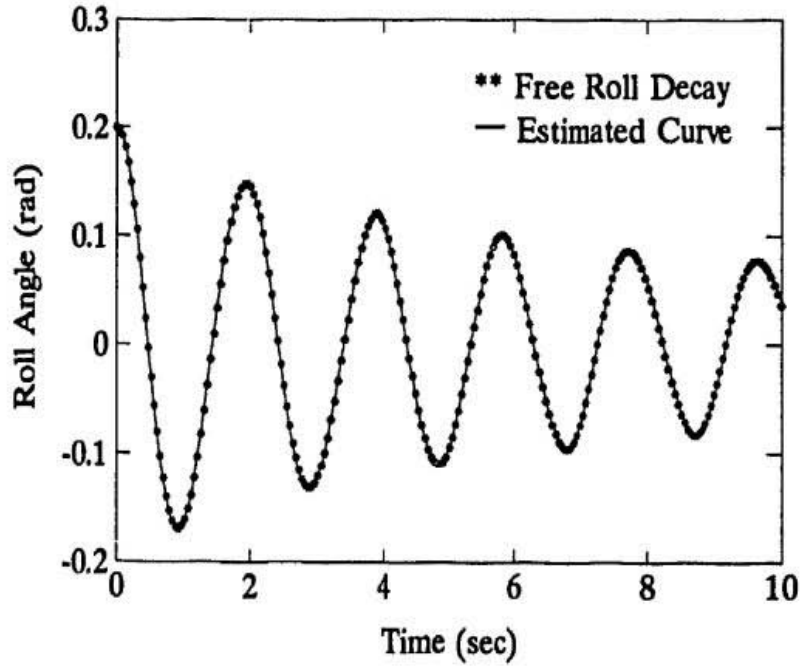

Fig. B.6: Free Decay and its Estimated Curve (M365: GM=3.26cm)

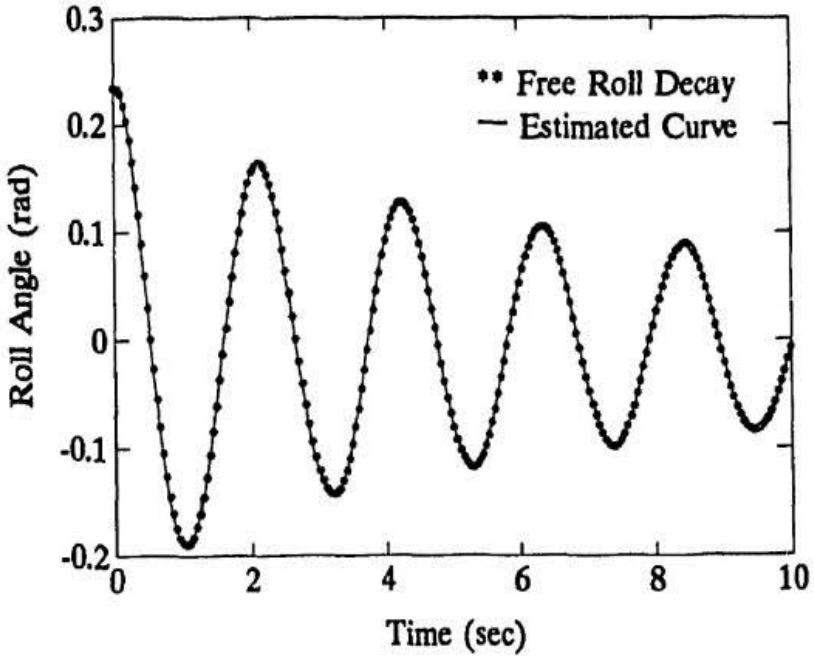

Fig. B.7: Free Decay and its Estimated Curve (M365: GM=2.75cm)

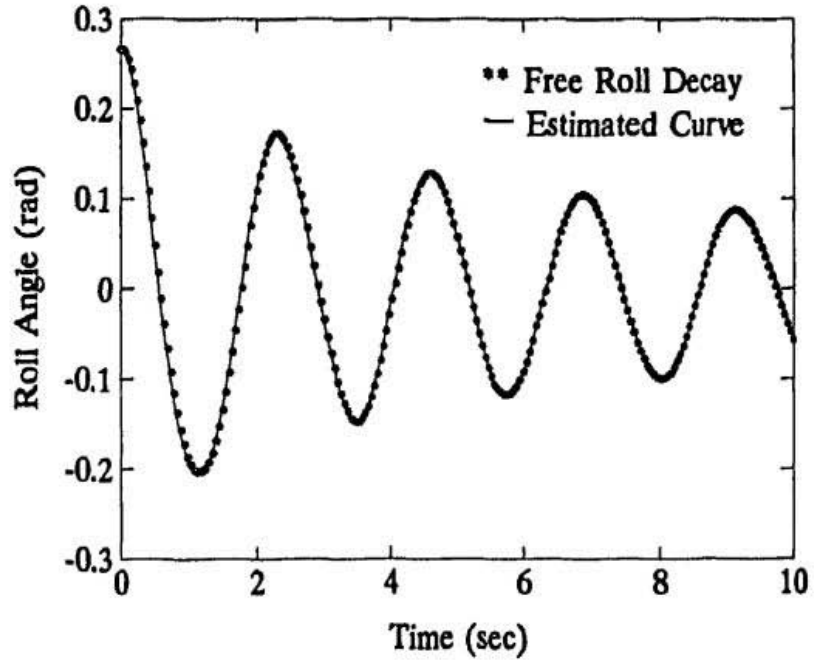

Fig. B.8: Free Decay and its Estimated Curve (M365: GM=2.39cm)

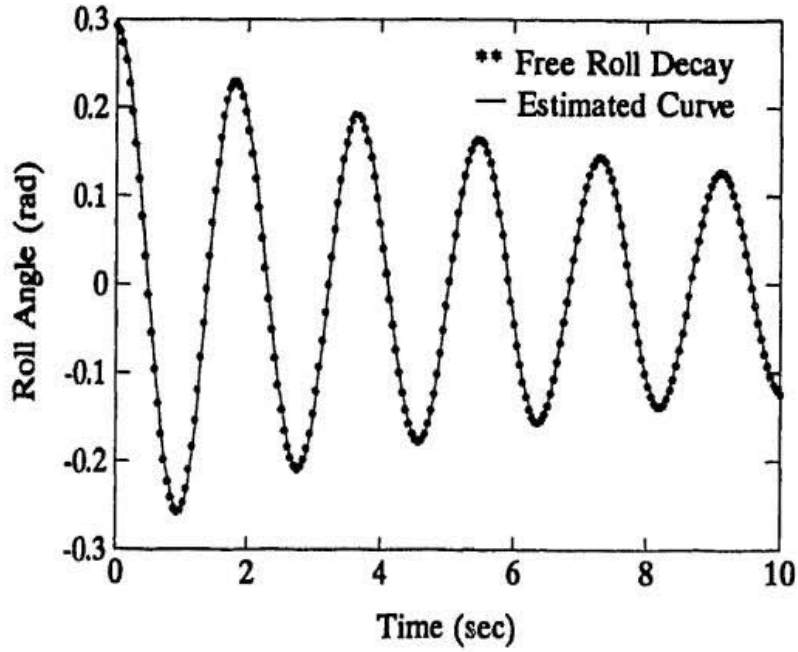

Fig. B.9: Free Decay and its Estimated Curve (M366: GM=5.29cm)

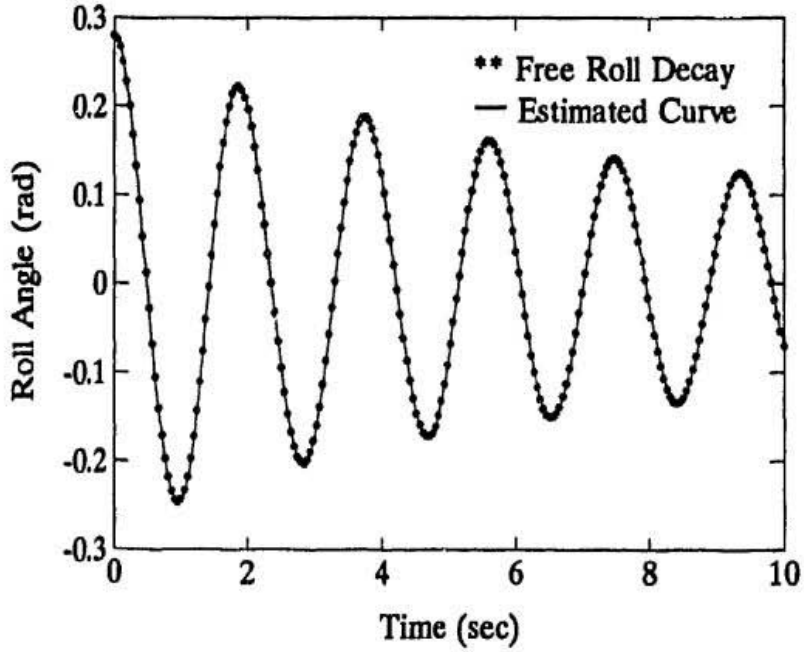

Fig. B.10: Free Decay and its Estimated Curve (M36b: GM=4.91cm)

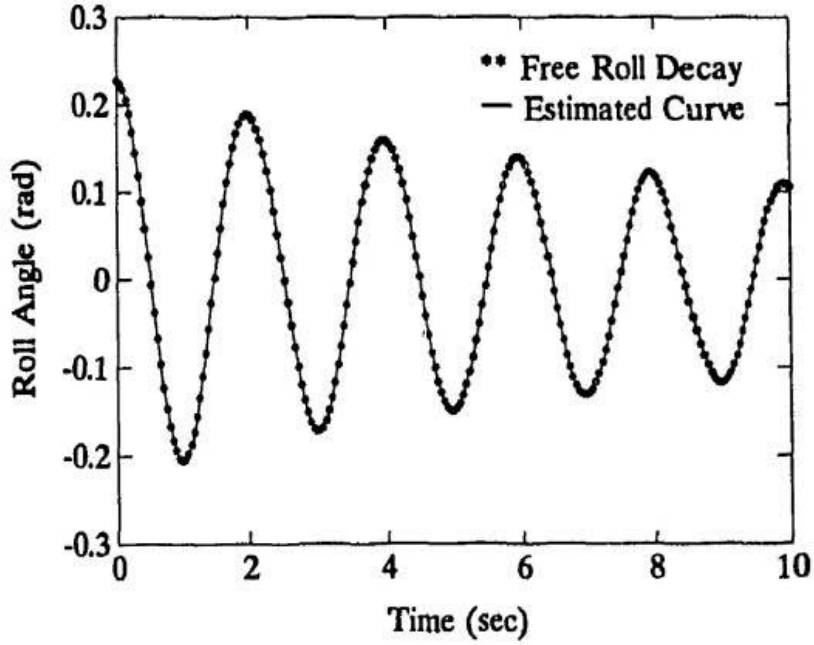

Fig. B.11: Free Decay and its Estimated Curve (M366: GM=4.51cm)

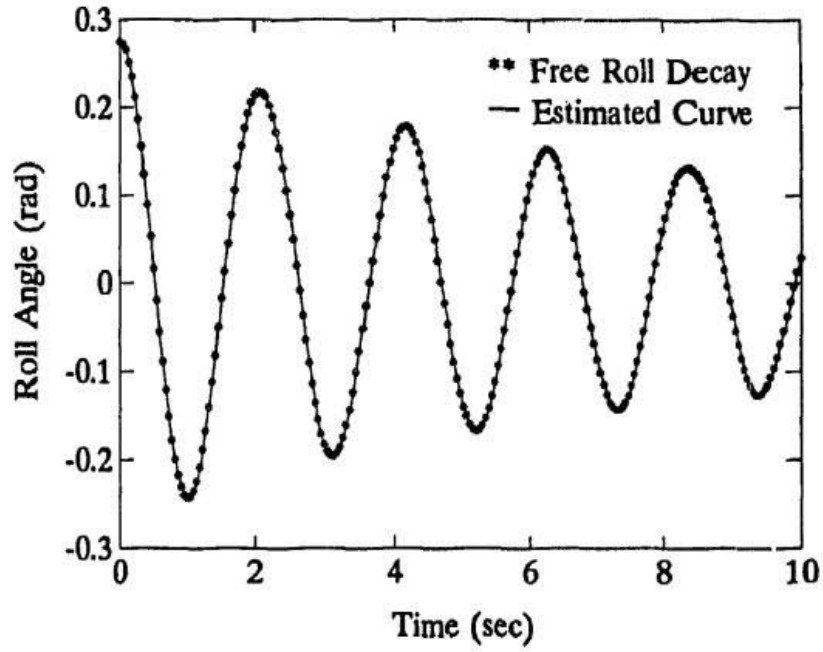

Fig. B.12: Free Decay and its Estimated Curve (M366: GM=3.92cm)

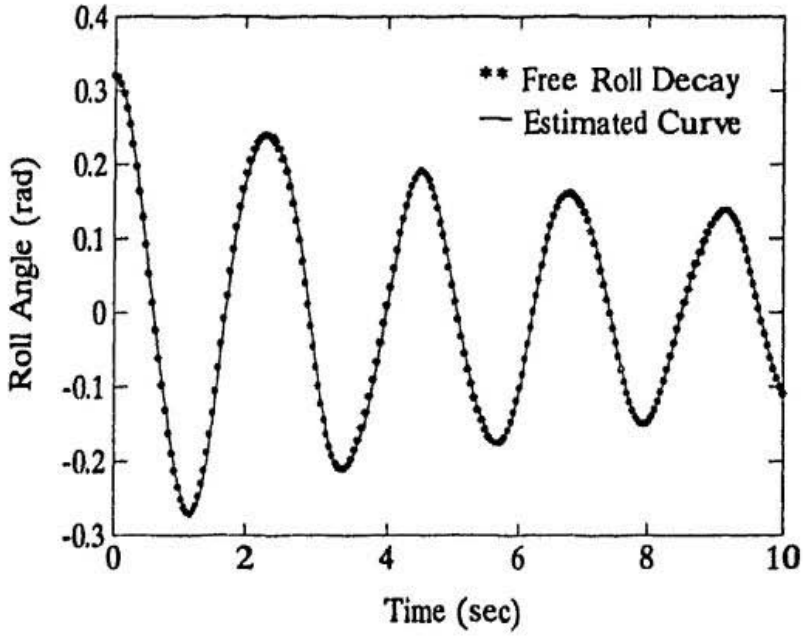

Fig. B.13: Free Decay and its Estimated Curve (M366: GM=3.38cm)

Appendix C

Random Decrement and its Estimated Curve

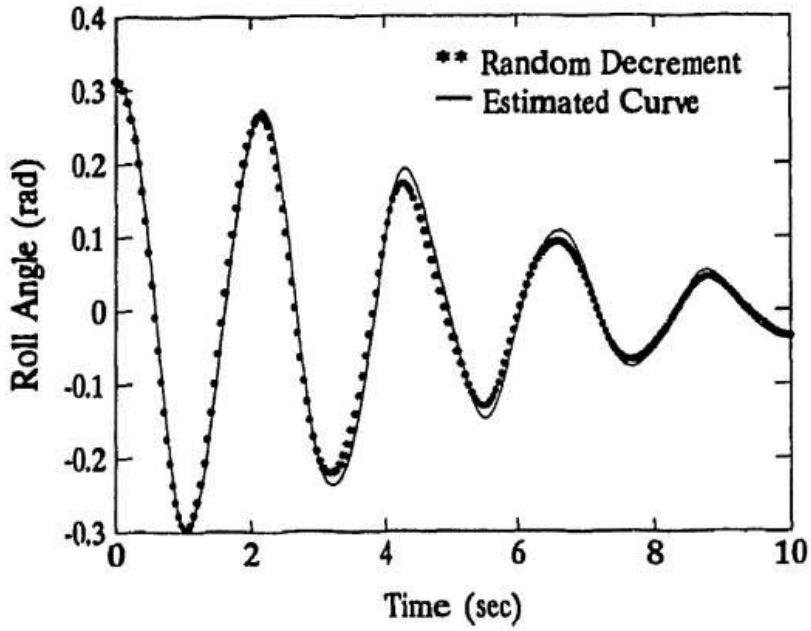

Fig. C.1: Random Decrement and its Estimated Curve (M363: GM=3.81cm)

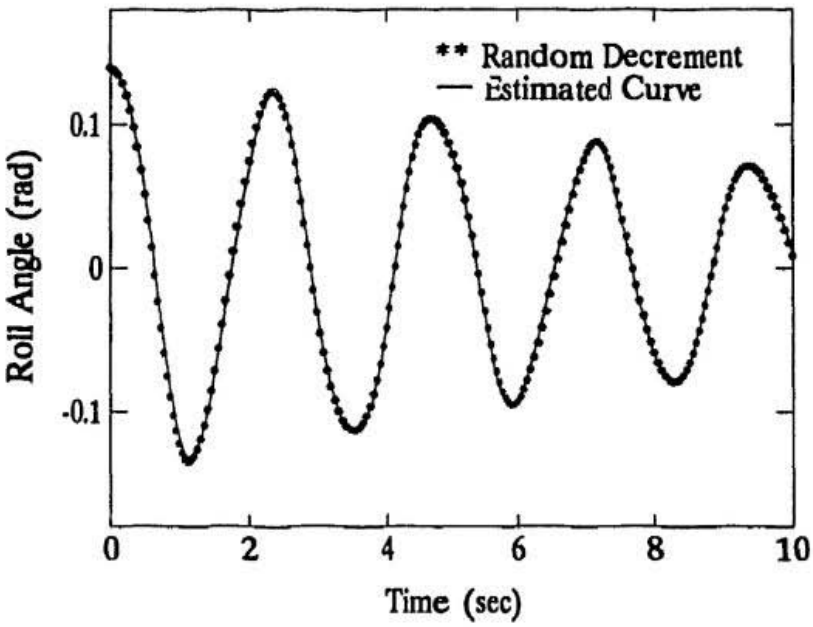

Fig. C.2: Random Decrement and its Estimated Curve (M363: GM=3.10cm)

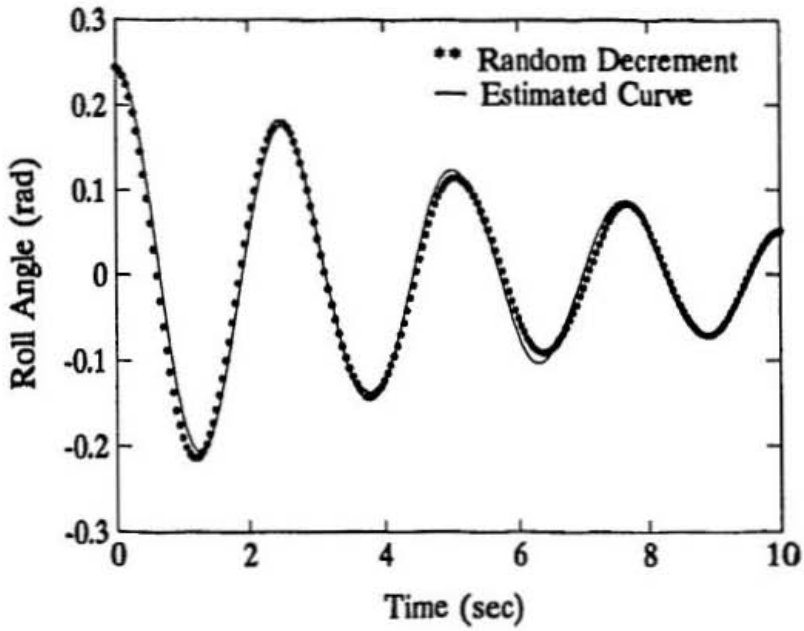

Fig. C.3: Random Decrement and its Estimated Curve (M363: GM=2.51cm)

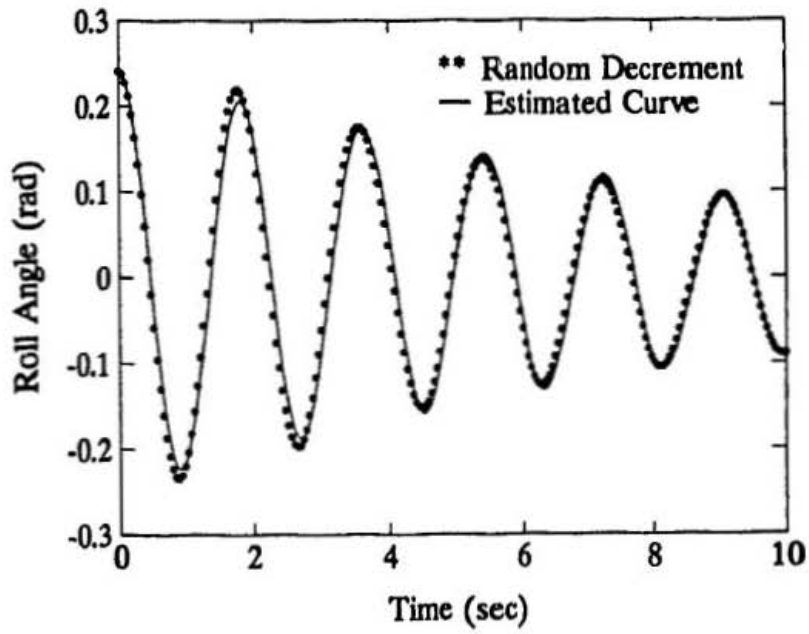

Fig. C.4: Random Decrement and its Estimated Curve (M365: GM=4.31cm)

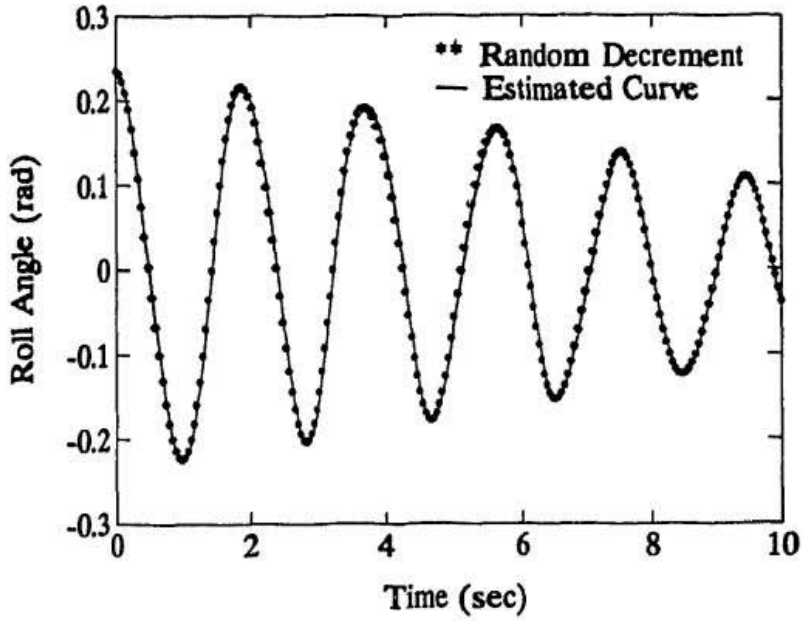

Fig. C.5: Random Decrement and its Estimated Curve (M365: GM=3.61cm)

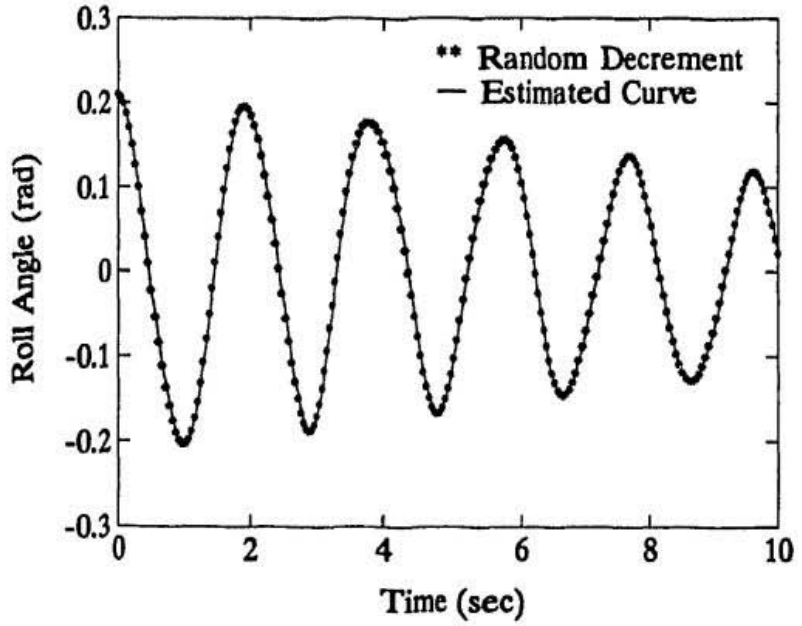

Fig. C.6: Random Decrement and its Estimated Curve (M365: GM=3.26cm)

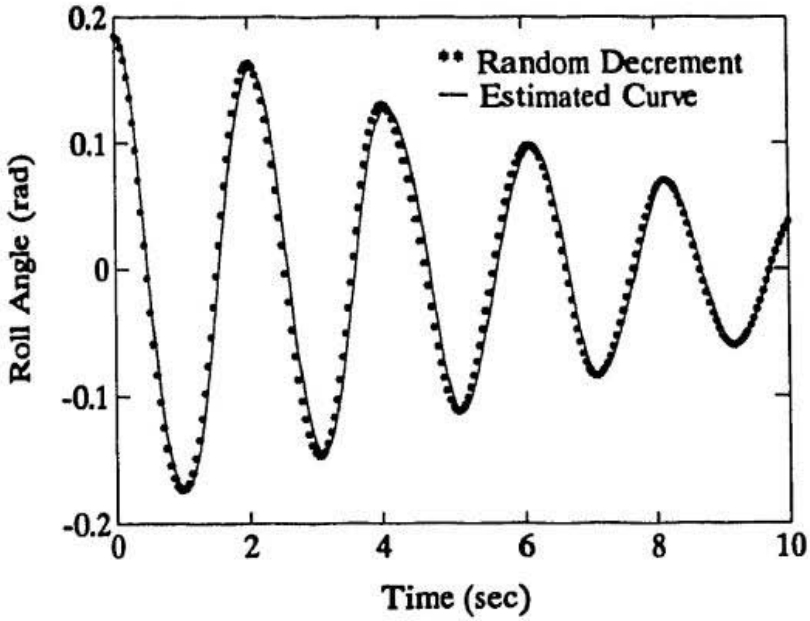

Fig. C.7: Random Decrement and its Estimated Curve (M365: GM=2.75cm)

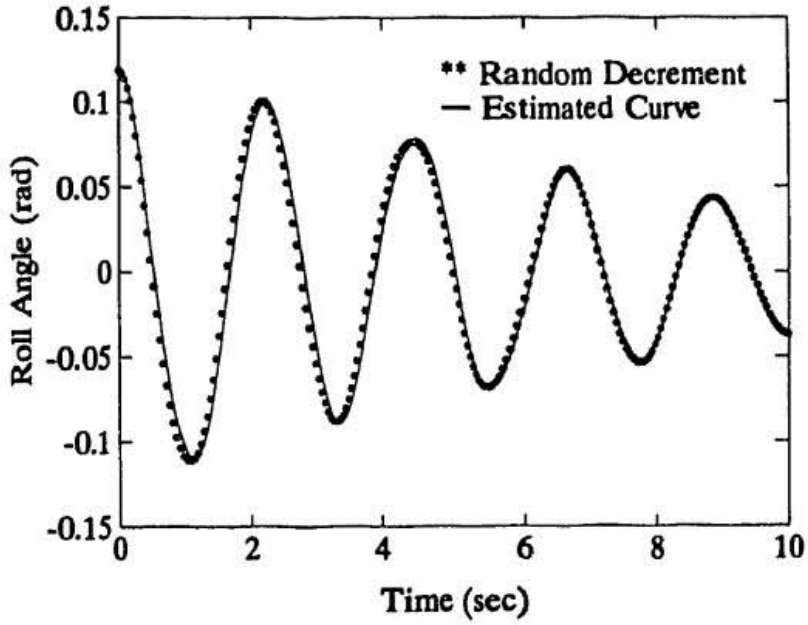

Fig. C.8: Random Decrement and its Estimated Curve (M365: GM=2.39cm)

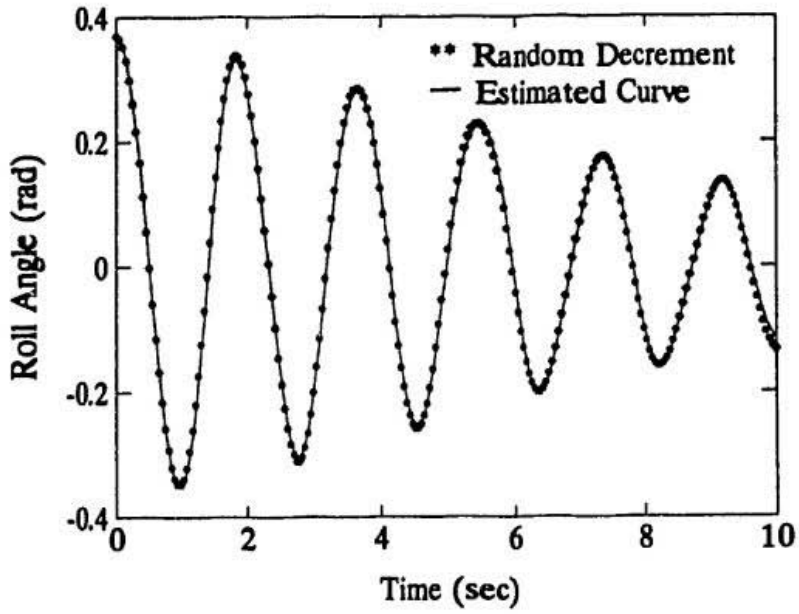

Fig. C.9: Random Decrement and its Estimated Curve (M366: GM=5.29cm)

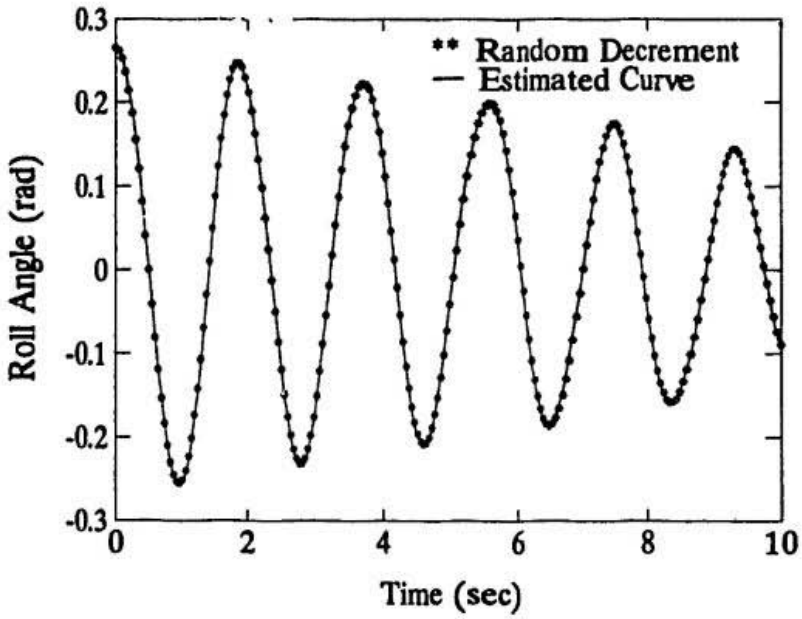

Fig. C.10: Random Decrement and its Estimated Curve (M366: GM=4.91cm)

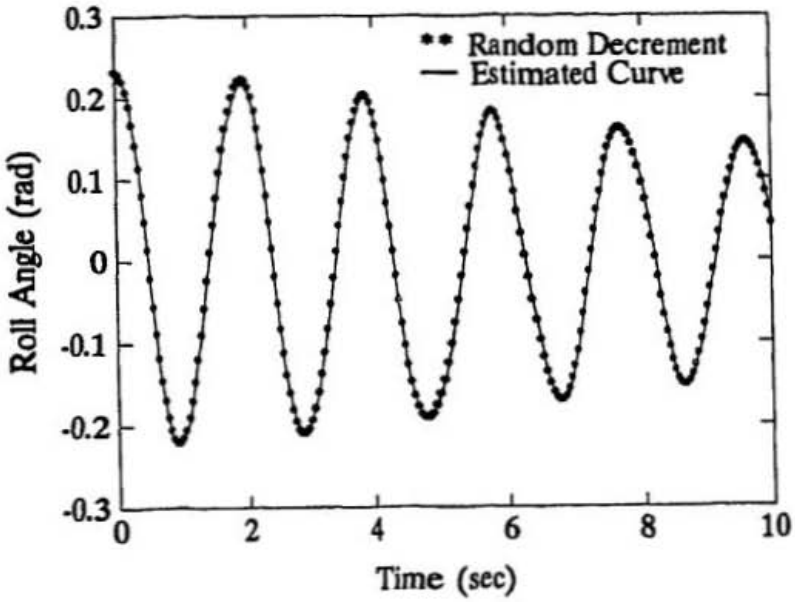

Fig. C.11: Random Decrement and its Estimated Curve (M366: GM=4.51cm)

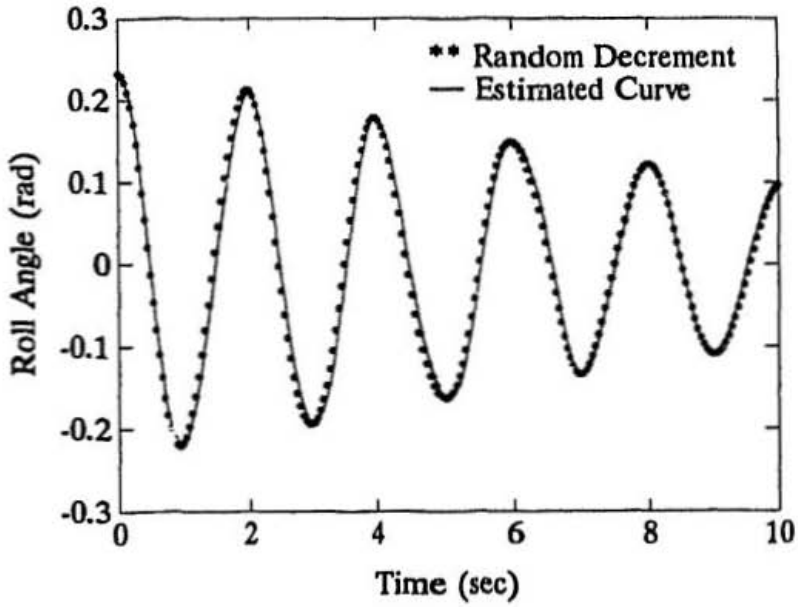

Fig. C.12: Random Decrement and its Estimated Curve (M366: GM=3.92cm)

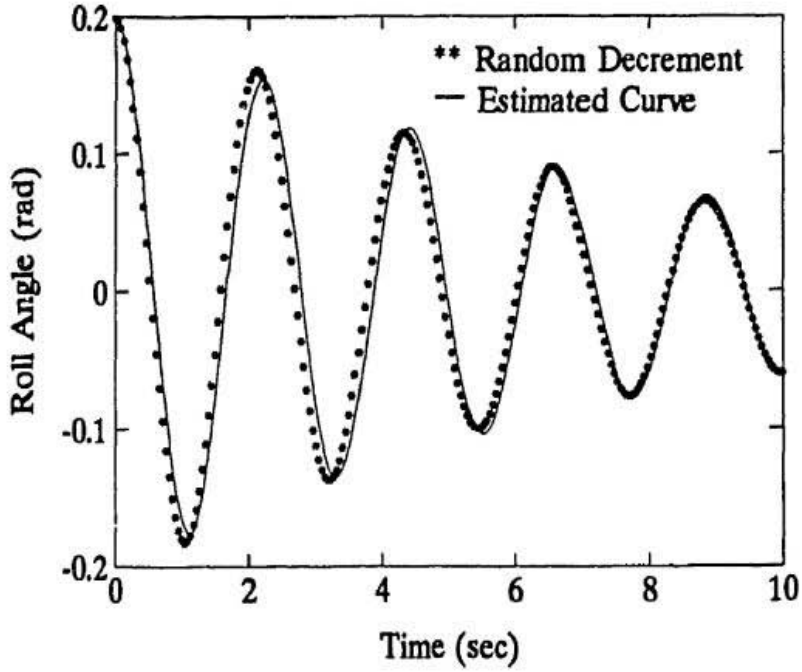

Fig. C.13: Random Decrement and its Estimated Curve (M366: GM=3.38cm)

Appendix D

Autocorrelation and its Estimated Curve

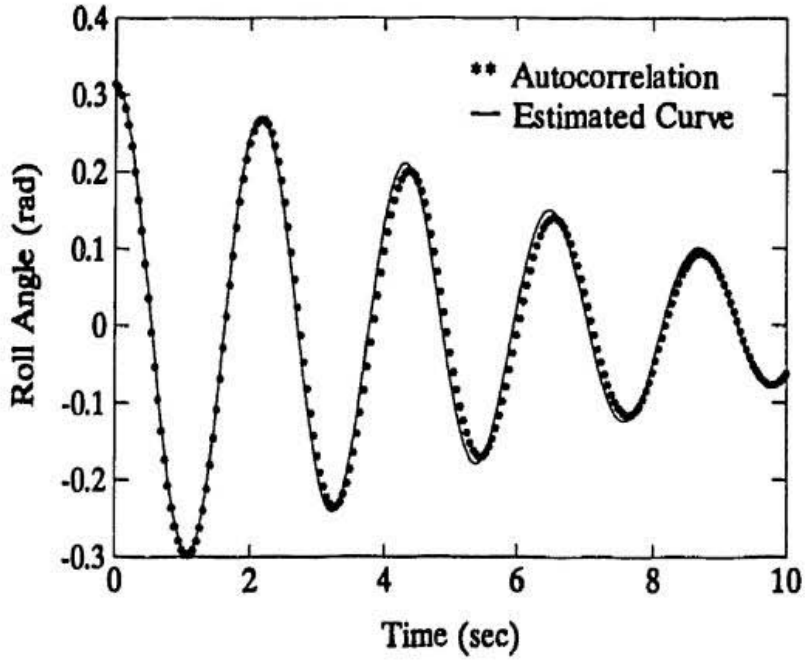

Fig. D.1: Autocorrelation and its Estimated Curve (M363: GM=3.81cm)

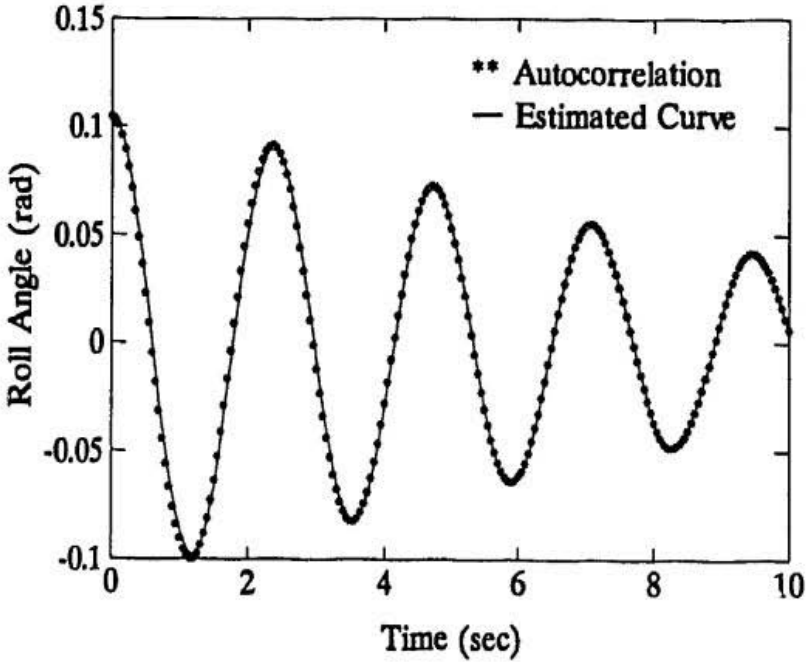

Fig. D.2: Autocorrelation and its Estimated Curve (M363: GM=3.10cm)

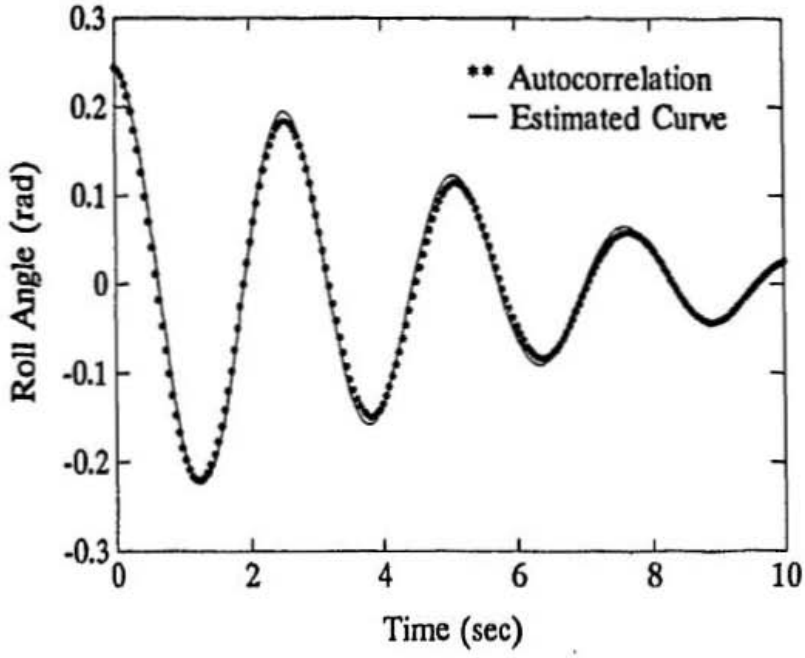

Fig. D.3: Autocorrelation and its Estimated Curve (M363: GM=2.51cm)

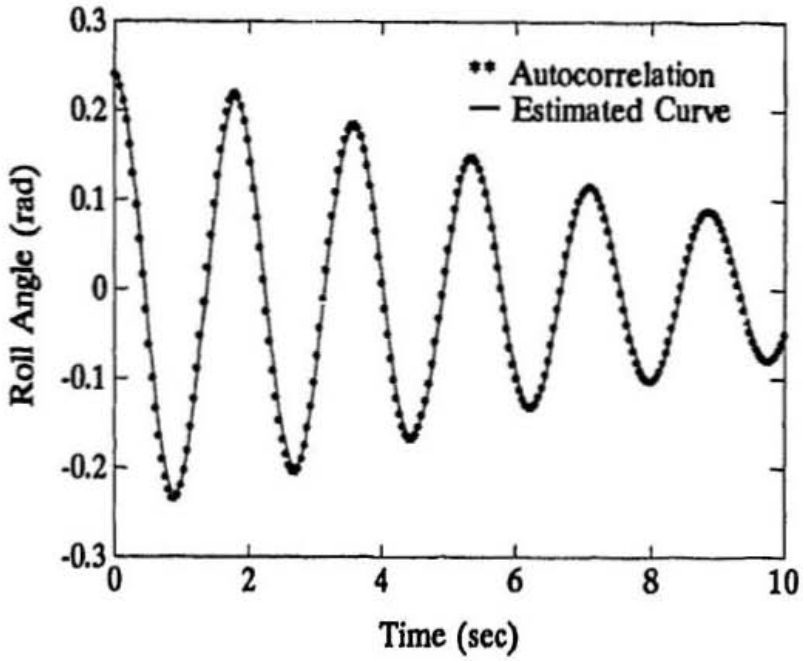

Fig. D.4: Autocorrelation and its Estimated Curve (M365: GM=4.31cm)

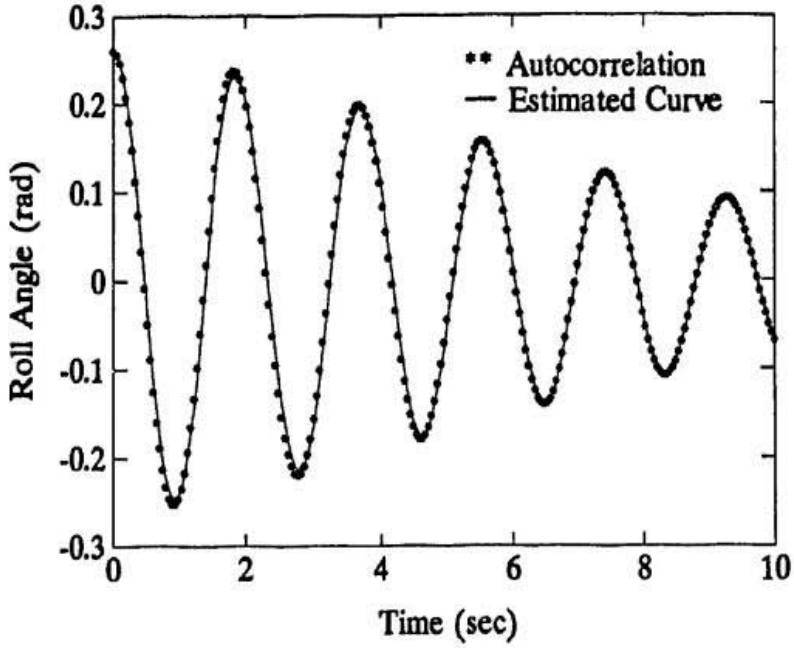

Fig. D.5: Autocorrelation and its Estimated Curve (M365: GM=3.61cm)

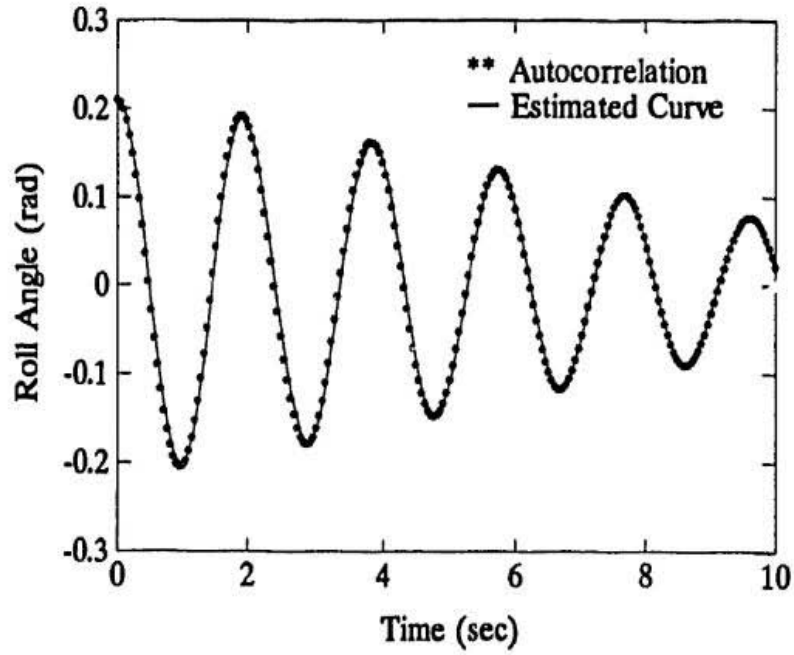

Fig. D.6: Autocorrelation and its Estimated Curve (M365: GM=3.26cm)

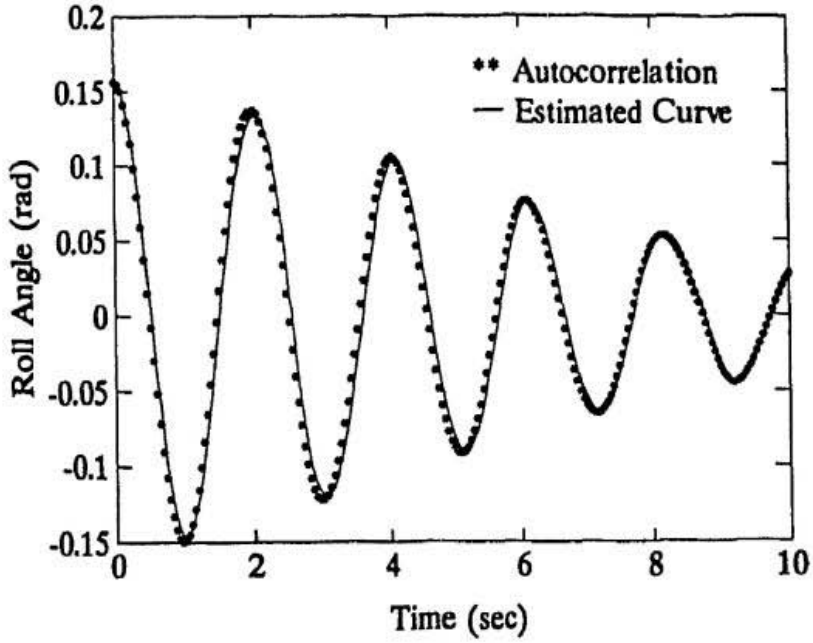

Fig. D.7: Autocorrelation and its Estimated Curve (M365: GM=2.75cm)

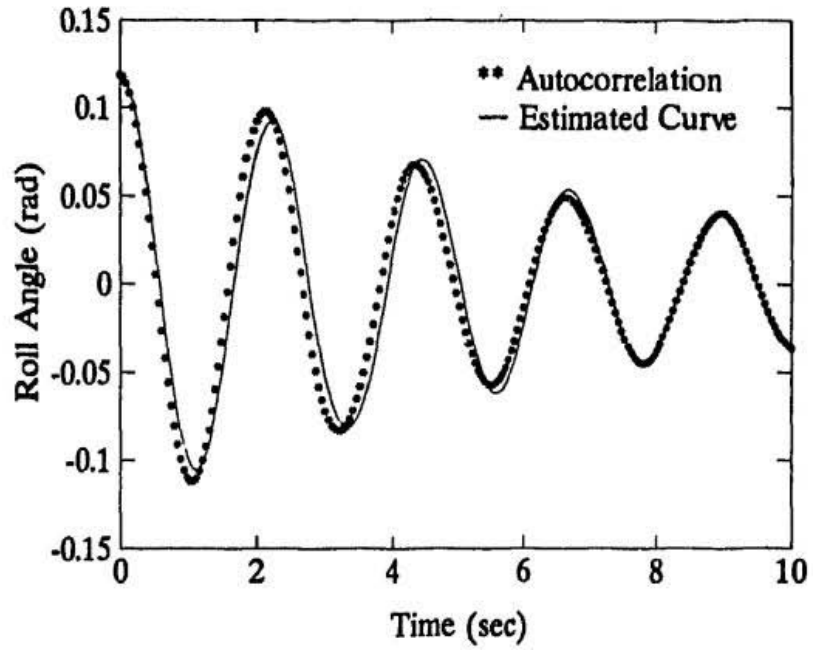

Fig. D.8: Autocorrelation and its Estimated Curve (M365: GM=2.39cm)

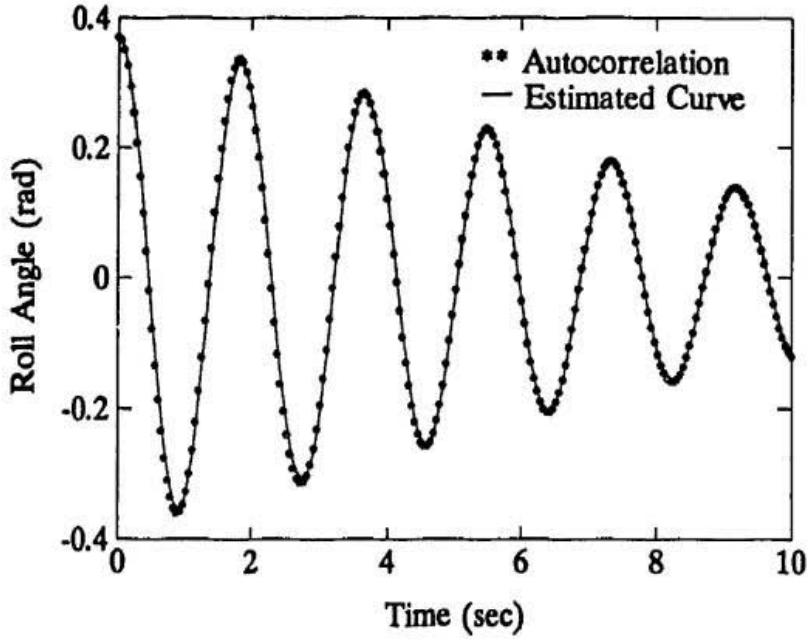

Fig. D.9: Autocorrelation and its Estimated Curve (M366: GM=5.29cm)

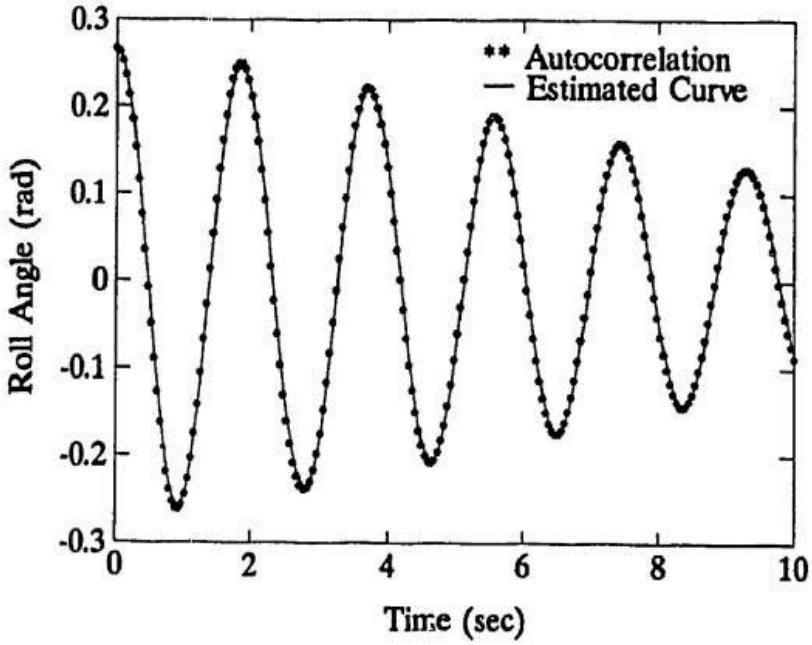

Fig. D.10: Autocorrelation and its Estimated Curve (M366: GM=4.91cm)

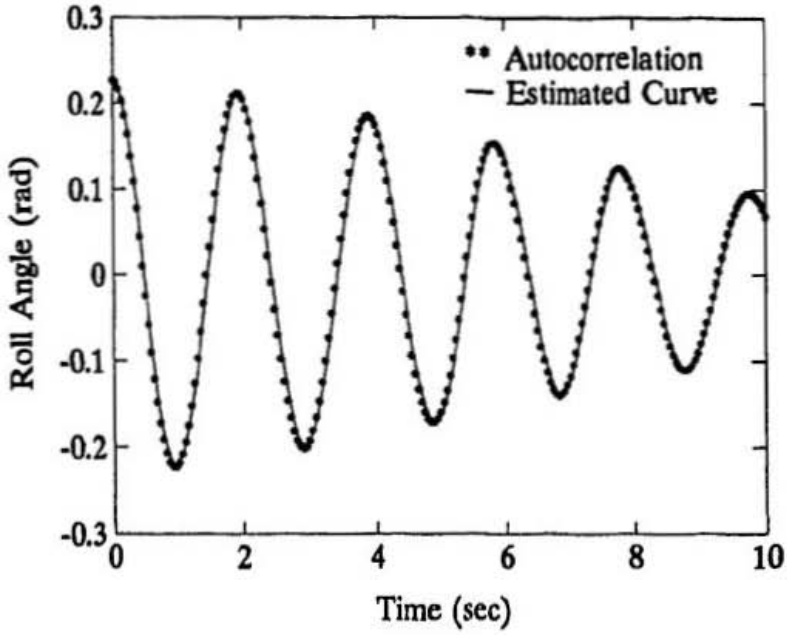

Fig. D.11: Autocorrelation and its Estimated Curve (M366: GM=4.51cm)

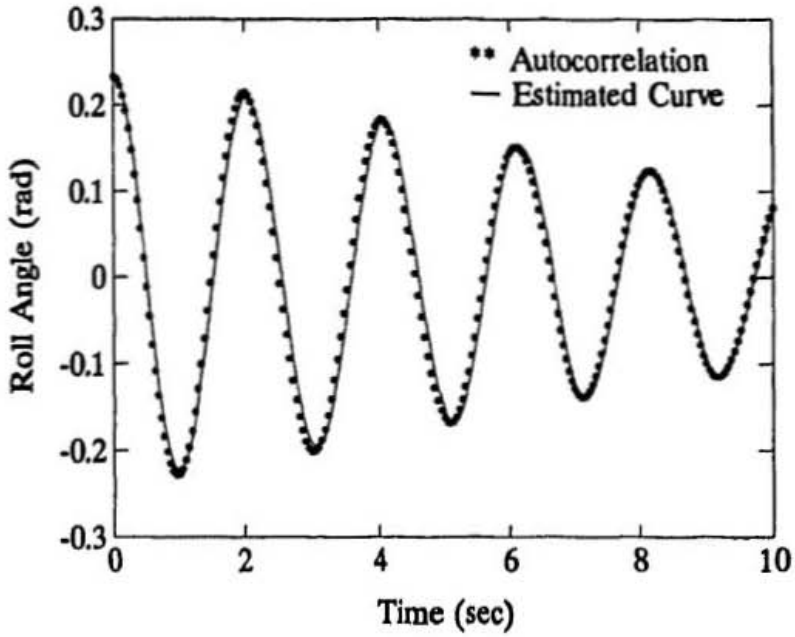

Fig. D.12: Autocorrelation and its Estimated Curve (M366: GM=3.92cm)

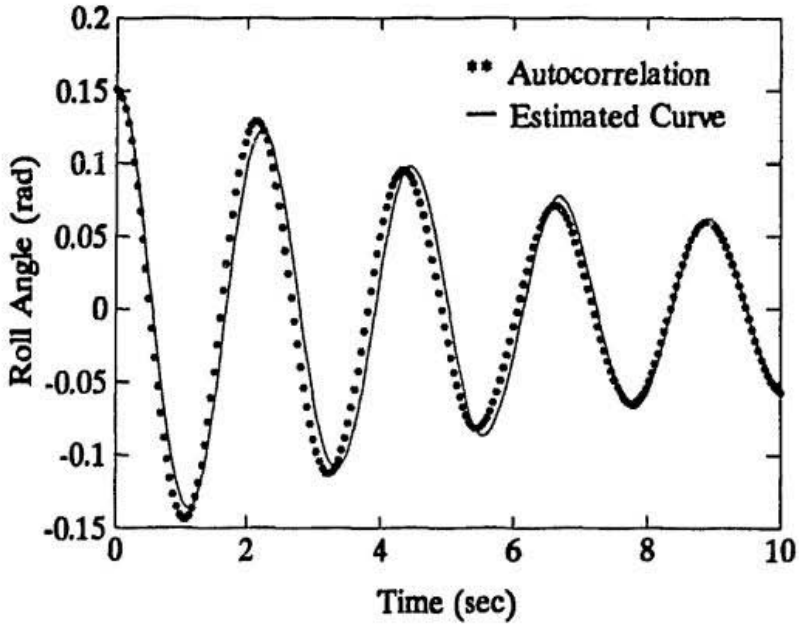

Fig. D.13: Autocorrelation and its Estimated Curve (M366: GM=3.38cm)

Appendix E

Loading Conditions of the Real Ship

Table E.2: Ship Loading Condition: No.2

Item	Weight (t)	V.C.G. (m)	F.S. MMT. (t.m.)
#1 Aft Peak Fuel Oil	12.97	4.42	24.53
#2 Fuel Oil Day Tank	11.74	3.64	16.30
#3 Fuel Oil Wing Tank	8.39	1.63	4.39
#4 (P) D.B. Fuel Oil	20.95	0.77	38.69
#4 (S) D.B. Fuel Oil	11.89	0.57	22.68
#5 (P) D.B. Water Ball	12.16	0.72	8.55
#5 (S) D.B. Water Ball	0	-	-
#6 Fresh Water	14.03	2.75	6.23
#7 Fore Peak Fresh Water	6.27	3.61	1.28
Miscellaneous Tanks	10.45	2.31	-
Provisions	1.59	5.20	-
Crew & Effects	1.5	6.5	-
Fishing Gear	1.5	6.00	-
Empty Fish Boxes	3.98	3.15	-
Ice in Boxes	43.23	2.21	-
Fish&IceinBoxes	40.53	2.63	-
Ice Accretion			
Deadweight	201.69		122.65
Lightship	406	4.74	-
Displacement	607.69	3.95	122.65

Table E.1: Ship Loading Condition: No.1

Item	Weight (t)	V.C.G. (m)	F.S. MMT. (t.m.)
#1 Aft Peak Fuel Oil	12.97	4.42	24.53
#2 Fuel Oil Day Tank	11.74	3.64	16.30
#3 Fuel Oil Wing Tank	8.39	1.63	4.39
#4 (P) D.B. Fuel Oil	20.95	0.77	38.69
#4 (S) D.B. Fuel Oil	13.51	0.62	25.66
#5 (P) D.B. Water Ball	12.16	0.72	8.55
#5 (S) D.B. Water Ball	0	-	-
#6 Fresh Water	14.86	2.85	7.07
#7 Fore Peak Fresh Water	6.27	3.61	1.28
Miscellaneous Tanks	10.45	2.31	-
Provisions	1.69	5.20	-
Crew & Effects	1.5	6.5	-
Fishing Gear	1.5	6.00	-
Empty Fish Boxes	4.34	3.02	-
Ice in Boxes	47.13	2.19	-
Fish & Ice in Boxes	31.11	2.65	-
Ice Accretion			
Deadweight	199.07		126.47
Lightship	406	4.74	-
Displacement	605.07	3.95	126.47

Table E.3: Ship Loading Condition: No.3

Item	Weight (t)	V.C.G. (m)	F.S. MMT. (t.m.)
#1 Aft Peak Fuel Oil	12.97	4.42	24.53
#2 Fuel Oil Day Tank	11.74	3.64	16.30
#3 Fuel Oil Wing Tank	8.39	1.63	4.39
#4 (P) D.B. Fuel Oil	20.95	0.77	38.69
#4 (S) D.B. Fuel Oil	10.44	0.53	19.88
#5 (P) D.B. Water Ball	12.16	0.72	8.55
#5 (S) D.B. Water Ball	0	-	-
#6 Fresh Water	13.30	2.67	5.50
#7 Fore Peak Fresh Water	6.27	3.61	1.28
Miscellaneous Tanks	10.45	2.31	-
Provisions	1.51	5.20	-
Crew & Effects	1.5	6.5	-
Fishing Gear	1.5	6.00	-
Empty Fish Boxes	3.36	3.71	-
Ice in Boxes	36.50	2.23	-
Fish&IceinBoxes	56.79	2.60	-
Ice Accretion			
Deadweight	208.33		119.13
Lightship	406	4.74	-
Displacement	614.33	3.94	119.13